THE UNIVERSITY
of EDINBURGH

On Three Use Cases of Multi-Connectivity Paradigm in Emerging Wireless Networks

Mohamed Kassem

Doctor of Philosophy
Institute of Computing Systems Architecture
School of Informatics
University of Edinburgh
2019

Abstract

As envisioned by global network operators, the increasing trend of data traffic demand is expected to continue with exponential growth in the coming years. To cope with this rapid increase, significant efforts from the research community, industry and even regulators have been focused towards improving two main aspects of the wireless spectrum: (i) spectrum capacity and (ii) spectral efficiency. Concerning the spectrum capacity enhancement, the multi-connectivity paradigm has been seen to be fundamentally important to solve the capacity problem in the next generation networks. Multi-connectivity is a feature that allows wireless devices to establish and maintain multiple simultaneous connections across homogeneous or heterogeneous technologies. In this thesis, we focus on identifying the core issues in applying the multi-connectivity paradigm for different use cases and propose novel solutions to address them.

Specifically, this thesis studies three use cases of the multi-connectivity paradigm. First, we study the uplink/downlink decoupling problem in 4G networks. More specifically, we focus on the user association problem in the decoupling context, which is considered challenging due to the conflicting objectives of different entities (e.g., mobile users and base stations) in the system. We use a combination of matching theory and stochastic geometry to reconcile competing objectives between users in the uplink/downlink directions and also from the perspective of base stations.

Second, we tackle the spectrum aggregation problem for wireless backhauling links in unlicensed opportunistic shared spectrum bands, specifically, TV White Space (TVWS) spectrum. In relation to this, we present a DIY mobile network deployment model to accelerate the roll-out of high-end mobile services in rural and developing regions. As part of this model, we highlight the importance of low-cost and high-capacity backhaul infrastructure for which TVWS spectrum can be exploited. Building on that, we conduct a thorough analytical study to identify the characteristics of TVWS in rural areas. Our study sheds light on the nature of TVWS spectrum fragmentation for the backhauling use case, which in turn poses requirements for the design of spectrum aggregation systems for TVWS backhaul. Motivated by these findings, we design and implement WhiteHaul, a flexible platform for spectrum aggregation in TVWS. Three challenges have been tackled in this work. First, TVWS spectrum is fragmented in that the spectrum is available in non-contiguous manner. To fully utilize the available spectrum, multiple radios should be enabled to work simultaneously. However, all the radios have to share only a single antenna. The key challenge is to design a system architecture that is capable of achieving different aggregation configurations while

avoiding the interference. Second, the heterogeneous nature of the available spectrum (i.e., in terms of bandwidth and link characteristics) requires a design of efficient traffic distribution algorithm that takes into account these factors. Third, TVWS is unlicensed opportunistic shared spectrum. Thus, the coordination mechanism between the two nodes of backhauling link is essential to enable seamless channel switching.

Third, we study the integration of multiple radio access technologies (RATs) in the context of 4G/5G networks. More specifically, we study the potential gain of enabling the Multi-RAT integration at the Packet Data Convergence Protocol (PDCP) layer compared with doing it at the transport layer. In this work, we consider ultra-reliable low-latency communication (URLLC) as one of the motivating services. This work tackles the different challenges that arise from enabling the Multi-RAT integration at the PDCP layer, including, packet reordering and traffic scheduling.

Lay Summary

Wireless and mobile services are an essential and integral part of daily life nowadays and different industries are based on wireless services now. Global mobile devices grew in 2017 to reach 8.6 billion devices compared to 7.9 billion in 2016. In addition, the global mobile data traffic increased by 71% in 2017 and reached 11.5 exabytes per month by the end of 2017 which was previously 6.7 exabytes per month by the end of 2016. With the rise of 5G Network and its wider deployment, this increasing trend is expected to continue to reach 131 exabytes per month by 2024.

Thus, the growing demand of global mobile data traffic is propelling the need for more capacity. In fact, regulators, industry, and research community are all busy working to address that from various angles. Allocating more spectrum and improving the efficiency (i.e., spectral efficiency) of its use is a well-known way to scale up the capacity of wireless and mobile networks. However, the spectrum is a limited resource, especially below 6 GHz where most wireless and mobile systems operate and will continue to do so in the future. In view of these constraints associated with an additional spectrum below 6 GHz that could be made available to the wireless and mobile services, regulators, around the globe, have introduced and regulated access for a new type of spectrum that is shared between different industries. The new concept of the shared spectrum allows opportunistic access to some spectrum bands between different sectors/industries (e.g., mobile services and military in 3.5 GHz band). This shared access concept created a new phenomenon named fragmented spectrum in which means the spectrum might not be found available in large chunks. Therefore, in order to boost the capacity, mobile and wireless systems have to leverage several chunks of available spectrum in different bands. This gives rise to the new multi-connectivity paradigm. Multi-connectivity is a feature that allows wireless and mobile systems to establish and maintain multiple simultaneous connections across homogeneous or heterogeneous technologies and spectrum bands.

In this thesis, we focus on three use-cases for the multi-connectivity paradigm, (i)

decoupled user association in LTE systems, (ii) TVWS spectrum aggregation to enable high capacity backhauling links and (iii) Multi-RAT integration. Thorough the coming chapters, we will identify the core issues when applying the multi-connectivity paradigm in these different use-cases and propose our novel solutions to largely alleviate these issues.

Acknowledgements

I would first like to thank my supervisor Mahesh K. Marina for all his support and guidance throughout my PhD. Not only did he teach me how to do quality research and always strive for the best result, but also taught me how to enjoy the process and find balance in my personal and professional life. He is a true mentor for me in every sense of the word. I also am very grateful to Dr. Cengis Hasan, Dr. Xenofon Foukas, Dr. Joerg Widmer, Dr. Claudio Fiandrino and Dr. Morteza Kheirkhah for all the helpful discussions that greatly influenced the outcome of my research.

Throughout my PhD, I have been very fortunate to work next to and collaborate with some amazing colleagues, Dr. Saravana Rathinakumar, Dr. Valentin Radu, Dr. Mah-Rukh Fida, Galini Tsoukaneri and Rajkarn Singh.

My deepest gratitude goes to my parents Mostafa and Hanaa. Both starting and finishing my PhD would have been impossible without the unconditional love and support they have shown me throughout all of these years. I am very thankful to my brother Amro and sister Dalia, who were always there for me when I needed it the most, with endless understanding, their unconditional love.

Declaration

I declare that this thesis was composed by myself, that the work contained herein is my own except where explicitly stated otherwise in the text, and that this work has not been submitted for any other degree or professional qualification except as specified. Some of the material used in this thesis has been published in the papers listed below. For the WhiteHaul work, the contribution of my co-authors, other than my supervisors, is limited to helping with the implementation of the MPTCP Linux kernel module.

- Kassem, Mohamed M., and Mahesh K. Marina. "Future wireless spectrum below 6 GHz: A UK perspective." 2015 IEEE International Symposium on Dynamic Spectrum Access Networks (DySPAN). IEEE, 2015.

- Kassem, Mohamed, Cengis Hasan, and Mahesh Marina. "Decoupled Uplink/Downlink User Association in HetNets: A Matching with Contracts Approach." Proceedings of the 12th ACM Symposium on QoS and Security for Wireless and Mobile Networks. ACM, 2016.

- Kassem, Mohamed M., Mahesh K. Marina, and Oliver Holland. "On the potential of TVWS spectrum to enable a low cost middle mile network infrastructure." 2018 10th International Conference on Communication Systems Networks (COMSNETS). IEEE, 2018.

- Kassem, Mohamed M., Mahesh K. Marina, and Bozidar Radunovic. "DIY Model for Mobile Network Deployment: A Step Towards 5G for All." Proceedings of the 1st ACM SIGCAS Conference on Computing and Sustainable Societies. ACM, 2018.

- Kassem, Mohamed M., Morteza Kheirkhah, Mahesh K. Marina, and Peter Buneman. "WhiteHaul: An Efficient Spectrum Aggregation System for Low-Cost and High Capacity Backhaul over White Spaces", to appear in the 18th ACM International Conference on Mobile Systems, Applications, and Services, MobiSys 2020.

(*Mohamed Kassem*)

Table of Contents

List of Figures

List of Tables

List of Abbreviations

TVWS	TV White Space
RAT	Radio Access Technology
PDCP	Packet Data Convergence Protocol
URLLC	Ultra Reliable Low Latency Communication
UHF	Ultra High Frequency
OSA	Opportunistic Shared Access
LSA	Licensed Shared Access
eLSA	Evolved Licensed Shared Access
GL-DB	Geo-Location Database
RSS	Received Signal Strength
CAPEX	Capital Expenditure
OPEX	Operational Expenditure
IoT	Internet of Things
CA	Carrier Aggregation
LTE-U	Long Term Evolution-Unlicensed
CB	Channel Bonding
BS	Base Station
DC	Dual Connectivity

SINR	Signal to Interference and Noise Ratio
MBS	Macro Base Station
SBS	Small Base Station
GDP	Gross Domestic Product
4G	4th Generation
5G	5th Generation
LWA	LTE-WiFi Aggregation
MPTCP	Multi-path Transport Control Protocol
NLOS	Non-Line of Sight
DIY	Do-it-Yourself
NR	New Radio
mmWave	Millimeter Wave
PHY	Physical
M2M	Machine to Machine
MoD	Ministry of Defence
WGFM	Working Group on Frequency Management
ECC	Electrical Communication Committee
LTE-TDD	Long Term Evolution-Time Division Duplex
QoS	Quality of Service
PUs	Primary User
SUs	Secondary User
DTT	Digital Terrestrial TV
PMSE	Programme Making and Special Events

MNO	Mobile Network Operator
ETSI-RRS	European Telecommunications Standards Institute Reconfigurable Radio Systems
DFS	Dynamic Frequency Selection
CCC	Common Control Channel
WSDB	White Space Database
WSD	White Space Device
GPS	Global Positioning System
WSDIS	White Space Devices Information System
FDD	Frequency Division Duplex
SDL	Supplemental Downlink
RSPG	Radio Spectrum Policy Group
PTP	Point to Point
PTMP	Point to Multi-Point
MP-QUIC	Multi-Path Quick UDP Internet Connection
WiLD	WiFi for Long Distance
LWIP	LTE-WLAN Radio Level Integration With Ipsec Tunnel
WT	Wireless Termination
FMS	First Missing Sequence
LWIPEP	LWIP Encapsulation Protocol
LWAAP	LWA Application Protocol
HetNet	Heterogeneous Network
UE	User Equipment
UL	Uplink

DL	Downlink
D2D	Device to Device
PPP	Poisson Point Process
DUDe	DL/UL Decoupling
UAV	Unmanned Aerial Vehicle
PoP	Point of Presence
MME	Mobility Management Entity
HSS	Home Subscriber Server
SGW	Serving Gateway
VMs	Virtual Machine
DEA	Diameter Edge Agent
IPX	IP Exchange
ITWOM	Irregular Terrain With Obstructions
EIRP	Equivalent Isotropically Radiated Power
TDD	Time Division Duplex
COTS	Commodity Off-The-Shelf
LPWAN	Low Power Wide Area Network
LO	Local Oscillator
VCO	Voltage Controlled Oscillator
SNR	Signal to Noise Ratio
USRP	Universal Software Radio Peripheral
SPDT	Single Pole Double Throw
PA	Power Amplifier

LNA	Low Noise Amplifier
MCS	Modulation and Coding Scheme
TDM	Time Division Multiplexing
OLIA	Opportunistic Linked-Increases Algorithm
LIA	Linked Increases Algorithm
OOB	Out-of-Band
RSSI	Received Signal Strength Indication
PRR	Packet Reception Rate
AI	Artificial Intelligence
eMBB	Enhanced Mobile Broadband
mMTC	Massive Machine Type Communication
BALIA	Balanced Linked Adaptation
PDU	Protocol Data Unit
RLC	Radio Link Control
RLC AM	RLC Acknowledged Mode
RLC UM	RLC Unacknowledged Mode
RTT	Round Trip Time
HoL	Head of Line
BLER	Block Error Rate
CQI	Channel Quality Indicator
NF	Noise Figure
eNB	eNodeB
MAC	Medium Access Control

RRC	Radio Resource Control
WLAN	Wireless Local Access Network

Chapter 1

Introduction

Wireless and mobile services are an essential and integral part of daily life, and many different industries are currently based on wireless services. Global mobile devices grew in 2017 to reach 8.6 billion devices compared to 7.9 billion in 2016 with expectations to grow to 12.3 billion by 2022 [40]. In addition, global mobile data reached 11.5 exabytes per month by the end of 2017, an increase of 71% from 6.7 exabytes per month by the end of 2016 [40]. It is expected that the global mobile data traffic will continue this growing trend to reach 77.5 exabytes per month in 2022 [40]. The growing demand of mobile data traffic is not only driven by smartphones usage but also by the rise in Internet-of-Things (IoT) devices. By early 2019, IoT devices accounted for 10 billion connections in the global mobile network whilst smartphones account for 5 billion [69]. With the rise of the 5G network and its wider deployment, this increasing trend is expected to continue and reach an estimated 131 exabytes per month by 2024 [56].

Thus, the growing demand of global mobile data traffic is propelling the need for more capacity. In fact, regulators, industry and the research community are all busy working to address that from various angles. Allocating more spectrum and improving the efficiency (i.e., spectral efficiency) of its use is a well-known way to scale up the capacity of wireless and mobile networks. However spectrum is a limited resource, especially below 6 GHz, where most wireless and mobile systems operate and will continue to do so in the future. In view of these constraints associated with additional spectrum below 6 GHz that could be made available to wireless and mobile services, regulators around the globe have introduced and regulated access to a new type of spectrum that is shared between different industries. The new concept of *shared spectrum* allows opportunistic access to some spectrum bands between different sectors/industries (e.g.,

mobile services and the military in 3.5 GHz band). This shared access concept created a new phenomenon named *fragmented spectrum*, which means the spectrum might not be found available in large chunks. Therefore, in order to boost the capacity, mobile and wireless systems have to leverage several chunks of available spectrum in different bands. This gives rise to the new *multi-connectivity* paradigm. Multi-connectivity is a feature that allows wireless and mobile systems to establish and maintain multiple simultaneous connections across homogeneous or heterogeneous technologies and spectrum bands.

The multi-connectivity paradigm has different forms and has been applied in various use cases. It is first introduced in mobile networks with the Carrier Aggregation (CA) concept in LTE systems. With intra-band/inter-band configurations, the mobile user can leverage up to five contiguous or non-contiguous carriers in order to increase the capacity up to 100 MHz. Another form of multi-connectivity is the LTE-Unlicensed (LTE-U) systems that utilize the unlicensed band 2.4 GHz and 5 GHz used by WiFi systems to increase the capacity in mobile networks [170]. In WiFi systems, Channel Bonding (CB) is another forms of the multi-connectivity paradigm in which multiple adjacent channels can be bonded into a larger channel [100].

1.1 Multi-Connectivity Use Cases in Wireless Systems

In this thesis, we focus on three use cases for the multi-connectivity paradigm, (i) decoupled user association in LTE systems, (ii) TV White Space (TVWS) spectrum aggregation to enable high-capacity backhauling links and (iii) Multi-RAT integration. The main theme of these use cases is boosting the system capacity and enhancing the user experience. Motivated by the benefit of the Dual Connectivity (DC) concept proposed by 3GPP, we study user association problem in LTE uplink/downlink decoupling scenario. With the main objective of enhancing the user experience and efficiently balancing the uplink and downlink system load, we propose a decentralized solution that can achieve near-to-optimal aggregated user throughput while balancing the base station load in uplink and downlink directions. In the second use case, we focus on a different form of multi-connectivity: spectrum aggregation. Aiming at connecting the offline population (i.e., people who live in regions with no Internet access), we highlight the bottleneck in the backhauling network and propose the WhiteHaul system that aggregates the TVWS spectrum in order to enable high capacity wireless backhauling links to bridge the Internet to remote and under-served regions. In the third use

case, we focus on the Multi-RAT architecture, which is one form of multi-connectivity paradigm that allows the mobile user to simultaneously establish and maintain connections to different technologies such as 5G, LTE and Wi-Fi, which in turn increase the system capacity and enhance the user experience. In the Multi-RAT architecture, we study the fundamental question of what is the right approach to realize the Multi-RAT integration. Throughout the coming chapters we will identify the core issues when applying the multi-connectivity paradigm in these different use cases and propose our novel solutions to largely alleviate these issues.

Decoupled Uplink/Downlink in LTE systems. From the first generation of mobile networks, the Uplink (UL) and Downlink (DL) sessions of a mobile user are coupled in a way in which mobile users are only allowed to associate with the same base station (BS) in both directions. However, with the introduction of the Dual Connectivity (DC) concept in LTE Rel.12 [12] and the growing interest in shifting towards the dense Heterogeneous Networks (HetNets) architecture, the efficiency of conventional coupled association is being questioned. The key limitations of the conventional user association can be seen twofold. First, the coupled user association is typically based on maximizing downlink Signal-to-Interference-Ratio (SINR), which means the mobile user associates to the base station with the highest received power. However, that might be inefficient from the uplink perspective. Consider the following example: if a mobile user is located in an overlapping coverage area between a Macro Base Station (MBS) and a Small Base Station (SBS). According to the coupled user association, the mobile user will associate with the MBS because the received power from MBS is higher than the received power from SBS; thus, that maximizes the downlink SINR. As the transmit power of both the MBS and mobile user are different, associating to the same MBS in the uplink direction does not necessarily achieve the optimal uplink SINR. On the contrary, that increases the interference level on the uplink direction because of the high transmit power that the mobile user will use to associate with the further MBS. Second, the differences between the uplink and downlink cell loads make the choice of associating the uplink user to the same downlink-preferred BS inefficient. In light of these limitations, an emerging body of work argues in favor of departing from the convention and instead adopting the more general *downlink/uplink decoupling model for user association* [30, 161, 54] in which a mobile user could be associated with different BSs in the uplink and downlink directions. These efforts quantitatively show gains of such decoupling in dense HetNets in terms of several aspects, including an increased uplink SNR and data rate, and different and better load

balancing in the uplink and downlink. Our first contribution is to address the problem of decoupled UL/DL user association in a HetNet context, given the diverse objectives, preferences and capabilities of the different types of entities involved: the users, the small base stations, and the macro base stations

TVWS Spectrum Aggregation. The Internet undoubtedly is an integral part of people's lives; it is changing the way they think, work and develop. The Internet has been widely acknowledged as a key infrastructure and as the propelling engine for the global economy. The ability of the Internet to foster economic growth has been well-recognized as, according to World Bank estimates, every 10% increase in broadband Internet access translates to a 1-2% rise in gross domestic product (GDP). Mobile networks can be seen as a potential enabler for wider Internet access, especially knowing that the global mobile phone penetration is 104%. Yet, we are quite some distance away from *Universal Internet Access*, as by now half of the world's population does not have access to the Internet. The root of the problem lies in the fact that the majority of the *offline population* lives in rural and low-income regions where mobile operators have little economic incentive to expand their infrastructure to these sparsely populated areas. Apart from mobile networks, all other traditional means (e.g., fiber, satellite) to provide Internet connectivity to these areas are considered to be expensive, limiting the affordability of the service in such areas. This is a twofold problem with a focus on both access and backhaul networks. The key question is how to enable and ease deployments of high-end (4G and beyond) mobile services at low cost by a new set of non-traditional operators (e.g., communities, local small-scale mobile network operators) in areas with market failure and limited availability of mobile services, thereby allowing these areas to have access to the Internet through bottom-up initiatives. Our second contribution is to leverage TVWS spectrum to enable low cost backhauling connectivity [1] to the Internet backbone by designing and implementing an efficient spectrum aggregation technique that allows high capacity backhaul infrastructure.

Multi-RAT Integration: PDCP and Transport Layers Approaches. Recent advances in computing, Artificial Intelligence (AI) and computer vision have enabled new services that are expected to create challenges for next generation networks. These challenges revolve around the diverse service requirements that are expected to evolve in the near future. For example, upcoming services like remote driving, virtual/augmented reality and tele-presence pose stringent requirements on both throughput and per-

[1] Henceforth, throughout this thesis, the terms backhauling and middle-mile are used interchangeably.

packet delivery delay guarantees [90, 150]. Remote driving requires real-time and reliable streaming between the vehicle and the operator while accounting for vehicular speed and network latency to maintain the vehicle at a safe speed. Virtual/augmented reality and tele-presence require very high capacity (e.g., 1Gbps) and continuous real-time feedback to enforce high-precision perception. To support such services, current network systems are required to boost capacity and support ultra low latency services. One approach is to enable multi-connectivity through Multi-RAT systems in which different Radio Access Technologies (RAT) coordinate to efficiently handle these service requirements. There are several forms of the Multi-RAT system including the scenarios where different systems share the same spectrum band such as LTE-U systems or use separate spectrum bands such as the LTE-WiFi Aggregation (LWA) concept. In our third contribution, we study the fundamental question of what is the right approach to realize the Multi-RAT integration by experimentally studying the two dominant approaches, transport layer approach (i.e., focusing on Multi-path TCP) and PDCP layer approach (i.e., focusing on LTE-WiFi Aggregation).

1.2 Thesis Contributions

The goal of this thesis is to address the various challenges that hinder the multi-connectivity paradigm to be leveraged in the aforementioned three use cases in emerging wireless networks. To this end, we examine all three use cases outlined above to identify the crucial roadblocks, and propose novel solutions to tackle these challenges.

1.2.1 Matching Theory based Decoupled User Association Mechanism

We focus on the user association problem in HetNets with uplink/downlink decoupling as one use case of multi-connectivity. The user association problem in HetNets is considered more challenging due to the conflicting objectives of different entities in the system, and applying classical user association schemes results in load imbalances and inefficient operation. Moving to the decoupled uplink/downlink setting, the problem of user association gets even more challenging because in addition to reconciling competing objectives from different angles (uplink, downlink, macro BSs, small-cell BSs), both uplink and downlink association should be *jointly* tackled, and cost associated with decoupling needs to be taken into account. Very little work exists on the de-

sign of user association mechanisms suitable for the decoupled context [55, 155, 152] and these works fail to capture the inter-dependent nature of uplink/downlink associations and the impact of decoupling related cost, with the latter being dependent on the bandwidth of the backhaul link connecting the two BSs involved in a decoupled user association.

To address the decoupled uplink/downlink user association problem in HetNets, we propose a novel mechanism based on matching theory and stochastic geometry. Matching theory is particularly proven to accommodate the heterogeneity of system entities and their objectives to obtain stable and optimal algorithms that can be implemented in a distributed (self-organizing) manner. Specifically we formulate the decoupled uplink/downlink user association problem as a *matching with contracts* game. We draw an analogy between the user association problem in the decoupled context with the doctor-hospital matching problem that exemplifies a matching with contracts game. In the doctor-hospital matching problem [76], there is a set of hospitals which seek to hire doctors by handing them contracts that respect the ranked preferences of hospitals and doctors. To map this problem to our setting, BSs play the role of hospitals and the User Equipments (UEs) are the doctors, and there can be two types of contracts between the two sets: UL and DL association. We show the effectiveness of our proposed mechanism based on the matching with contracts approach via simulations in comparison with a traditional coupled user association approach, a conventional (one-to-many) matching based decoupled user association mechanism proposed in [155] and another recently proposed uplink-oriented user association mechanism for decoupled context from [55]. The gains from our mechanism stem from its holistic nature, accounting for the additional cost incurred by decoupling while choosing the specific BSs to associate in the uplink and downlink directions. Our solution is also shown to result in performance that is close to a centralized and computationally expensive optimal solution representing the approach taken in [152]. It is also important to note that this is the first work that proposes using the matching with contracts game in the wireless communication context. The contributions of this work can be summarized as follows:

- Using tools from matching theory, we formulate the decoupled uplink/downlink user association problem as a *matching with contracts* game.

- We use stochastic geometry to derive a closed-form expression for matching utility function in both uplink and downlink directions. In addition, we formulate

the decoupled user association problem as an optimization problem to benchmark our solution.

- We model the decoupling cost as a function of backhaul links between base stations to tackle the inter-dependent nature of uplink/downlink association in decoupling scenario. This highlights the advantages of our approach which jointly optimizes both uplink and downlink association in order to maximize the overall mean rate for the UE.

- Via simulation results, we show the superiority of our solution over the existing works in literature and the feasibility of the proposed solution in both fast and slow fading environments.

1.2.2 Aggregated TVWS Spectrum for Backhaul in Rural and Developing Regions

TV White Space (TVWS) spectrum has the potential to be a significantly lower cost alternative for backhauling connectivity in rural areas. TV white spaces at any given location and time refer to the portions of spectrum in the Ultra High Frequency (UHF) TV bands (e.g., 470 - 790 MHz in the UK) which are not used by TV transmitters and wireless microphone users (the primary users of this spectrum). TVWS spectrum is attractive for rural and backhauling connectivity for two reasons. First, it has superior propagation characteristics compared to other higher frequency bands in terms of range and non-line-of-sight (NLOS) propagation in the presence of foliage and obstructions. For example, measurement studies confirm that it is possible to get four times greater range with TVWS spectrum compared to 2.4GHz unlicensed spectrum used by WiFi(i.e., using the same transmission power, 4W EIRP) [37]. This means lesser amount of infrastructure (fewer base stations) for connectivity over a given distance with TVWS spectrum and corresponding reduction in deployment costs. Second, there is a large amount of TVWS spectrum likely available in rural areas (in the region of 200+ MHz) with fewer TV transmitters and rare wireless microphone use. In developing countries, almost all of the UHF band is available as white space due to the non-existence or limited presence of over-the-air TV. This aspect is also beneficial for backhauling connectivity as it allows high bandwidth connections like the other expensive alternatives (e.g., fiber).

The problem of providing high-capacity backhauling links for rural areas can be

seen from three perspectives. First, we need to understand/quantify the usage of mobile services in rural and remote areas, which will give better insight into the required capacity of the backhauling link. Second, identifying the key characteristics of TVWS spectrum (i.e., focusing on rural areas), in terms of the amount and nature of spectrum, the operation constraints (e.g., transmit power) and the channel quality, is essential in order to understand the major system requirements of the backhauling links. Third, leveraging all these insights in order to design and implement an efficient backhauling system that fully utilizes the available resources of TVWS spectrum.

We start this work by studying the nature of mobile traffic usage in rural areas to identify the average capacity that the backhauling link should provide for these areas. The lack of any commercial mobile network in rural Scotland has motivated us to propose a do-it-yourself (DIY) model for deploying mobile networks in under-served regions, aiming at provisioning high-end (4G and beyond) mobile services. Our proposed model is in tune with the increasing openness (in terms of ecosystem with IT/cloud vendors and verticals, platforms, spectrum types, services, etc.) and cloud-ification of mobile networks in the run up to 5G. We demonstrated the feasibility of our proposed deployment model in practice, doing a trial deployment of a particular instance of this model in Balquhidder, a small village in rural Scotland with a cohesive and vibrant community of 200 households and supporting more than 95 diverse businesses. Due to the poor broadband and mobile infrastructure in this area, an initiative driven by the community is in process to bring fiber connectivity to a majority of the properties. However, about 15% of them would be too expensive to reach through the community fiber roll-out initiative, so we targeted those households through this trial deployment in a partnership involving The University of Edinburgh, the Balquhidder community, Microsoft Research (Cambridge) and WhitespaceUK[2]. As a backhauling link for our DIY model, we leveraged a commercial TVWS solution from Adaptrum that provided a backhauling link of 1.6KM using one TV channel of 8 MHz. We conducted a measurement campaign which concluded that the backhauling link is the crucial part of the end-to-end connectivity to bridge local access networks with the wider Internet, and also dictates their effective capacity and reliability. In addition, it motivates the need for a high-capacity backhauling solution that is vital to enable high-end mobile services in rural areas.

From our experience in the Balquhidder deployment, we understand that the narrow TV channels (i.e., 6 or 8 MHz) are the limiting factor in allowing a high-capacity

[2] https://www.whitespaceuk.com/

backhauling solution for 4G/5G services in rural areas. Therefore, aggregating multiple TV channels is essential in order to achieve the high-capacity link. Towards that objective, we analytically studied the nature of TVWS spectrum in a representative rural region in the UK. Unlike the several previous studies on TVWS spectrum availability (e.g., [81]), we focus on the *quality* of the available TVWS spectrum to be able to enable backhauling links by accounting for not only the topography of the region but also the aggregate interference from nearby TV transmitters and relays. To this end, we introduce a novel TVWS receiver-oriented notion of *usable* TVWS spectrum that differs from the commonly used TVWS transmitter side perspective on spectrum availability. Our analysis shows that aggregate interference from nearby TV transmitters can in fact have a significant negative impact on the usable TVWS spectrum for establishing backhauling links. Our analysis also sheds light on the nature of TVWS spectrum fragmentation for this use case, and this in turn poses requirements for the design of spectrum aggregation systems for TVWS backhauling link.

As a result of these two studies, we identified the system requirements for TVWS backhauling solution as follows:

- First, TVWS spectrum is fragmented and that requires the proposed system to leverage multiple wireless interfaces to be able to fully utilize the available spectrum and to increase the capacity of the backhauling link. However, unlike the previous Multi-Radio works in literature, the radios in this context are constrained to share a single antenna. The system should be able to allow these multiple interfaces to share a single antenna without causing any harmful interference to each other.

- Second, TVWS spectrum varies significantly in terms of transmit power, channel conditions and the size of available chunks. The system should be able to evaluate all the available choices and choose the right combination that maximizes its performance.

- Third, the traffic volumes in backhaul networks are asymmetric, yet dynamic. In addition, different than the other WiFi backhauling solution, the transmit power between both ends of the link are different. Therefore, the system should be able to provide a traffic distribution mechanism that dynamically allocates the time resources between both ends of the link.

Addressing these requirements, we designed and implemented the WhiteHaul system,

which is, to the best of our knowledge, the first flexible and efficient backhauling system capable of aggregating a large number of spectrum chunks in TVWS spectrum. The contributions of this work can be summarized as follows:

- We analytically studied the quality of the TVWS spectrum by using a new and more reliable receiver-oriented notion of usable TVWS spectrum. Our study shows that TVWS spectrum is fragmented even in rural areas and cost-effective solution for intra-band spectrum aggregation is essential.

- Designed and implemented, WhiteHaul , a flexible and efficient system for high capacity backhaul over TVWS that addresses all the system requirements which we identify in the previous studies.

- Designed and implemented MPTCP congestion control that is tailored to enable efficient operation of MPTCP over the hardware architecture of the WhiteHaul system.

- Thoroughly evaluated the performance of the WhiteHaul system to quantify the aggregate backhaul link throughput it can achieve in various network settings (e.g., number and width of TVWS spectrum chunks) and link conditions. In particular, we show that WhiteHaul can aggregate almost the whole of TV band with 3 interfaces and achieve nearly 600Mbps TCP throughput.

1.2.3 Assessing the Protocol Layer to Integrate Multiple RATs

Multi-RAT integration has attracted a lot of attention from industry and the research community since the early work of LTE traffic offloading on WiFi [77, 72, 38, 141]. Different than these efforts, the focus of this work is to identify the right protocol layer to realize the Multi-RAT integration. considering not only LTE and WiFi integration but also other different technologies, including 5G New Radio (NR) and the IEEE 802.11ad which operates in Millimeter Wave (mmWave) bands. Towards that objective, we considered two dominant approaches in Multi-RAT integration: the transport layer approach represented by Multipath TCP (MPTCP), and the Packet Data Convergence Protocol (PDCP) layer approach, represented by the LTE-WiFi Aggregation (LWA). The Multi-RAT integration is a non-trivial task because it aims at enabling a seamless simultaneous operation of various technologies with different protocol stacks. We considered both MPTCP and LWA to be the most feasible integration approaches

due to the very fact that the lower layers of the protocol stack are more technology-specific where each RAT has its own standards; for example, the physical (PHY) layer in LTE and WiFi have different frame structure, modulation and channel coding, and the representation of the PHY resources are different. Hence, trying to realize the Multi-RAT integration at the lower layers of the protocol stack is considered to be infeasible due to the high complexity and lower performance gain compared to other higher protocol layers. The contributions of this work can be summarized as follows:

- Provide a quantitative comparison between MPTCP and LWA integration approaches in different scenarios and channel conditions.

- Propose a rate-based scheduler at the PDCP layer that leverages a feedback mechanism to estimate the different interfaces rate and distribute the traffic between different RATs in order to maximize the user throughput and increase the system capacity.

1.3 Thesis Organization

The reminder of this thesis is organized as follows:

Chapter 2 provides a detailed description of the background of the current and future status of the spectrum below 6 GHz used by the wireless and mobile industry. We examine the amount and nature of future spectrum below 6 GHz. We also highlight that, unlike the currently allocated spectrum, most of the new spectrum (close to 80%) would be shared spectrum and would be accessed via either licensed shared access (LSA) or opportunistic spectrum access (OSA) models. Parts of this chapter have been published in the IEEE International Symposium on Dynamic Spectrum Access Networks (DySPAN 2015) [92].

Chapter 3 provides an overview of the related literature and the evolution of research for the three multi-connectivity use cases. In this chapter, we also discuss the limitations and shortcomings of the previous works, that necessitated the need for our novel solutions.

Chapter 4 presents our mechanism to address the decoupled user association problem in the HetNets environment. This work has been published in the 12th ACM Symposium on QoS and Security for Wireless and Mobile Networks (Q2SWinet 2016) [91].

Chapter 5 presents our DIY network deployment model and the trial deployment that we did in the Balquhidder area. This chapter motivates the need for high-capacity low-cost backhauling solution. This work has been published in the 1st ACM SIGCAS Conference on Computing and Sustainable Societies (COMPASS 2018) [94].

Chapter 6 presents our analytical study on the nature of TVWS spectrum in rural areas. This work has been published in the 10th International Conference on Communication Systems Networks (COMSNETS 2018) [93].

Chapter 7 presents our WhiteHaul system for enabling a flexible and efficient low-cost high-capacity backhauling link over TVWS for rural and remote areas. The work presented in this chapter is accepted and will appear in the 18th ACM International Conference on Mobile Systems, Applications, and Services, MobiSys 2020.

Chapter 8 presents our experimental study on examining the performance of different Multi-RAT integration approaches. The work presented in this chapter is under submission.

Finally, **Chapter 9** presents our concluding remarks and summarizes the work presented in this thesis. In this chapter we also discuss some limitations of the presented work and future research directions.

Chapter 2

Outlook for Future Wireless Spectrum below 6GHz

This chapter provides a detailed description of the current and the future state of the spectrum below 6 GHz where most mobile and wireless systems currently operate. We present the UK perspective on the future wireless spectrum below 6 GHz, including plans and strategy of Ofcom (the UK telecommunications regulator) to make more spectrum available for wireless and mobile services. We first start with highlighting how the need for more capacity (especially indoors) is the major drivers that are expected to influence spectrum regulation in the coming future. We then examine the amount and nature of future spectrum below 6 GHz. We find that, unlike currently allocated spectrum, most of the new spectrum (close to 80%) would be shared spectrum and it will be accessed via either licensed shared access (LSA) or opportunistic spectrum access (OSA) models. We finalize with the different spectrum access techniques that is expected to evolve in the near future to deal with shared spectrum bands.

2.1 Capacity Scaling Challenge for Wireless Networks

Scaling capacity is the need of the hour for wireless broadband industry. The growing demand for wireless and mobile services is fuelling the need for more capacity. The latest Ofcom Communications Market Report [131] indicates that smartphone and tablet ownership in the UK has already reached 66% and 54% of adults, respectively. Furthermore, the growth of machine-to-machine (M2M) communication and Internet of Things (IoT) paradigm will keep this increasing trend in the coming years.

Traffic offloading is one current solution to handle the increasing trend in wireless

Table 2.1: UK Government 500 MHz Target [45]

Band	Lead Department	Expected Release	Quantum (MHz)
Release Completed			
VHF and L-Band	Emergency Services	2012	13 MHz
870-872 MHz and 915-917 MHz	MoD	H1_2013	4 MHz
2025 - 2070 MHz	MoD	H2_2013	45 MHz (shared)
Total released to date:		**62 MHz**	
Upcoming Releases			
2.3 - 2.4 GHz	MoD	2015	40 MHz
3.4 - 3.6 GHz	MoD	2015	190 MHz
4.8 - 4.9 GHz	MoD	2015	55 MHz (shared)
1427 - 1452 MHz	MoD	2015	20 MHz (shared)
Total upcoming releases:		**305 MHz**	
Longer term releases			
2.7 - 2.9 GHz	DfT	2016 - 2020	100 MHz
Other	Various	2014 - 2020	Up to 35 MHz
Total longer time releases:		**135 MHz**	
Total targeted releases by 2020:		**500 MHz**	

services demands. Mobile data traffic can be offloaded via WiFi which is considered a cost-efficient approach as it uses the freely accessible 2.4 and 5 GHz bands. Also, traffic offloading can be through femtocells which are quickly deployed base stations that has a potential advantage over the deployment of macrocells that take much longer time due to purchase of radio infrastructure and backhaul. Moreover, starting from year 2010 around 80% of the generated data traffic comes from indoor environment [68]. Both WiFi and femtocell offloading solutions are promising due to the fact that most of the data usage occurs indoors which make these indoor deployed technologies useful to offload the data traffic. A complete study on data traffic offloading via WiFi or femtocells can be found in [20, 51, 105].

2.1.1 Spectrum for Mobile Networks

Despite the use of approaches like traffic offloading, it will become necessary to free up more spectrum at some point in the future to address the capacity scaling problem. Towards this end, WRC-15 discussed adding additional allocations for mobile broadband services and whether to allocate additional spectrum which could be used for WiFi around 5 GHz. Within the UK, Ofcom is in the process of releasing up to 500

MHz public sector spectrum below 5 GHz by 2020 as per the the government target set in 2010 [45].

As shown in Table 2.1, the UK Ministry of Defence (MoD) planned to release 40 MHz of spectrum within 2.3 GHz band (2350 – 2390 MHz). The harmonization process for the 2.3 GHz band over Europe is currently ongoing. In March 2015, Working Group on Frequency Management (WGFM), a part of Electrical Communication Committee (ECC), submitted a final report of technical conditions for using 2.3 GHz band in high power 4G LTE networks while ensuring the protection for currently used systems. According to the 3GPP standard, only unpaired band plan is considered in 2.3 GHz band (2300 – 2400 MHz) which make it suitable only for LTE-TDD. Currently, the UK mobile operators are focusing on LTE-FDD technology and only one operator (UK Broadband) runs a LTE-TDD network currently in bands 42 and 43. Although Vodafone and BT were awarded unpaired (LTE-TDD) spectrum in 2.6 GHz in the 2013 4G auction, they are yet to use that spectrum. The advantage of using 2.3 GHz for LTE and beyond mobile networks is that the propagation characteristics of 2.3 GHz band are very similar to the 2.6 GHz band that is already used for 4G networks in the Asian market. Moreover, as of October 2014, there are 207 LTE-enabled user devices (smartphones, tablets, etc.) supporting the 2.3GHz band [128].

However, using the 2.3 GHz band for high power mobile networks can lead to potential interference with the adjacent 2.4 GHz band used by WiFi, Bluetooth and ZigBee devices. Although there will be 10 MHz separation between the new 2.3 GHz mobile band and 2.4 GHz WiFi band that will provide some protection, the licence-exempt devices are not designed to deal with or take into account the high power users in the adjacent band. In [128], Ofcom concluded that there is no need for any intervention to protect WiFi devices from potential interference arising due to 2.3 GHz band mobile operation. Instead, very simple migration activities such as moving the WiFi routers away from windows, using 5 GHz band instead of 2.4 GHz band especially for WiFi routers, using improved filters in the routers will be developed as part of the natural evolution of the market over the next few years and would solve any light interference between the two adjacent bands.

In addition to 2.3 GHz band, MoD plans to release 150 MHz of spectrum within 3.4 GHz band (3410 – 3480 MHz and 3500 – 3580 MHz). 3.4 GHz band has inferior propagation characteristics than 2.3 GHz band. Nevertheless, mobile services (4G and beyond) are the potential use of this band and it could alleviate the spectrum crunch/capacity problem, especially for small cells. ECC decision (11)06 provides

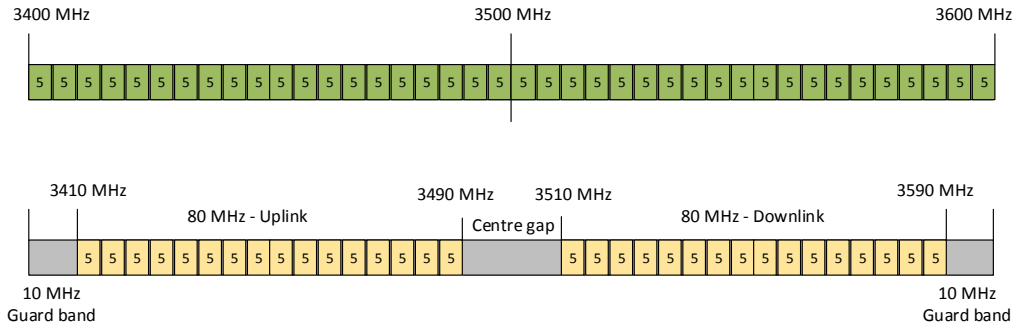

Figure 2.1: Unpaired (at top) and paired (at bottom) band plans for 3.4 GHz.

two harmonized band plans in 3.4 GHz. Fig. 2.1 demonstrates the proposed unpaired and paired band plans for 3.4 - 3.6 GHz band. With the paired band plan, there is a need to separate the band into two frequency blocks with a guard band in between. In addition, we need two 10 MHz block at the start and the end of the band to avoid interference with adjacent bands. Due to the inefficient use of 3.4 GHz band under paired band option (30 MHz unused spectrum) and due to the preferences of industrial and national organizations for unpaired band, ECC decided in its 36th meeting, March 2014, to allow TDD or unpaired option to be the preferred mode of operation in the 3.4 – 3.6 GHz band, whilst allowing FDD as an alternative. Ofcom believes that the unpaired band plan is best suited for realizing the most benefits from this 3.4 GHz spectrum. UK/Ofcom have another problem to solve to free up the 3.4 GHz band. UK Broadband (a mobile/wireless operator in the UK) is currently allocated two separate 20 MHz blocks in this band: 3480-3500 MHz and 3580-3600 MHz. Ofcom needs to relocate the UK broadband blocks to allow larger contiguous assignments which, in turn, give operators the flexibility to deploy larger channel sizes and to reduce the technical constraints due to the lower number of spectrum boundaries between licensees. In fact, the 3.4 GHz band is considered promising for capacity scaling especially indoors. The 3.4 GHz not only has a higher bandwidth than 2.3 GHz band but also the higher propagation loss makes it suitable for small coverage (e.g., femtocells). This small coverage capability helps in the interference management in dense cellular deployment or to avoid the potential interference with the adjacent band where maritime and aeronautical radars operate.

Ofcom plans to make the 2.3 and 3.4 GHz bands accessible for mobile services operator on a licensing basis. To realize this plan, Ofcom decided to migrate the amateurs out of 2350 – 2390 MHz band because of the harmful interference caused by them to

Table 2.2: Proposed Changes for 2.3 and 3.4 GHz bands

Band	Affected Industry	Proposed changes
2.3 GHz	2.4 GHz Wi-Fi band	Light interference expected and the natural evolution of the market over the next few years will solve it
	Amateur services	Migrate from 2.3 GHz band and will migrate from adjacent band if they cause interference to users in 2.3 GHz or adjacent bands
3.4 GHz	PMSE	Work only in specific area where new services have not been rolled out yet.
	Radar in 2.7 – 3.1 GHz band	Limit the power flux density (pfd) per MHz to $+5dBm/m^2$ across the band

the new users [125]. However, the amateurs can continue using adjacent bands (2310 – 2350 MHz and 2390 – 2400 MHz) but with required clarification of the notice period needed by amateur use to cease if amateurs cause interference to other users in the newly released band or the adjacent bands [128]. Amateur radio is hobby and a service that uses some radio frequencies (e.g., 2.3GHz) to communicate with other amateur radios for non-commercial purposes such as self-training or volunteering emergency services.

In addition to amateurs, the release of 2.3 and 3.4 GHz bands will reduce the number of PMSE channels to 19 channels (in 2 – 4 GHz range) from the previous 33 channels. Moreover, nine of these channels are currently exclusively assigned to news broadcasters. The remaining 10 channels will be sufficient for 98% of events. However, there are some migration actions needed to support the other events which require more than these 10 available channels such as allocate more spectrum for PMSE uses in other bands (e.g., 7 GHz band) or re-use news channels as appropriate. Due to the fact that the migration to 7 GHz band may take some time to implement, Ofcom is studying the possibility of allowing on-going PMSE access to the new licensed band (2.3 GHz and 3.4 GHz) in specific areas where the new services have not been rolled out yet.

The use of 3.4 GHz band for 4G (high power) networks will raise concern regarding the radar performance in 2.7 – 3.1 GHz band. Due to the lack of selectivity within these radars (s-band), an inter-modulation interference will affect its operation. A similar concern arised earlier when 2.6 GHz band was allocated to 4G networks. Ofcom suggests limiting the power flux density (pfd) per MHz to $+5dBm/m^2$ across the 3.4 GHz band, the same as with the case of 2.6 GHz band. This limit will alleviate the risk of multiple bands illuminating the radar, especially the case of 2.6 GHz and 3.4 GHz bands being simultaneously within the radar beam-width [128].

Table 2.2 summarizes the changes needed to support the operation of mobile networks in 2.3 and 3.4 GHz bands.

2.1.2 WiFi Spectrum

WiFi is the dominant carrier of wireless data traffic. A report commissioned by the European Commission showed that over 71% of all wireless data traffic that delivered to smartphones and tablets was delivered through WiFi. In 2013, Ofcom identified that the 2.4 GHz band is much more heavily used than 5 GHz band; on average occupancy of the 2.4 GHz band is approximately ten times that of the 5 GHz band [127]. Although the current use of the 5 GHz band is relatively low, another study [130] commissioned by Ofcom found that the current spectrum allocation for WiFi at 2.4 and 5 GHz is likely to be under pressure by 2022 and the additional spectrum will be required to support the expected demand. Moreover, by 2019 the amount of traffic offloaded from smartphones and tablets will be 54% and 70 %, respectively [40].

A proposal to increase the amount of spectrum allocated to WiFi at 5 GHz band is being discussed in the preparation of WRC-15 under agenda item 1.1. The proposal explores the possibility of making 5350 – 5470 and 5725 – 5925 bands available. Moreover, CEPT is currently working to identify harmonized compatibility and sharing conditions for a shared use of these two bands for wireless access systems [35]. This proposal will create a contiguous 775 MHz block of spectrum for WiFi between 5150 and 5925 MHz. Moreover, the removal of the current gap in the 5GHz WiFi bands would increase the number of wider bandwidth channels (e.g., 80 and 160 MHz) which can be exploited by the latest 802.11ac standard higher data rates.

2.2 Spectrum Access Models and the Nature of Future Spectrum

In this section, we focus on analyzing the amount and nature of future spectrum below 6 GHz. It would however be helpful to first give an overview of various spectrum access models. Traditionally, the spectrum use for mobile/wireless communications was authorized in only two ways: (i) licensed and (ii) unlicensed (or licence-exempt). With licensed authorization, a spectrum band (or pair of bands) is allocated to an operator for their exclusive use, typically via an auctioning process (e.g., UK 4G auction held in February 2013 covering 800MHz and 2.6 GHz mobile spectrum). On the other hand, unlicensed spectrum bands allow devices to use those bands without the need for license but they are obliged to abide by certain technical requirements or spectrum etiquette rules (e.g., power limits, restrictions on usage to indoors). The 2.4 GHz band

used by WiFi, Bluetooth, ZigBee and other low power devices is the famous example of unlicensed spectrum access model. The exclusive use nature of licensed spectrum offers better control over the interference environment than the open access unlicensed spectrum and thus more likely able to provide quality of service (QoS) guarantees.

Making a spectrum band accessible via either licensed or unlicensed models first requires clearing that band from incumbent use. Below 6 GHz, it is becoming increasingly harder to be able to clear bands as they are held by incumbents unconnected with mobile/wireless communication that have strategic or operational reasons to continue doing so (e.g., military, radars, satellite earth stations). This necessitates sharing that ensures incumbent protection as the only viable approach to make such bands accessible for mobile services. Although there are several sharing based spectrum access models proposed in the recent past (e.g., pluralistic licensing), the two main ones that are gaining traction in practice are Opportunistic Spectrum Access (OSA) and Licensed Shared Access (LSA), which are briefly described next.

2.2.1 Opportunistic Spectrum Access (OSA)

The essential idea behind the OSA model is as follows. In a band licensed to *Primary Users (PUs) (also called incumbents)*, *Secondary Users (SUs)* are allowed to opportunistically exploit temporal/spatial spectrum holes (or white spaces) in that band in such a way that the PU operations are protected from SU induced interference. Examples of the OSA model in practice are 5 GHz WiFi spectrum [87] and TVWS spectrum [63]; in the former case, the PUs are radars, satellites etc. whereas digital terrestrial TV (DTT) transmitters/receivers and Programme Making and Special Events (PMSE) microphone devices are the PUs in the latter case. The OSA model can be viewed as the unlicensed model with the addition of PU protection requirement. As such, there can be any number of SUs attempting to use the OSA band at a given time and location, which makes PU protection a non-trivial task. In the next section, we will give an overview of different spectrum access techniques that can be used for PU protection. This concept is adapted globally by different regulators such as FCC and Ofcom.

TVWS spectrum is a well-known example of OSA spectrum access. The UHF TV band (470-790MHz, in the UK) is allocated to the Digital Terrestrial Television (DTT) broadcasting; however, the majority of the UHF TV is unused by the DTT broadcasting. The main reason behind that is because the DTT transmitters use very high trans-

mission power (e.g., kW), and to avoid interference when using the same TV channels, the geographical separation is essential. Thus, that creates gaps where some TV channels are unused within some locations. These unused TV channels defined as white spaces. Led by FCC, the TV UHF band is opened for opportunistic access in order to utilize these unused spectrum resources. That decision faced resistance by the TV broadcasters who were worried about their service quality when sharing the spectrum with other users. However, the FCC (and Ofcom later) worked closely with different industrial partners to identify the system requirements that the secondary users should follow in order to not cause any harmful interference to the DTT broadcasting services.

2.2.2 Licensed Shared Access (LSA)

The LSA model [113] aims to enable secondary access in a band licensed to a PU in a way that resembles the licensed model for the SU. Essentially the idea is for the SUs to sub-license a portion of the PU owned spectrum band in the frequency, space and time dimensions; as such, SUs in the LSA model are referred to as LSA licensees. In the LSA model, an entity called LSA repository continually keeps track of the amount of spectrum available at each time instant and location, and acts as the intermediary responsible for dynamically generating the licenses to LSA licensees. The 3.6 – 4.2 GHz band is an example of a band that could be made available via the LSA model in the future; PUs in this band are satellite earth stations and fixed terrestrial wireless links. The LSA model is attractive for mobile network operators (MNOs) to acquire additional spectrum without risking the ability to provide QoS guarantees because LSA licensees obtain a time-limited *license* on the fly to a slice of incumbent's spectrum band in frequency and space. Limited number of SUs (LSA licensees) in the LSA model eases the task of ensuring PU protection compared to the OSA model.

eLSA is the evolved version of the LSA spectrum access model that focuses on allowing vertical operators (e.g., automotive, industry, and entertainment) to have access to a shared spectrum in order to provide high-quality local services. The European Telecommunications Standards Institute Reconfigurable Radio Systems (ETSI RRS) technical committee has published two technical documents [59, 57] to describe the system requirements of the eLSA model and the enhancement over the LSA model. As the number of licensees is expected to increase (as we move toward the shared spectrum concept), therefore, the eLSA model should be able to enable a secure coexistence between the incumbents (i.e., the primary users) and the large number of

licensees.

One of the key characteristics of both eLSA and LSA models is that the spectrum sharing will be restricted within a geographical area where the eLSA licensees will have the right to access certain frequency bands within predefined area/region. Hence, that motivates the need to introduce a new concept in the eLSA model, which is the allowance zone concept. The allowance zone is a geographical area in which the eLSA licensees are allowed to operate with a certain frequency range. The allowance zone is not only be defined by a geographical but also by measurement thresholds such as maximum allowed signal strength and maximum field strength level (i.e., dB V/m/MHz) and time period.

2.2.3 Amount and Nature of Future Spectrum Below 6 GHz

Now we look into the key question of how much new spectrum below 6 GHz is expected to become available in the coming future and the distribution of that spectrum between the different types of access models described above (licensed, unlicensed, OSA, LSA). We compiled this date primarily from Ofcom's various spectrum related publications, including its 2014 spectrum management strategy statement [129]. Resulting data is summarized in Table 2.3 and Fig. 2.2. For comparison, currently allocated spectrum for mobile/wireless services in the UK obtained via Ofcom's UK Spectrum Map[1] is shown in Fig. 2.2.

We briefly elaborate on how we obtain the figure for TVWS. In [117], the authors stated that on average there is 150 MHz TVWS spectrum available spectrum in the UK. But this figure includes the 700 MHz band which Ofcom has recently decided to allocate to mobile operators on a licensing basis by 2022. So we proportionately reduced the available TVWS spectrum to reflect the reduced TVWS frequency range after discounting 700 MHz band, which gives us 80 MHz.

Regarding 3.6 – 4.2 GHz band, currently this band has permanent satellite earth stations and terrestrial fixed links as primary users and UK Broadband (an operator in the UK) as the secondary user. The UK broadband is allocated two blocks of spectrum, 84 MHz each (3605 – 3689 MHz and 3925 – 4009 MHz), shared on a geographic basis with the primary users. In our estimates of new spectrum, we assume that in the best case the whole 600 MHz in this band (3.6 – 4.2 GHz) will be available via the LSA model for mobile and wireless services. But it is worth noting that there are obstacles

[1] http://www.ofcom.org.uk/static/spectrum/map.html

Table 2.3: Distribution of New Spectrum Below 6 GHz

Frequency Range	Amount (MHz)	Notes	Spectrum Access Model
694 - 790 MHz	286 MHz	MNOs	Licensed
2350 - 2390 MHz			
3410 - 3480 MHz			
3500 - 3580 MHz			
863 - 876 MHz	20 MHz	SRDs (M2M)	Unlicensed
915 - 921 MHz			
470 - 682 MHz	80 MHz	TVWS	OSA
5350 - 5470 MHz	320 MHz	5 GHz Wi-Fi	
5725 - 5925 MHz			
1427 - 1452 MHz	25 MHz	PUs: Military & Satellite	LSA
4.8 - 4.9 GHz	55 MHz		
3.6 - 4.2 GHz	600 MHz		

to be overcome before this can happen. Chief among them is migrating satellite earth stations to a different set of frequencies, which can prove to be expensive.

From Fig. 2.2 , it is clear that most of the new spectrum will be shared (either LSA or OSA). To appreciate the changing nature of spectrum, in Fig. 2.3 , we show the pie charts for current and new spectrum showing the distribution by access model. We see that 58.3% of the current spectrum is licensed and 9.3% is available for unlicensed use (primarily in the 2.4 GHz band). The remaining 32.4% of the currently allocated spectrum is the 5 GHz WiFi spectrum that follows the OSA model as that band has various radars as primary users and radar protection is mandatory through the spectrum sensing based dynamic frequency selection (DFS) mechanism [87]. Looking at the breakdown for new spectrum, almost half of it is LSA type spectrum and close to 80% is shared (LSA or OSA). Thus as we go into the future, there is a remarkable shift in the nature of spectrum. Note that in this analysis we have not considered 2 GHz mobile satellite service spectrum and 2.7-2.9 GHz spectrum used by aeronautical radars. Even considering those bands, we expect our general conclusion that shared spectrum will be the norm in the future to still hold.

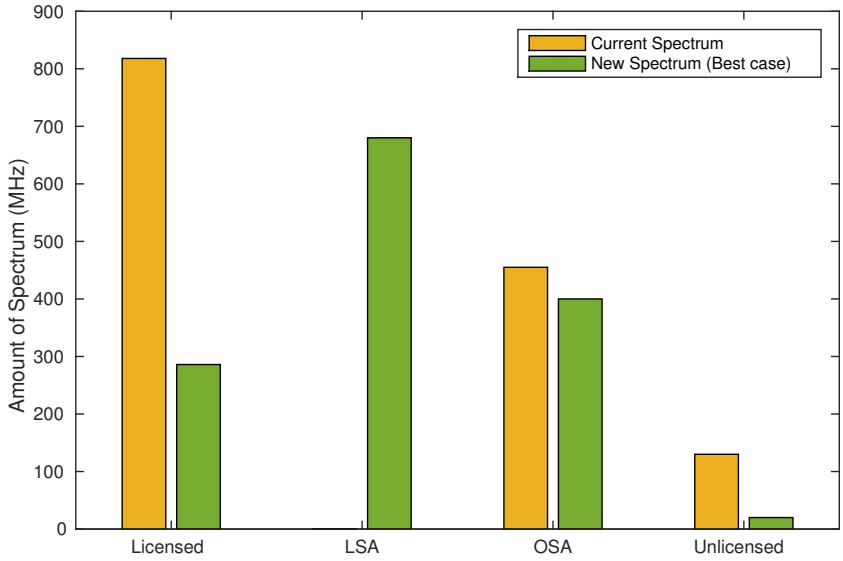

Figure 2.2: Amount of future spectrum below 6 GHz in comparison with currently allocated mobile and wireless spectrum.

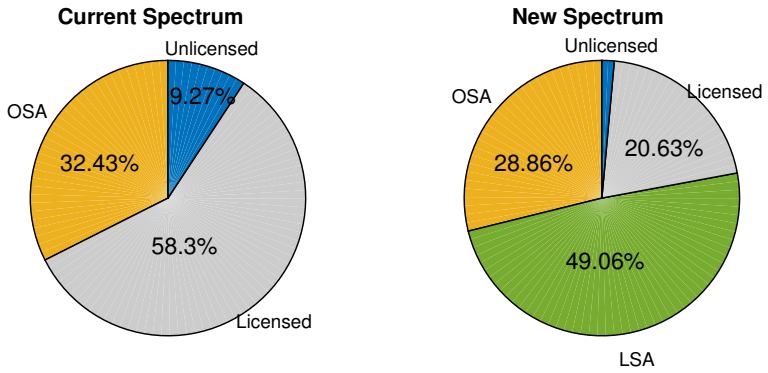

Figure 2.3: Nature of future spectrum below 6 GHz in comparison with currently allocated mobile and wireless spectrum.

2.3 Spectrum Access Techniques

In this section, we give an overview of different spectrum access techniques that could be used for accessing shared spectrum.

2.3.1 Spectrum Sensing

Spectrum sensing is an old and commonly used spectrum access technique to detect the presence of primary user (PU) or equivalently to determine a spectrum white space. The radar detection feature underlying the DFS mechanism in 5 GHz WiFi systems [87] is an example of spectrum sensing use in practice.

2.3.1.1 Local Spectrum Sensing

In this basic form of spectrum sensing, each secondary user (SU) senses the spectrum locally and independently using one of the following methods: *(i) Energy Detection*; *(ii) Waveform Sensing*; *(iii) Feature Detection*; and *(iv) Matched Filtering*. Energy detection is the most common method employed for spectrum sensing because of its low complexity. But it has poor performance since it cannot differentiate between primary user signal and the interference and noise. The other methods overcome some of these limitations, the detailed discussion on different types of local spectrum sensing can be found in [169].

There are some issues that should be taken into consideration when designing spectrum sensing algorithms such as *Hidden terminal problem, PU Diversity* and *Sensing Efficiency and Sensitivity*. Due to severe multipath fading and shadowing problem, local spectrum sensing techniques suffer from hidden terminal problem in which the primary user could not be detected due to its location. In addition, different type of primary users could exist in shared spectrum and hence new local sensing techniques should handle PU diversity. Due to the dynamic characteristics of future shared spectrum, both sensing time and threshold should set appropriately in order tackle the trade-off between the complexity and the efficiency and sensitivity of sensing techniques.

2.3.1.2 Cooperative Spectrum Sensing

The shortcomings of local spectrum sensing can be overcome by sharing sensing information between multiple sensors to enhance the ability of SUs to detect and exploit spectrum holes. This mechanism is called cooperative spectrum sensing. The common control channel (CCC) is used by SUs to report and share their sensing data. Therefore based on the bandwidth of CCC, SUs report different forms and sizes of sensing data. The sensing data can be combined in three different ways: *(i) soft combining*, *(ii) quantized soft combining*, *(iii) hard combining* and the detailed discussion on these methods can be found in [21]

There are some issues that should be taken into consideration when designing cooperative sensing algorithms such as *Spatial diversity* and *Exposed node problem*. Although spatial diversity in cooperative sensing increases its gain especially in the cases like hidden terminal problem but also more spatially correlated SUs participating in cooperative sensing can be detrimental to the detection performance [21]. Moreover, in high mobility scenario, the spatial diversity between the captured measurements can degrade the performance of cooperative sensing techniques. The exposed node problem leads to inefficient utilization of spectrum which occurs when SUs on the boundaries of PUs' exclusive zone share their information with SUs outside the exclusive zone. Therefore, the SUs which are outside the exclusive zone will have inaccurate information about channel occupation. In general, spectrum sensing mechanism introduces overhead especially in case of cooperative sensing which have a significant overhead on common control channel. Therefore, a more cost-efficient access techniques is needed to overcome the spectrum sensing limitation.

2.3.2 Geo-Location Database (GL-DB)

With this spectrum access technique, the SUs query a centralized database to get information about the available free channels to use. The centralized database stores PU locations and the channels they use, thus the database has a complete image of the current spectrum usage. Instead of sensing the spectrum, SUs estimate their locations (e.g. using GPS, or other localization techniques) and send their location coordinates to the database which replies to SUs with a set of free channels to be used in their locations. The centralized database decides on the free channels based on theoretical propagation models to estimate the interference among PUs and SUs. In case of mobility, and according to regulators, portable or mobile devices are also allowed to utilize the TVWS spectrum using the geolocation database, however, with more restrictions. For instance, Ofcom classified the portable white space devices as WSD class 5 with limited antenna height and to lower allowed transmission power [126]. Not only Ofcom, FCC as well, requires the portable white space devices to query the geolocation database with every 100m change in its location [80].

There are some issues that should be taken into consideration when designing geolocation database algorithms such as *Hidden terminal problem* and *propagation model complexity-accuracy trade-off*. Although the geo-location database approach looks promising to solve the hidden terminal problem but this only depends on having all

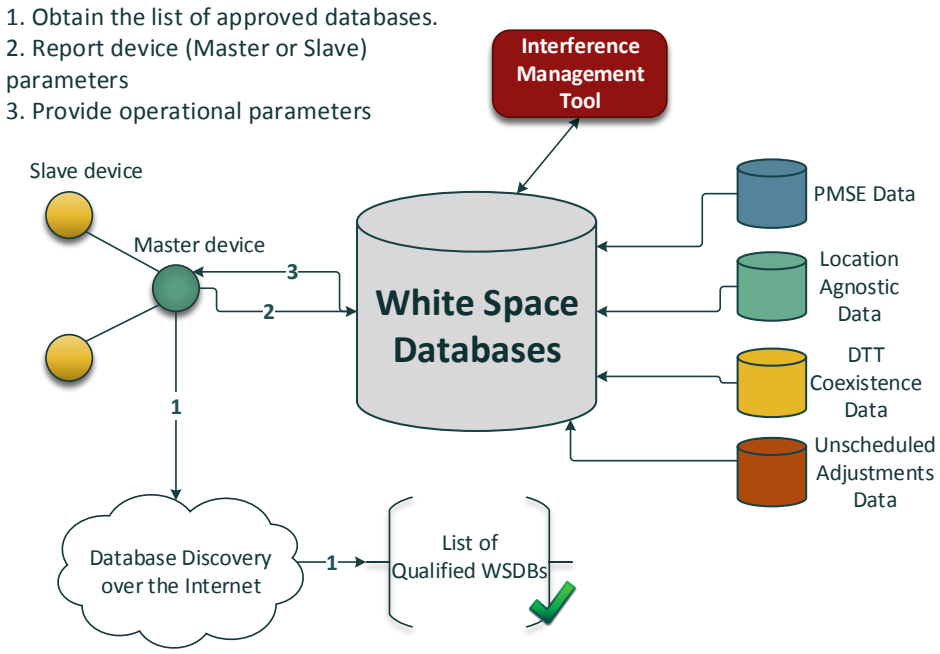

Figure 2.4: Ofcom Geo-location TVWS Database Model

PUs registered in the database. That may be optimistic and may not always be practical. For example, in the case of TVWS, it is hard to register the wireless microphone users which would seriously affect using the geo-location database technique in TV band. In addition to hidden terminal problem, achieving the right complexity-accuracy trade-off for the used propagation model is a non-trivial task. Unlike the sensing techniques, the geo-location depends on theoretical propagation model instead of real RF measurement. In this technique, the database periodically updates the spectrum occupation of PUs which increases the complexity of geo-location database especially in the case of mobility. In the following, we will review Ofcom's geo-location database technique and how this model addresses the above mentioned issues.

2.3.2.1 Ofcom GL-DB for TV White Spaces

Ofcom [121, 122, 123, 133] allows the secondary users to exploit the holes or white spaces in the TV band via a White Space Database (WSDB); these secondary users called White Space Devices (WSDs). WSDs are classified into two categories: Master and Slave WSDs. Master WSDs will contact the geo-location database directly to obtain the list of available channels and its operation parameters, whereas Slave WSDs operate under the control of Master WSDs. The WSDBs have information from differ-

ent data sets provided by Ofcom. (i) DTT Coexistence Data: a set of data containing the allowable transmission power in each 100 x 100 m pixel in the UK taking into consideration the minimum probability of interference with DTT. According to Ofcom the PMSE devices will work on channel 38 to prevent WSDs from interfering with them or with other services in TV adjacent bands, (ii) Location Agnostic data set is added. Location Agnostic data is a set of maximum allowable power for each channel in the TV band regardless the location of WSDs. (iii) PMSE data is the data set of licensed PMSE (different than in channel 38) that work in TV band. (iv) Unscheduled Adjustment data is a set of revised allowable transmission power in certain areas. The complete architecture of Ofcom geo-location database is showed in Fig.2.4.

The WSD operation is controlled by White Space Databases (WSDBs). First, the Master WSD sends its parameters to the WSDB (e.g. location) in which the WSDB computes the *operational parameters* and sends them to the Master WSD. These operational parameters could be the available channels, and the allowable transmission power. The WSDBs calculate these parameters based on information that obtained from the different data sets, we defined earlier. Finally, the Master WSD sends the *used parameters* (the chosen parameters from the list) to the WSDBs. In case of Slave WSDs operation, the Master WSD requests *generic operational parameters* to its slaves. These generic operational parameters are restrictive because the database does not take into account the device parameters of Slave WSD. The Master WSD forwards these parameters to its slaves. The Slave WSDs could use these restrictive parameters or they could send to the Master WSD their device parameters to get better operational parameters. At the end, the Master WSD informs the database with the used operational parameters by its slave WSDs.

Ofcom has a very restrictive the out-of-block emission or spectral efficiency which is calculated by [123]:

$$P_{OOB(dBm/(100khz))} <= max(P_{IB(dBm/(8MHz))} - AFLR(dB), -84)) \tag{2.1}$$

Where $P_{OOB(dBm/(8MHz))}$ is the WSD's in-block emission within 8 MHz channel. AFLR is the WSD's adjacent frequency leakage ratio. Ofcom classified the WSD devices into four classes where Class 1 WSDs produces the cleanest signal in term of spectral leakage or AFLR.

As discussed before, in Ofcom's geo-location database model the WSDs are required to send several device parameters to geo-location database to be able to obtain the operational parameters. These device parameters are unique device identifier,

emission class, technology identifier, device type, device master/slave category, antenna latitude/longitude coordinates and accuracy. Based on these detailed parameters, the geo-location database calculates the allowable operational parameters within specific period of time and geo-location. The geo-location validity is within 50 meters difference between the current position and the position reported to the geo-location database when the operation parameters calculated. Therefore Ofcom's geo-location model is flexible where the operational parameter such as transmission power and allowable time are different from device to another (due to device parameters differences). In addition to these detailed parameters, the white space devices information system (WSDIS) will guarantee to avoid any harmful interference to other devices working on the TV band. WSDIS is an information system which identify the WSDs that causing the interference and allow Ofcom to act accordingly to resolve the interference. Ofcom's geo-location database model solves the hidden terminal problem by allowing the PMSE devices that did not register in the database to operate on channel 38 and hence, the other devices will not interfere with them.

2.3.3 Beacon signaling

To avoid the latency associated with accessing the geolocation database, PUs can instead share information regarding their spectrum usage with SUs directly through *beacons*. A transmitter beacon consists of four types [34]: *(i) pre-transmitter beacon*, *(ii) area beacon*, *(iii) unlicensed signalling* and *(iv) receiver beacon*. A detailed discussion on different types of transmitter beacon can be found in [34].

There are some issues that should be taken into consideration when designing beacon signalling algorithms such as *Standardization* and *Cost*. Since beacons can operate in different frequency bands with different policies and regulatory requirements, a standard beacon design is needed to satisfy the different requirements of these bands. Although the beacon approach has the potential to enable more efficient spectrum use and sharing, it requires significant changes in the current infrastructure [121] which in turn increase the cost of implementing this approach on a large scale, making it impractical for legacy systems.

2.4 An Update on Ofcom's Spectrum Allocation plans

In order to improve the mobile network coverage in rural and remote areas, Ofcom has proposed to award 80MHz of spectrum in the 700MHz band to mobile network operators [134]. The 80MHz spectrum is within the 694-790MHz frequency range. More specifically, the 80MHz spectrum is divided into two 30MHz blocks of paired spectrum configured based on the Frequency Division Duplex (FDD). The 703 - 733MHz block will be used for the uplink traffic, while the downlink traffic will be carried on the second spectrum block ranges from 758 to 788MHz. Another 20MHz block of spectrum is used as a gap between both the uplink and downlink bands. Ofcom proposed that the 20MHz central gap can be used by mobile operators to enable supplemental downlink (SDL) services to enhance the downlink capacity of the mobile services. Ofcom proposed some coverage obligations associated with this 700MHz band award. Within the four years of license, Ofcom requires the obligated operator, first, to provide a certain level of quality for outdoor mobile services in the majority of the UK landmass. Second, to provide a good quality of outdoor service for at least 140,000 premises, which they currently do not have coverage. Third, to deploy at least 500 new mobile sites. The 80MHz spectrum is expected to be awared in May/June 2020 [134].

To increase the capacity and enable the 5G services in the UK, Ofcom proposed to award 120MHz of spectrum in the 3.6-3.8GHZ band for mobile operators [134]. The 120MHz will be available in a contiguous spectrum chunk between 3680MHz and 3800MHz. This spectrum band has been harmonized for 5G services in Europe by the Radio Spectrum Policy Group (RSPG). Although Ofcom is planning to allow this spectrum band to be available to the mobile operators by June 2020, yet, not everywhere, and some location constraints may remain until the band is completely cleared from the current fixed links and satellite services, by the end of 2022 [134].

To cope with the growing use of Wi-Fi networks and the development of new Wi-Fi standards (e.g., Wi-Fi 6), Ofcom proposed to enable unlicensed spectrum access to the lower spectrum chunk of 6GHz band and make it available for Wi-Fi and other related wireless technologies [135]. The target frequency range is between 5925MHz and 6425MHz. That will open up an additional 500MHz spectrum for Wi-Fi use in the near future. Hence, that will allow additional wide channels for the sixth generation of Wi-Fi, 802.11ax, that promises higher data rate up to 4.8Gbps [41]. Ofcom suggested that the maximum allowed power for unlicensed users in that band should be 250mW (24dBm) for indoor use and 25mW (14dBm) for outdoor use [135], in order to not

interfere with the incumbent users. Ofcom also proposed to remove the Dynamic Frequency Selection (DFS) restrictions on the Wi-Fi devices operate in the 5.8GHz band. The DFS requires the Wi-Fi devices to vacuate the Wi-Fi channel if a radar transmission is detected on that channel. Removing the DFS requirements will enable more Wi-Fi devices to use the 5.8GHz band.

Chapter 3

Related Work

In this chapter we present an overview of the literature related to the use cases discussed in the context of this thesis. For each use case, we present the most characteristic works, and show how the research evolved throughout the years. We also discuss shortcomings that drive the need for the novel solutions presented in the following chapters.

3.1 Decoupled User Association

Fair amount of research attention has been drawn towards the resource allocation/cell association problem in HetNets. Most of these works focus on coupled scenario either in downlink direction [24, 53, 120, 29] using different techniques such as game theory [24, 120], markov decision processes [53] and stochastic geometry [29], or in uplink direction and joint downlink and uplink association [149, 32]. [149] tackles the uplink user association problem using matching theory, where authors have used college admission framework (so called, one-to-many matching) to model the mobile users as students and the BSs as colleges. However, this work does not consider the decoupled uplink/downlink user association, the focus of our work.

In [155], authors extend the work in [149] to decoupled user association by applying matching algorithm similar to that in [149] separately for uplink and downlink associations, but it fails to consider the inter-dependency between uplink and downlink associations, and it also does not account the decoupling related cost. In [55], authors tackled the decoupled user association based on load and backhaul capacity, however, this work only focuses on the uplink association and does not consider the

downlink perspective and BSs' objectives. Another recent work [152] proposed a centralized approach to solve the decoupled user association problem with expensive solution in terms of communication overhead where each BS needs to continually send some statistics of system parameters to a centralized controller which decides the optimal association. In contrast to these related works, our proposed solution captures the inter-dependence between uplink and downlink associations and the impact of decoupling related cost. Moreover we propose a fully distributed solution by formulating the user association problem in decoupled context as a matching with contracts game and using stochastic geometry for modeling utility functions.

3.2 TVWS Spectrum Availability Analysis

TV White Spaces for Connectivity in Rural and Developing Regions. Rural broadband has been one of the key use cases for TVWS spectrum given its characteristics (see [124], for example). Similar arguments apply for exploiting this spectrum to address Internet connectivity challenges in developing regions [147, 89, 102] and emerging market such as in Africa [95, 108, 112] and Asia [160, 115, 103]. Recent work in this area has started investigating how TVWS spectrum can be used in the context of current and future cellular network standards to enable rural coverage. CellFi [27] leverages TVWS and LTE standards to realize an unlicensed cellular network with some additional changes to standard LTE to handle the opportunistic nature of channel access in TVWS spectrum and unplanned interference experienced by TVWS secondary users. [97] consider the use of TVWS in the 5G architecture, supporting it with a cost analysis.

From the perspective of the particular use case of middle mile connectivity targeted in this thesis, only one prior work [102] from the literature considers TVWS based point-to-point (PTP) links and that too over short distances up to a few kilometers. Other existing work largely focuses on the use of TVWS spectrum for last mile connectivity via point-to-multipoint (PTMP) links (e.g., [147]).

TVWS Spectrum Availability Studies and Measurements. Broadly speaking, TVWS spectrum can be accessed using either spectrum sensing or by consulting a geolocation database [92]. Early research and standards using TVWS spectrum employed the spectrum sensing approach (e.g., IEEE 802.22 [43], WhiteFi[26]). However, in view of the reliability and complexity concerns with the spectrum sensing approach, TV white space regulations in the US, UK and elsewhere have opted for

the alternative geolocation database approach (e.g., [132]), which has also become the basis for newer TVWS standards (e.g., 802.11af [65]). Geo-location database systems in practice rely on mathematical propagation models along with the knowledge of primary user locations, similar to the several TVWS spectrum availability studies in the literature (e.g., [81, 163, 74, 117]). This has been argued to be too much in favor of incumbent protection, thus conservative and limit white space usage opportunities for secondary users [143]. These concerns along with increasing interest in using TV white spaces indoors have led to hybrid spectrum access techniques that augment geolocation databases with measurements [168, 171, 107, 172, 36].

Despite these efforts, none of these works have addressed the several key aspects towards TVWS based backhauling connectivity which can be summarized as: (i) considering the effect of interference from multiple TV transmitters; (ii) studying the benefit of directional antennas in mitigating this interference; and (iii) understanding the nature of spectrum fragmentation that is crucial from the perspective of aggregating spectrum to establish high-bandwidth backhauling links.

3.3 Spectrum Aggregation for TVWS and Beyond

3.3.1 Spectrum Aggregation Approaches

The state of the art on Spectrum Aggregation can be traced back to the earlier works on Carrier Aggregation (CA) in LTE Release.10. Broadly speaking, three types of aggregations, named (i) Intra-band contiguous aggregation, (ii) Intra-band non-contiguous aggregation and (iii) Inter-band non-contiguous aggregation, have been introduced. The contiguous type of aggregation allows for spectrum aggregation of adjacent chunks of the spectrum while the non-contiguous type can leverage the non-adjacent/fragmented spectrum chunks. The recent LTE Release.16 will enable Inter-band non-contiguous aggregation for 5 carriers (i.e., up to 100MHz) [18]. Carrier Aggregation has been classified as low-layer spectrum aggregation technique which takes the traffic steering decisions at the MAC layer. The cross-carrier scheduler has been introduced in LTE Release.10 to efficiently manage the resources of different carriers. Another example for low-layer spectrum aggregation is the channel bonding techniques in WiFi network (e.g., 802.11n/ac). Unlike carrier aggregation, WiFi channel bonding has lack of flexibility in terms of the type of the channel bonding (i.e., only one use case of non-contiguous bonding, 80+80MHz) and the size of the bonded channels (i.e.,

20,40,80MHz).

In addition to CA and channel bonding techniques, Multi-Radio Access Technology (Multi-RAT) aggregation under the name of LTE-WiFi Aggregation (LWA) has been standardized for LTE in Release.13 [16]. LWA is inherited from the dual-connectivity concept proposed for LTE systems that allows the User Equipment (UE) to transmit/receive data simultaneously to/from different eNodeBs (eNB) to boost the performance. Unlike the low-layer aggregation techniques (e.g., CA and channel bonding), LWA enables the Multi-RAT aggregation at relatively higher layer, specifically, at the PDCP layer of LTE protocol stack. PDCP layer, in LWA, is responsible for packet reordering and traffic steering across different RATs [17].

Recently, more attention has been drawn towards the high-layer aggregation techniques (e.g., Transport layer) such as Multipath TCP (MP-TCP) transport protocol [67, 66]. The major focus given to the high-layer aggregation has been driven by the fact that these techniques can aggregate the spectrum across different technologies (e.g., LTE and WiFi). In other words, moving to the upper layers releases the aggregation technique from being technology-specific. Thus, that enables flexible type of aggregation such as aggregation between 5 GHz and 2.6 GHz spectrum. The major focus of these works [62, 70, 75, 101, 106, 104, 151] is on the design of an efficient scheduling algorithm while considering the different characteristics of the underlying technologies (e.g., bandwidth, latency, etc.). The recent extension of QUIC transport protocol, Multipath QUIC (MP-QUIC) [46, 165, 47, 114, 166] is another example of high-layer spectrum aggregation technique.

3.3.2 Spectrum Aggregation in TV White Space

There have been significant efforts to analyze the TVWS spectrum availability under different conditions (e.g., rural, dense areas) [81, 117, 163, 102, 74, 93]. These works have advocated the wide availability of TVWS spectrum in rural and remote areas. However, none of these works have studied the spectrum aggregation techniques in TVWS. To the best of our knowledge, [82] is the only work proposed in the literature to address the fragmented TVWS spectrum. Holland et al. [82] demonstrated the implementation of TVWS device that capable of aggregating up to 4 contiguous or non-contiguous channels. However, the aggregation technique proposed in this work lacks of flexibility and considered to be inefficient for the backhaul networks due to two reasons. First, as we will discuss in the next Chapters, TVWS spectrum is frag-

mented and leveraging only 4 channels as proposed in [82] is not sufficient to enable high capacity backhaul network. Second, in Multi-Radio context, traffic management mechanism is essential in order to enable efficient traffic distribution between different radios. Packet reordering and duplicate packet handling is the basic functionality of such traffic management mechanisms, [82] lacks of any traffic management handling and thus that hinders its performance in the large scale such as backhaul networks. Third, the backhaul network has different characteristics (in terms of available spectrum, channel condition and MAC layer protocols as will be discussed in Chapter.7) compared to the indoor deployment which make this work inefficient and incapable of handling the different characteristics of backhual network.

3.3.3 Backhauling solutions for rural and remote areas

Not only the TVWS [97, 111] but also a variety of other different approaches have been taken in the literature to provide efficient solutions for backhauling networks in rural areas. The earlier work on WiFi for Long Distance (WiLD) [140] is the first effort to assess the feasibility of using WiFi to provide a backhaul solution for rural areas. This, then, is commercialized into different products such as [8]. In addition, Tarana Wireless solutions that leverage Wi-Fi to enable rural area connectivity [7]. With the increasing development of Millimeter wave (mmWave) technology, some works in the literature have showed the potential benefits of using the higher-frequency band for backhauling networks [110, 109]. In addition, Project AirGig by AT&T [2] is initiated to provide connectivity to the rural areas through mmWave and LTE spectrum.

3.4 Multi-RAT Integration

LTE and WiFi integration has already been standardized in Release 13 [16] and 14 [13, 14] with two different solutions named LTE-WLAN Radio Level Integration with IPsec Tunnel (LWIP, Rel.13) and LTE-WLAN Aggregation (LWA, Rel. 14). The LWA architecture leverages the same principles of LTE Dual Connectivity introduced in Rel. 12. More specifically, the eNB is connected to wireless termination (WT) through Xw interface. The WT can be either an access point or central controller that control multiple APs. The PDCP layer is responsible for the traffic distribution functionality and the PDUs reordering that means it decides where to route the PDCP PDUs and to perform the reordering process before passing the PDUs to the higher

layers. A flow control mechanism between the WT and the LTE PDCP layer has been standardized to allow the flow of information such as first missing sequence (FMS), highest received WiFi sequence number and count of missing SN between the two interfaces LTE PDCP. This type of report named LWA status report sent periodically along with the PDCP status report from the UE to the eNB. In addition to LWA status report, the eNB configures the UE to send a periodic reports on the WiFi channel conditions which asset in the mobility decision.

In addition to the LWA approach, another simpler protocol for LTE and WiFi integration, named, LTE-WLAN Radio Level Integration with IPsec Tunnel (LWIP) has been proposed in LTE Rel. 13. This integration is achieved by establishing an IPsec tunnel between eNB and UE and carried over the WLAN network. This integration occurs at LWIP Encapsulation Protocol (LWIPEP) layer above the PDCP layer in which the traffic steering algorithm decides which bearers, flows or packets to be transmitted over LTE or WiFi. Different than LWA, LWIP needs no flow control or Xw interface between the eNB and WiFi node. This approach can be seen as an intermediate solution between transport layer integration approach (e.g., MPTCP) and LWA integration approach (i.e., PDCP layer). An implementation of LWIP on OAI has been introduced and presented in [139, 138]

A very early work has been introduced in [96] to discuss the impact of LWA on TCP performance. It proposed a very simple mechanism to detect and correct packet errors that could occurs on WiFi interface and two basic traffic steering functionality that either offload all the traffic to WiFi interface or distribute it between the two interfaces based on the eNB status report on LTE part. Another work in [83] studies the performance of higher layer protocols (e.g., TCP and UDP) when the LWA is enabled. The author realized the LWA by implementing the LWA Application Protocol (LWAAP) layer which is a virtual layer below the PDCP layer adds an adaptation header if the PDUs are passed to the WiFi part. This header contains the bearer ID and it is essential to allow the AP to distinguish between the traffic coming from LTE part or the other traffic handled by the AP. Three simple offloading policies have been proposed.

All of these works only focus on LWA approach and tried to realize it on an open-source platforms such as srsLTE or OpenAirInterface. However, none of these efforts have addressed the fundamental question of what are the key differences between the PDCP layer approach and the transport layer approach? More specifically, what is the right protocol layer to perform the Multi-RAT integration?

Chapter 4

Decoupled Uplink/Downlink User Association in HetNets: A Matching with Contracts Approach

In this chapter we address the decoupled uplink/downlink user association problem in HetNets. Over the last years, it is widely agreed that shifting to a multi-tier heterogeneous cellular network (HetNet) architecture, with dense deployments of low-cost small cells (e.g., micro, pico, femto cells) overlaid within the coverage area of a macro cell, is a cost-effective way to cope with the growing traffic demand. Unlike the traditional homogenous architecture with macro cells all using similar transmit power, dense HetNets feature base stations (BSs) with widely different transmit powers and deployment topologies. This has implications on several aspects including interference management and resource allocation but of particular relevance to this work is the issue of *user association* that concerns which BS a mobile device (UE) associates in the uplink (UL) and downlink (DL) directions.

The conventional approach to user association is to have a UE associates with the same BS in both directions and this is sometimes referred to as coupled user association, typically based on maximizing downlink SINR. In light of the shift towards dense HetNets, the limitations of coupled user association are coming to the fore. There is now an emerging body of work that argues in favor of departing from the convention and instead adopting the more general *downlink/uplink decoupling model for user association* [30, 161, 54] in which a UE could be associated with different BSs in the uplink and downlink directions. In [31], authors discuss the need for uplink/downlink

decoupling in the context of device-centric architectures for 5G. Boccardi et al. [30] quantitatively show gains of such decoupling in dense HetNets in terms of several aspects, including: increased uplink SNR and data rate, different and better load balancing in the uplink and downlink, and allowing more device-to-device (D2D) transmissions that will share uplink bands as per 3GPP Rel. 12.

The user association problem in HetNets is considered more challenging due to the conflicting objectives of different entities in the system and applying classical user association schemes results in load imbalances and inefficient operation. Moving to the decoupled uplink/downlink setting, the problem of user association gets even more challenging because in addition to reconcile competing objectives from different angles (uplink, downlink, macro BSs, small-cell BSs), both uplink and downlink association should be *jointly* tackled and cost associated with decoupling needs to be taken into account. While (coupled) user association in HetNets has received a fair amount of attention recently and there are several simulation and analytical studies investigating the decoupling benefits (e.g., [30, 161, 54]), very little work exists on the design of user association mechanisms suitable for the decoupled context [55, 155, 152] and these works fails to capture the inter-dependent nature of uplink/downlink associations and the impact of decoupling related cost, latter dependent on the bandwidth of the backhaul link connecting the two BSs involved in a decoupled user association.

To address the decoupled uplink/downlink user association problem in HetNets, we propose a novel mechanism based on matching theory and stochastic geometry.

Matching theory is particularly proved to accommodate heterogeneity of system entities and their objectives to obtain stable and optimal algorithms that can be implemented in distributed (self-organizing) manner. Specifically we formulate the decoupled uplink/downlink user association problem as a *matching with contracts* game. We draw an analogy between the user association problem in the decoupled context with the doctor-hospital matching problem that exemplifies a matching with contracts game. In the doctor-hospital matching problem [76], there are a set of hospitals which seek to hire doctors by handing them contracts that respect ranked preferences of hospitals and doctors. To map this problem to our setting, BSs play the role of hospitals and UEs are the doctors, and there can be two types of contracts between the two sets: UL and DL association.

In our model, users have different objectives determining their BS preferences in the uplink and downlink directions: based on *long-term* throughput in the UL and DL directions; long-term throughput is used instead of instantaneous throughput to limit

the need to frequently redo associations (by computing a new matching) in response to time-varying channel conditions. We use stochastic geometry to model this long-term throughput[1] as the average ergodic rate of a typical user and its associated BS. Users, then, use this model to rank their BS preferences in both uplink and downlink directions. From the perspective of BSs, the preferences capture the need to offload the traffic from the macro-cell BS to small-cell BSs. We present a matching algorithm that considers these diverse objectives and the decoupling related cost; this algorithm results in a stable allocation and we also empirically demonstrate its convergence. We show the effectiveness of our proposed mechanism based on matching with contracts approach via simulations in comparison with traditional coupled user association approach, conventional (one-to-many) matching based decoupled user association mechanism proposed in [155] and another recently proposed uplink oriented user association mechanism for decoupled context from [55]. The gains from our mechanism stem from its holistic nature, accounting for the additional cost incurred by decoupling while choosing the specific BSs to associate in the uplink and downlink directions. Our solution is also shown to result in performance that is a close to centralized and computationally expensive optimal solution representing the approach taken in [152]. It is also important to note that this is the first work that proposes using matching with contracts game in the wireless communication context.

The work presented in this chapter has been published in the 12th ACM Symposium on QoS and Security for Wireless and Mobile Networks (Q2SWinet 2016) [91].

4.1 System Model

4.1.1 Network Model

We consider a multi-tier HetNet including set of BSs $B = S \cup m$ where we denote by small-cell BSs (SBSs) $S = \{1, \ldots, |S|\}$, one macro-cell BS (MBS) m, and set of users $N = \{1, \ldots, |N|\}$ which are deployed and seek to transmit in both uplink and downlink directions. We consider that SBSs, and users are arranged in space following homogeneous Poisson point process (PPP) Φ of intensity λ_S, λ_N in the Euclidean plane, respectively. SBSs are overlaid on the MBS area to increase coverage and improve the performance of users. Each SBS j has a maximum *quota* q_j which is the maximum number of users that it can serve. We also assume that there is no intra-cell interfer-

[1] Henceforth, the terms throughput and rate are used interchangeably.

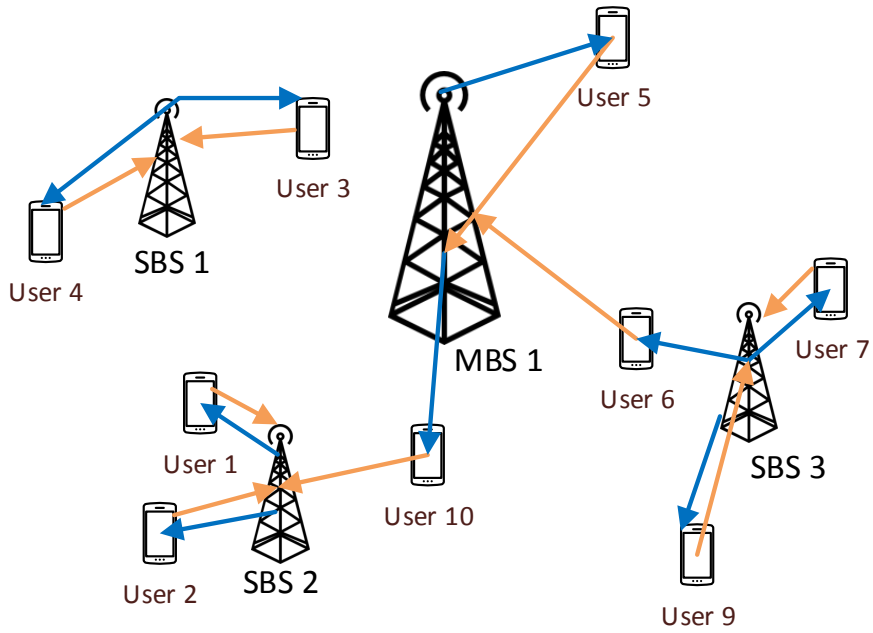

Figure 4.1: Illustration of decoupled uplink/downlink user association in a HetNet.

ence between users within a same cell as they can be assigned non-interfering set of resource blocks; however, the cell-edge users could suffer from inter-cell interference. We assume Rayleigh fading channel model. Transmit power is denoted by P_i where i can be either users, MBS or SBSs, i.e. $i \in \{m, S, N\}$. In this case, the received power at a typical user i in DL (or BS i in UL) at distance $d_{i,j}$ from BS j in DL (or user j in UL) is $P_j g_{i,j} d_{i,j}^{-\alpha}$, where $g_{i,j}$ is a random variable that follows an exponential distribution, and α is path loss exponent.

4.1.2 User Association: Decoupled Scenario

From DL perspective, in *traditional coupled user association*, the common criterion to drive user-BS association is the max downlink SINR [44], where each user by default shares the same BS both in UL and in the DL, which makes the association scheme unfair and inefficient for UL traffic in a dense HetNet architecture with BSs widely varying in terms of their transmit powers. Therefore, in order to achieve better network operation, it is potentially beneficial to decouple the UL and DL associations.

An illustrative scenario is shown in Figure 4.1 where the network consists of one MBS, 3 SBSs, and 10 users. The main purpose of SBSs is to offload traffic from MBS

and would provide better performance to users. As a result, the main objective for each user is to associate with the BS enhancing its performance. The concept of traffic offloading is very clear from Figure 4.1. Instead of having 10 users associated with the MBS, only two users are connected to the MBS and the remaining are connected to the other 3 SBSs. Figure 4.1 also shows that every user attempts to maximize its own utility by connecting to the best BS for the UL and DL directions. For example, user 10 prefers to connect to the MBS in DL and SBS 2 in UL. In uplink association, the users use the fractional path loss compensation power control mechanism for UL power control which depends on the path loss model. Consequently, the users prefer to associate with BS with respect to the path-loss, which will allow the users to reduce their transmission power and the interference on the BS in turn. In other words, the users prefer to associate with the nearest BS in the UL direction in order to reduce its transmission power as well as the interference level at the BS. Thus, this makes the boundaries of BS to be different in UL and DL.

Based on the above network model, we seek to address the following question: *What is the best user-BS association in UL and DL directions?*

This is non-trivial because UL and DL associations are inter-dependent and decoupling related cost also needs to be accounted.

4.1.3 Decoupling Cost

From the foregoing discussion and recent literature on DL/UL decoupling (DUDe), decoupled user association is seen to offer advantages over the coupled association in term of UL user throughput and UL/DL traffic load balancing. Dual connectivity is considered as an easier to realize practical route for deploying decoupled association where the user can connect to one BS in DL (e.g., max-SINR) and another BS in UL (e.g., based on path-loss). In such a decoupled user association deployment, there are two type of BSs, called, master-BS (M-BS) and secondary-BS (S-BS). Based on 3GPP specification, there are two type of architecture that agreed by 3GPP to support dual connectivity, named, *1A* and *3C alternatives*. 1A considers no bearer split. In this architecture, the core network deals with UL/DL BSs as two disjoint cells where no coordination is needed. Due to this core network separation, S-BS mobility is visible to core network which significantly increases the signalling overhead. In addition, utilization of radio resources for the same bearer across two BSs is not possible. Furthermore, security impact due to the fact that ciphering will be required for both UL/DL

BSs. The alternative 3C architecture that assumes bearer split (at the BS chosen for user association in the DL direction) does not share these limitations. In 3C architecture, only M-BS is visible to the core network which makes the mobility at S-BSs to be hidden from core network which limits the signalling overhead problem in 1A architecture. However, a coordination and flow control is needed at M-BS to forward traffic to S-BS.

In case of bearer split (i.e. 3C architecture), the key question is how much data should be forwarded between S-BS and M-BS. The nature of link between two BSs is the main factor to consider.

The limitation of backhaul link capacity (between S-BS and M-BS) compared to access link would cause buffer overflow at S-BS, high packet loss and performance degradation. On the other hand, if the backhaul link capacity is over-provisioned and the limitation is on access link side, then S-BS would not forward enough data to the M-BS, and the S-BS buffer may often run out of data, thus limiting the user performance. Therefore, the decoupling scenario has a cost function mainly in UL direction due to bearer split architecture.

Considering the dual connectivity (3C) architecture and given the fact that uplink association in a HetNet context with DUDe would likely be via a nearby small cell, S-BS would correspond to the UL direction. Bandwidth of the backhaul link (X2 interface) between M-BS and S-BS could therefore be a limiting factor and affect the UL throughput in a decoupled user association so we account for this backhaul communication effect as a decoupling cost.

The decoupling cost is modelled as follows: let us assume that BSs reserve a queue for each user associated with it. We denote by τ_{slot} as the duration of a time-slot. Let $\Pi^R_{i,j}(t)$ be the number of received bits from user i to BS j in time-slot t:

$$\Pi^R_{i,j}(t) = \tau_{\text{slot}} w_{i,j} \log_2 \left(1 + \frac{P_i g_{i,j}(t) d_{i,j}^{-\alpha}}{I + w_{i,j} N_0}\right),$$

where $w_{i,j}$ is the access link bandwidth between user i and BS j, and N_0 is noise power spectral density. Similarly, $\Pi^O_{j,k}(t)$ is the number of output bits from BS j to BS k at time-slot t:

$$\Pi^O_{j,k}(t) = \tau_{\text{slot}} w_{j,k} \log_2 \left(1 + \frac{P_j g_{j,k}(t) d_{j,k}^{-\alpha}}{w_{j,k} N_0}\right),$$

where $w_{j,k}$ is the backhaul link bandwidth between BSs j and k which we assume as a wireless link.

Ergodic mean of received and output bits can be calculated as:

$$\mathbb{E}[\Pi^R_{i,j}] = \lim_{T\to\infty} \frac{1}{T} \sum_{t=1}^{T} \Pi^R_{i,j}(t),\ \mathbb{E}[\Pi^O_{j,k}] = \lim_{T\to\infty} \frac{1}{T} \sum_{t=1}^{T} \Pi^O_{j,k}(t)$$

and we define the ratio of mean of output bits from BS j to k and mean of all received bits at BS j as:

$$r_{j,k} = \frac{\mathbb{E}[\Pi^O_{j,k}]}{\sum_{i\in N} \mathbb{E}[\Pi^R_{i,j}]}. \tag{4.1}$$

Then, the decoupling cost is given by:

$$c_{\mathrm{DC}}(j,k) = \begin{cases} r(j,k), & \text{if } r(j,k) \le 1 \\ 0, & \text{otherwise.} \end{cases} \tag{4.2}$$

This cost can essentially be viewed as capturing the mismatch between access bandwidth of cell used for UL association and bandwidth between BSs involved in the decoupled user association.

4.2 Reference Problem: Doctor-Hospital Matching

The user-BS matching describes the matching of users to BSs by allowing the decoupling of UL and DL associations. We model this problem as a matching with contracts. Basically, we assume that the contract between a particular user and BS is to choose UL or DL or neither.

The many-to-many matching with contracts[148] has been introduced to tackle problems such as United Kingdom Medical Intern match [148], the market used to allocate blood from blood banks to hospitals [88], worker-firm matching problem [50]. These works model the interaction between two set of agents in which one of them has limited quota and with conflict preferences in term of contracts, it is of interest to study how the assignment can occur between both sets of agents while satisfying, as much as possible, all preferences. We believe that this model is suitable for user association in a multi-tier HetNet architecture with DUDe as it naturally captures the dependency between UL/DL associations in our scenario, accommodates diverse objectives of system entities and allows stable associations.

We draw an analogy between our user association problem and the doctor-hospital matching problem [76]. As an illustrative example scenario for matching with contracts, consider a setting with a set of 3 doctors, i.e. $\{d_1, d_2, d_3\}$ and a set of 2 hospitals, i.e. $\{h_1, h_2\}$. Contracts can specify one or two of the following terms: a doctor works

in the morning (MO) shift only; works in the afternoon (AF) shift only; works in both the morning and the afternoon, a full-time (FT) shift.

Suppose that the set of contracts the hospitals can offer to doctors is given by $\{\mathrm{MO}_{11}, \mathrm{MO}_{12}, \mathrm{MO}_{21}, \mathrm{AF}_{21}, \mathrm{AF}_{32}, \mathrm{MO}_{32}, \mathrm{FT}_{22}, \mathrm{FT}_{31}\}$ where MO_{ij}, AF_{ij} and FT_{ij} denote different contracts involving doctor d_i and hospital h_j. This list of contracts reflect constraints for the matching. For example, the hospital 1 is only willing to hire doctor 3 on full-time basis and not for morning or afternoon shifts. Now consider following example that shows the preferences of doctors and hospitals as follows:

$$\text{Preferences of } d_1 : \{h_1^{\mathrm{MO}}, h_2^{\mathrm{AF}}\} \succ_{d_1} \{h_1^{\mathrm{MO}}\} \succ_{d_1} \{h_2^{\mathrm{MO}}\} \succ_{d_1} \emptyset$$
$$\text{Preferences of } d_2 : \{h_1^{\mathrm{AF}}\} \succ_{d_2} \{h_1^{\mathrm{MO}}\} \succ_{d_2} \emptyset$$
$$\text{Preferences of } d_3 : \{h_2^{\mathrm{AF}}\} \succ_{d_3} \{h_2^{\mathrm{MO}}\} \succ_{d_3} \emptyset$$
$$\text{Preferences of } h_1 : \{d_1^{\mathrm{MO}}, d_2^{\mathrm{MO}}\} \succ_{h_1} \{d_1^{\mathrm{MO}}, d_2^{\mathrm{AF}}\} \succ_{h_1} \{d_2^{a}\} \succ_{h_1} \emptyset$$
$$\text{Preferences of } h_2 : \{d_3^{\mathrm{MO}}\} \succ_{h_2} \{d_3^{\mathrm{AF}}\} \succ_{h_2} \emptyset$$

From the above, we can observe that doctor 1 prefers the contract combining hospital 1 in the morning and hospital 2 in the afternoon over all other contracts. Similarly, hospital 2 prefers to hire doctor 3 for morning shift d_3^{MO} over all other possibilities. The null contract $\emptyset$ for a doctor means that the doctor remains unemployed in the doctor-hospital matching problem, while null contract for a hospital means no doctors are hired at that hospital.

4.3 The Game Model and Association Rules

Based on the discussion in the previous section, the user-BS matching game can be defined by four components $\langle N, B, X, \succ \rangle$ where

- X is the set of *contracts* acting as possible connection between users and BSs in which each user can have either UL or DL connection or both with a BS, and

- *preference relations* $\{\succ_1, \ldots, \succ_{|N|}\}$ and $\{\succ_1, \ldots, \succ_{|B|}\}$ for users and BSs, respectively allowing them to build preferences over the available contracts. The preference relations are defined as a *complete*, *transitive*, and *reflexive* binary relations over the set of all contracts including the null contract $\emptyset$. The null contract in our setting implies that there is no association between the user and BS in question.

Note that *with this matching with contracts approach, the preference relations are over the available set of contracts* rather than building the preferences over one another as in conventional matching (e.g., one-to-many matching in [149, 155]).

4.3.1 Performance Objectives in Downlink and Uplink

Consider DL transmission where each user $i \in N$ chooses a BS $j \in B$ and this choice corresponds to a certain SINR. It is reasonable to assume that the performance objective for DL would be to maximize the DL rate which is a function of SINR. The SINR of a user i from its associated BS j can be expressed as:

$$\mathsf{SINR}_{i,j}^{\mathrm{DL}} = \frac{P_j g_{i,j} d_{i,j}^{-\alpha}}{\sum_{k \in B \setminus j} P_k g_{i,k} d_{i,k}^{-\alpha} + N_0} \tag{4.3}$$

where P_j (P_k) is equal to P_s, the transmit power of a SBS, if j (k) is a SBS; P_m, the transmit power of a MBS, otherwise.

Lemma 4.3.1 *We consider the average ergodic rate of a typical user i and its associated BS j in DL direction as follows:*

Case 1: If BS j is a SBS:

$$\begin{aligned}\theta_{i,j}^{\mathrm{DL}} &\triangleq \mathbb{E}\left[\ln\left(1+\mathsf{SINR}_{i,j}^{\mathrm{DL}}\right)\right] \\ &= \int_{t>0} \frac{P_s d_{i,j}^{-\alpha}}{(e^t-1)P_m d_{i,m}^{-\alpha} + P_s d_{i,j}^{-\alpha}} \left(\frac{e^t N_0}{P_s d_{i,j}^{-\alpha}} \right. \\ &\quad \left. + \frac{\lambda_S \pi d_{i,j}^2 e^t}{(e^t-1)^{1-\frac{2}{\alpha}}} \frac{4\pi/\alpha^2}{\sin(2\pi/\alpha)} \right) \\ &\quad \cdot \exp\left(-\frac{(e^t-1)N_0}{P_s d_{i,j}^{-\alpha}} - \frac{\lambda_S \pi d_{i,j}^2}{(e^t-1)^{-\frac{2}{\alpha}}} \frac{2\pi/\alpha}{\sin(2\pi/\alpha)} \right) t dt\end{aligned} \tag{4.4}$$

Case 2: If BS j is the MBS:

$$\begin{aligned}\theta_{i,j}^{\mathrm{DL}} &\triangleq \mathbb{E}\left[\ln\left(1+\mathsf{SINR}_{i,j}^{\mathrm{DL}}\right)\right] \\ &= \int_{t>0} \left(\frac{e^t N_0}{P_m d_{i,j}^{-\alpha}} + \frac{\lambda_S \pi d_{i,j}^2 e^t}{(e^t-1)^{1-\frac{2}{\alpha}}} \left(\frac{P_s}{P_m}\right)^{2/\alpha} \frac{4\pi/\alpha^2}{\sin(2\pi/\alpha)} \right) \\ &\quad \cdot \exp\left(-\frac{(e^t-1)N_0}{P_m d_{i,j}^{-\alpha}} - \frac{\lambda_S \pi d_{i,j}^2 e^t}{(e^t-1)^{-\frac{2}{\alpha}}} \left(\frac{P_s}{P_m}\right)^{2/\alpha} \frac{2\pi/\alpha}{\sin(2\pi/\alpha)} \right) t dt\end{aligned} \tag{4.5}$$

See Section 4.6 for the proof of the Lemma[2].

In UL, as in [55], we also consider the rate as the objective for the user and this also depends on SINR. The SINR for user i which is associated with BS j is given by (as in [155]):

$$\mathsf{SINR}_{i,j}^{\mathrm{UL}} = \frac{P g_{i,j} d_{i,j}^{-\alpha}}{\sum_{k \in N \setminus i} P g_{k,j} d_{k,j}^{-\alpha} + N_0} \tag{4.6}$$

We consider the average ergodic rate of typical user and its associated BS as follows:

$$\begin{aligned} \theta_{i,j}^{\mathrm{UL}} &\triangleq \mathbb{E}\left[\ln\left(1+\mathsf{SINR}_{i,j}^{\mathrm{UL}}\right)\right] \\ &= \int_{t>0} \left(\frac{e^t N_0}{P d_{i,j}^{-\alpha}} + \lambda_N \pi d_{i,j}^2 e^t (e^t-1)^{\frac{2}{\alpha}-1} \frac{4\pi/\alpha^2}{\sin(2\pi/\alpha)}\right) \\ &\cdot \exp\left(-\frac{(e^t-1)N_0}{P d_{i,j}^{-\alpha}} - \lambda_N \pi d_{i,j}^2 (e^t-1)^{\frac{2}{\alpha}} \frac{2\pi/\alpha}{\sin(2\pi/\alpha)}\right) t\, dt \end{aligned} \tag{4.7}$$

4.3.2 Ranking Criteria

4.3.2.1 The Users' Ranking Criterion

Assume that each user $i \in N$ selects a BS $j \in B$ so as to optimize its rate. For this purpose, we propose a utility function that captures the user's rate in the UL and DL directions. For a particular user $i \in N$, the utility function is defined as follows:

$$\theta_i(j,k) = \begin{cases} \theta_{i,k}^{\mathrm{DL}} + (1 - c_{\mathrm{DC}}(j,k))\theta_{i,j}^{\mathrm{UL}}, & \text{if } j \neq k \\ \theta_{i,k}^{\mathrm{DL}} + \theta_{i,j}^{\mathrm{UL}}, & \text{if } j = k \end{cases} \tag{4.8}$$

4.3.2.2 The Base Stations' Ranking Criterion

Basically, each SBS has two objectives: 1) traffic offloading from the MBS, to extend its coverage, and enhance the user's performance, which is achieved by accepting the users from MBS; this objective is indirectly captured by the following objective; 2) to select users that can potentially experience good rate on that base station.

Therefore, in general, the benefit or utility that any BS $j \in B$ obtains by serving user $i \in N$ is given by $H_j(i) = f(\theta_{i,j}, \theta_{i,m})$, where $\theta_{i,j}$ is UL or DL rate that user i can achieve if it is associated with BS j and $\theta_{i,m}$ is UL or DL rate that user i can achieve if it is associated with the MBS. We let $f(\cdot)$ to be a function increasing with respect to

[2]The proof presented in section 4.6 is done in collaboration with Cengis Hasan

total rate and use the following function to define the ranking criteria of BSs in the DL and UL directions, respectively:

$$\text{for DL}: H_j^{\text{DL}}(i) = \frac{\theta_{i,j}^{\text{DL}}}{\theta_{i,m}^{\text{DL}}} \quad \text{and for UL:} \quad H_j^{\text{UL}}(i) = \frac{\theta_{i,j}^{\text{UL}}}{\theta_{i,m}^{\text{UL}}} \tag{4.9}$$

4.3.3 The Contracts

A set of contract specify a user, a BS and a connection between the user and the BS, i.e., UL or DL connection, $X \equiv N \times B \times T$, where $T = \{\text{UL}, \text{DL}\}$ is considered as contract terms which are in our model UL and DL associations, respectively. The contracts can either consist of two contract elements such as the users' contracts or only one contract element such as base stations' contract (see the next subsections 4.3.3.1, 4.3.3.2). We now give some essential definitions.

Definition 4.3.1 (The Allocation) A set of contract $Z \subseteq X$ is an allocation if it contains at most one contract element (UL) and one contract element (DL) for each user-BS pair. Note that the empty set is considered as an assignment. The objective of matching with contracts problem is to find the stable allocation.

Definition 4.3.2 (Chosen Set) User i's chosen set is denoted by $C_i(X')$ where $X' \subseteq X$. Chosen set is either the null set, if no acceptable contracts are offered, or the set of most preferred contracts. Similarly, the chosen set of a BS j *chosen set* $C_j(X')$ is a subset of contracts based on the preferences of BS j. Now consider $C_N(X') = \cup_{i \in N} C_i(X')$ as a the set of contracts chosen across all users from the set of contracts X'. Hence, the remaining offers from the set of contracts is called the *rejected set* which is formalized as: $R_N(X') = X' - C_N(X')$. Similarly, the chosen and rejected sets of the BSs are formalized as: $C_B(X') = \cup_{j \in B} C_j(X')$ and $R_B(X') = X' - C_B(X')$.

Definition 4.3.3 (Stable Allocation) The allocation $Y \subseteq X$ is *stable allocation* if and only if: (i) Y is individually rational, and (ii) there are no blocking contracts in Y.

An allocation is said to be *individually rational* if no user and BS deviates from the allocation.

A *blocking contract* x is a contract in which user i strictly prefers BS j with contract x to its current BS and contract, and/or the BS j strictly prefers user i with contract x over a currently allocated user and associated contract.

4.3.3.1 The Users' Contracts

Each user $i \in N$ can sign a contract which includes the identity of UL and DL BSs. We denote by $x = \{\mathrm{UL}_j, \mathrm{DL}_k\}$ a contract of user i. Think of a two BS example. Let possibilities for contract be the following: user i can sign UL contract with BS 1 and DL contract with BS 2. For example, user 1 prefers contract $\{\mathrm{UL}_1, \mathrm{DL}_2\}$ means that user prefers association with BS 1 in the UL direction and BS 2 in the DL direction based on the utility function in (4.8). For the two BS example, if we write the preferences as following: $\{\mathrm{UL}_1, \mathrm{DL}_2\} \succ_1 \{\mathrm{UL}_1, \mathrm{DL}_1\} \succ_1 \emptyset$. Then, this implies that user i prefers to transmit its UL traffic over BS 1 and receive the DL traffic from BS 2 in comparison with transmitting UL and receiving DL traffic both via BS 1. The contract $x \in X$ is acceptable for user i if $x \succ_i \emptyset$ else it would reject that contract. For any user $i \in N$, a preference relation over the set of contracts X is defined as follows: for any two contracts $x, y \in X, x \neq y$, the preference relation becomes

$$x \succeq_i y \iff \theta_i(x) \geq \theta_i(y) \tag{4.10}$$

where $\theta_i(x) = \theta_i(\mathrm{UL}_j, \mathrm{DL}_k) = \theta_i(j,k)$ as given in equation (4.8).

4.3.3.2 The Base Stations' Contracts

For each BS $j \in B$, we define two separate list of preference relations for UL and DL direction, over the set of contracts X. For example, a contract may be user i in UL direction, i.e. $x = \{\mathrm{UL}_i\}$, or another contract may be user i' in UL direction, i.e. $x' = \{\mathrm{UL}_{i'}\}$. For any two contracts $x, x' \in X, x \neq x'$:

$$\mathrm{UL}: \quad x \succeq_j x' \iff H_j(x) \geq H_j(x') \tag{4.11}$$

Similarly for downlink, a contract may be user i in DL direction, i.e. $y = \{\mathrm{DL}_i\}$, or another contract may be user i' in DL direction, i.e. $y' = \{\mathrm{DL}_{i'}\}$. For any two contracts $y, y' \in X, y \neq y'$:

$$\mathrm{DL}: \quad y \succeq_j y' \iff H_j(y) \geq H_j(y') \tag{4.12}$$

4.3.4 The Matching Algorithm

As per the solution to the user-BS matching problem posed above, we propose an algorithm, shown in Algorithm 1, which seeks to provide a stable and close-to-optimal allocation.

Algorithm 1: The proposed matching with contracts algorithm for DUDe user association.

1 **Initialization:**

(a) The network starts where no users are assigned to any BS.

(b) Let $X \equiv N \times B \times T$ denote all possible contracts.

(c) Initialize the chosen set of contracts for the users as $C_N(0) = X$ where X is all the available contracts at iteration = 0.

Main Phase:

(a) Each user builds its preference list over the available set of contracts based on the utility function as per (4.8).

(b) Each user chooses its most preferred set of contracts, and generates the rejected set as $R_N(\text{iteration}) = X - C_N[\text{iteration}]$.

(c) Each BS builds its preference list over the available set of contracts based on the utility function as per (4.9).

(d) After all users submit their requests, each BS $j \in B$ chooses user contracts as per its preference list (and limited by quota q_j for each SBS $j \in S$) while rejecting the rest of the user contracts.

(e) From the previous step, the chosen set $C_B[\text{iteration}]$ which is the complement of $R_N(\text{iteration})$ is generated, and the rejected set is $R_B(\text{iteration})$

Repeat (iteration = iteration + 1)**:**

(a) The rejected users re-apply to their next best choice, in which $C_N[\text{iteration}]$ is the complement of $R_B(\text{iteration} - 1)$.

(b) Each BS j picks the top ranked contracts considering its previous preference list, new user contracts and its quota (if SBS), and rejects the rest.

Until: $R_B(\text{iteration}) = R_B(\text{iteration} - 1)$. At this stage, no more allocation is possible and the algorithm converges.

At the initial network state, there is no user associated with any BS. We also assume that any user can be associated with any BS in order to maximize its utility function. Therefore, we generate a set of all possible contracts that the BS can offer to the users.

Besides, we only have two terms in the set of contracts, either to accept UL user's connection then the contract will be UL_j or to accept DL user's connection and the contract will be DL_j where these two kind of contracts are between the user and BS j. As a result, we will have a list $X \equiv N \times B \times T$, where $|T| = 2$. Finally, at the initial stage, we assume that users accept all available contracts. In the main phase, users start ranking their preferences over the available set of contracts according to the utility function defined in (4.8) and start by submitting their requests for assignment to the most preferred contracts with the corresponding BSs. At this step, the algorithm generates two set of contracts. The first set is the chosen set of contracts which contains the most preferred contracts between the users and the BSs from the users' perspective based on their utility function. The second set is the rejected set of contracts which is the complement of the chosen set, such that given $X' \subset X$, $R_N(X_N) = X' \setminus C_N(X_N)$. Note that at the initial state $X' = X$. Then, each SBS $j \in S$ receives the requests and place the top q_j requests between the user and the BS on the waiting list and rejects the rest. Note that the MBS does not have a quota limitation (i.e., as no physical constraints) so all users not associated with a SBS in the UL or DL direction are associated with the MBS. The BSs order their preferences based on different utility function given in (4.9).

In our model, since the user's preferences are not singleton sets like in conventional matching, we consider that an accepted preference must include both UL and DL contracts. For example, for a set of contracts $\{\mathrm{UL}_j, \mathrm{DL}_k\}$ of user i, if only BS j accepts the UL transmission and BS k rejects the DL transmission, then this set of contracts is considered as rejected. At this step, the rejected set of contracts, named as $R_B(X_B)$, is generated from BSs' perspective. The algorithm repeats as the rejected users submit requests for assignment to their next preferred set of contracts in which the remaining set of contracts $X' = X \setminus R_B(X_B(\text{iteration} - 1))$. Again, each SBS $j \in S$ creates a new waiting list of the top ranked q_j users among the previous waiting list and the new users, and rejects the rest. This algorithm is repeated and converges once $R_B(X_B(\text{iteration})) = R_B(X_B(\text{iteration} - 1))$ which means that every user $i \in N$ is associated with some BSs based on both users' and BSs' preferences. The following lemma states that the above described matching algorithm results in a stable allocation.

Lemma 4.3.2 *Let $(X_N, X_B) \subset X \times X$ is a solution to the system of equations, $X_N = X \setminus R_B(X_B)$ and $X_B = X \setminus R_N(X_N)$, then $X_N \cap X_B$ is a stable allocation and $X_N \cap X_B = C_N(X_N) = C_B(X_B)$. Conversely, for any stable collection of contracts X', there exists*

some pair (X_N, X_B) *satisfying the above two equations such that* $X' = X_N \cap X_B$.

As our matching algorithm is an adaptation of the doctor-offering algorithm in [76], we refer to [76] for detailed proof.

4.4 Optimal Decoupled User Association

The matching based algorithm described in the last section results in feasible and stable associations, and can also be implemented in a distributed (self-organizing) manner. To benchmark our matching based solution in terms of nearness to optimality, here we formulate the optimal user association problem in the decoupled context as a mixed integer linear program. It also serves as a centralized computationally expensive but optimal alternative (representative of [152]) to other approaches considered in the evaluation, including our proposed solution. We consider maximizing total rate across DL and UL directions as the objective for the optimization problem. We define the following variables:

$$z_{i,j}^{\mathrm{DL}} = \begin{cases} 1, & \text{user } i \text{ is associated with BS } j \text{ in DL} \\ 0, & \text{otherwise} \end{cases} \tag{4.13}$$

$$z_{i,j}^{\mathrm{UL}} = \begin{cases} 1, & \text{user } i \text{ is associated with BS } j \text{ in UL} \\ 0, & \text{otherwise} \end{cases} \tag{4.14}$$

The UL rate can be calculated by taking into account the decoupling in the following way:

$$z_{i,j}^{\mathrm{DL}} z_{i,k}^{\mathrm{UL}} (1 - c_{\mathrm{DC}}(j,k)) \theta_{i,k}^{\mathrm{UL}} \tag{4.15}$$

where note that $c_{\mathrm{DC}}(j,j) = 0, \forall j \in B$.

We need to define a new set of variables given by

$$y_{i,j,k} = z_{i,j}^{\mathrm{DL}} z_{i,k}^{\mathrm{UL}}, \quad \forall i \in N, \forall j,k \in B \tag{4.16}$$

Thus, the optimal total rate can be calculated as following:

$$\max_{z,y} \sum_{i\in N}\sum_{j\in B}\left\{\theta^{\mathrm{DL}}_{i,j} z^{\mathrm{DL}}_{i,j} + \sum_{k\in B}(1-c_{\mathrm{DC}}(j,k))\theta^{\mathrm{UL}}_{i,k} y_{i,j,k}\right\} \text{ s. t.}$$
$$\sum_{j\in B} z^{\mathrm{DL}}_{i,j} = 1, \quad \forall i \in N$$
$$\sum_{j\in B} z^{\mathrm{UL}}_{i,j} = 1, \quad \forall i \in N$$
$$\sum_{i\in N} z^{\mathrm{DL}}_{i,j} \leq q_j, \quad \forall j \in S$$
$$\sum_{i\in N} z^{\mathrm{UL}}_{i,j} \leq q_j, \quad \forall j \in S$$
$$z^{\mathrm{DL}}_{i,j} + z^{\mathrm{UL}}_{i,k} - y_{i,j,k} \leq 1, \quad \forall i \in N, \forall j,k \in B$$
$$z^{\mathrm{DL}}_{i,j} + z^{\mathrm{UL}}_{i,k} - 2y_{i,j,k} \geq 0, \quad \forall i \in N, \forall j,k \in B \tag{4.17}$$

First and second constraints ensure that a user must be associated to only one BS. Third and fourth constraints mean that at most q_j users can be associated with SBS $j \in S$. Last two constraints come from linearization of the product of two binary variables.

4.5 Evaluation

We evaluate our matching with contracts approach in three stages. First, we assess the goodness of the user associations using our approach compared to the optimal solution obtained from solving the optimization problem presented in subsection 4.4 (that also represents [152] from the literature). Then, we compare our matching with contract approach with the decoupled user association based on conventional matching approach from [155], another recent work on decoupled user association [55] which we refer to as Decoupling with Backhaul awareness ($BH_{\mathrm{Awareness}}$), and the coupled association case where each user uses the same BS in UL and DL based on classical max-SINR criterion applied in DL direction [44]. We use uplink and downlink average rates (i.e. bits/s/Hz) (corresponding to those presented earlier in section 4.3) to evaluate the performance of our algorithm. Lastly, we study the conditions where long-term matching has better performance result compared to instantaneous matching with different BS intensity (spatial density) levels and fading duration.

Concerning the first set of evaluations, Fig. 4.2 shows the results as a function of varying number of users, $|N| = 10$ to $|N| = 19$ (results for higher number of users are not included because of very high computational times needed to compute the optimal

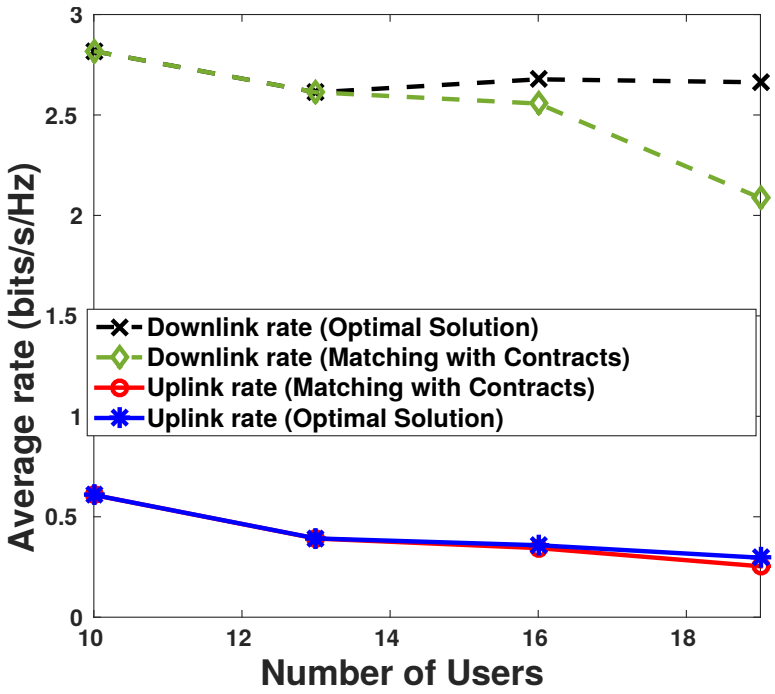

Figure 4.2: Performance comparison with the optimal, in terms of average UL and DL rates with varying number of users

solution.) and with number of SBSs $|S| = 3$, and with one MBS. We see that our matching with contracts approach performs close to optimal solution in terms of the average UL and DL rate. However, the performance of DL rate is slightly different from UL rate. This due to the fact that in matching approach, base stations play a role in association problem where it decide either to accept user association or not based on preferences list. Consider this example: user 1 prefers contract $\{UL_1, DL_2\}$ over contract $\{UL_1, DL_3\}$; on the other hand, in downlink direction BS 2 prefers contract $\{DL_3\}$ over $\{DL_1\}$, this means that BS 2 could accept user 3 association over user 1 which in turn affect the downlink performance as user 1 would associate with BS 3 which has lower DL performance compared to BS 2. Hence, this role of base stations is not reflected in optimal solution.

Fig. 4.3 shows the average number of iterations, the matching with contracts algorithm needs for convergence with increasing number of users compared to the conventional matching algorithm. We observe that the convergence time is almost the same in both cases which can be explained by the fact that both algorithms are based on Gale-Shapley deferred acceptance algorithm. In fact, we notice that as the number of users becomes large relative to the number of BSs, i.e., at $|N| \geq 50$ for $|B| = 10$, the average number of iterations becomes almost constant.

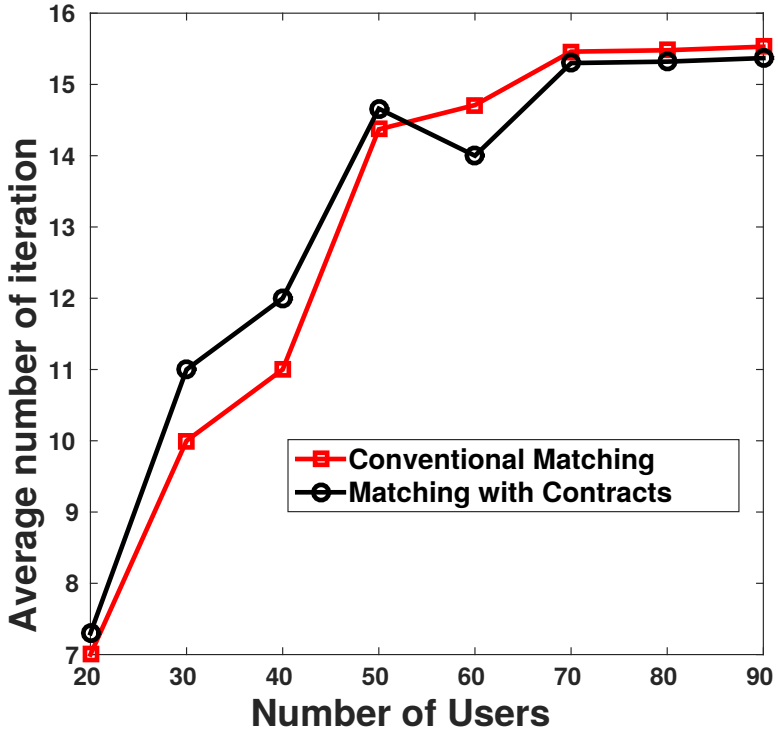

Figure 4.3: Average number of iterations till convergence of matching with contracts algorithm with varying number of users.

This is due to the fact that SBSs have limited quota and so when number of users increases total number of users become greater than total available quota on all SBSs, the number of iteration will be almost constant as SBSs will accept the same preferred users and not require further iterations.

In the second set of evaluations, we compare our approach against alternative approaches mentioned above using simulations and with larger number of users and SBSs. For simulation parameters, we consider simulation parameters similar to those in [149], which model a macro-cell in a square area of $50m \times 50m$ with the MBS at the center, however, our approach is not limited only to these parameters. In this macro-cell area, we randomly deploy the SBSs and users. We set all users' transmit powers to $13dBm$, transmit power of SBSs to $20dBm$, MBS transmit power to $40dBm$ and the quota of the SBS is set to a typical value of $q_j = 4$, $\forall j \in S$. Each data point in the plots is an average of 1000 runs, over various possible locations of the SBSs and users. For approaches in [155] and [55], we run the simulation for uplink and downlink separately with the same parameters we used in matching with contracts approach and then we consider the cost of decoupling after getting the result; this is justified as neither of these approaches are designed to account for decoupling cost.

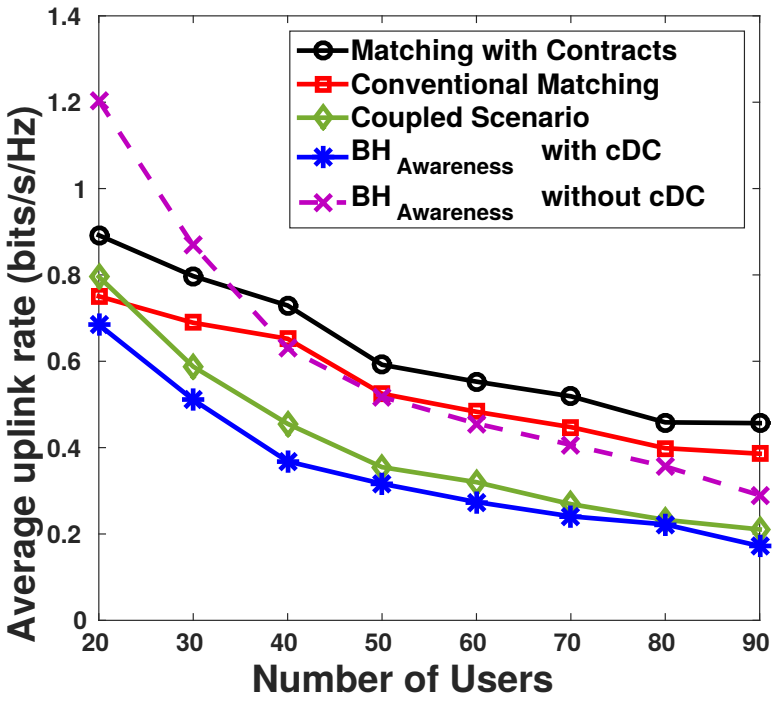

Figure 4.4: Uplink average rate results for different approaches with varying number of users.

Fig. 4.4 shows the uplink rate gain in case of matching with contracts compared to conventional matching approach, $BH_{\text{Awareness}}$ approach and coupled association case. We observe that matching with contract approach has advantage over other approaches aided by its awareness of decoupling cost that helps avoid user associations with BSs with high decoupling cost (lower uplink rate). As a result, matching with contracts algorithm has the highest average uplink average rate. It improves the average uplink rate compared to the conventional matching algorithm in the case of number of users varies from $|N| = 20$ to $|N| = 90$, and number of base station equals 10 with intensity, $\lambda_S = 0.004$. When the number of users increases, the matching with contracts approach still has better performance compared to other approaches. The $BH_{\text{Awareness}}$ without cDc approach ignores the decoupling cost; that is the reason why when the number of users is less than 30, it has slightly higher performance compared to other approaches. However, when we consider the same algorithm with a realistic scenario that considers the decoupling cost as in $BH_{\text{Awareness}}$ with cDc, the performance drops. That drop in the performance is due to the fact that the utility function of this algorithm does not take into account the decoupling cost in which it only tries to maximize the total throughput of uplink and downlink independently. On the other hand, the performance of downlink rate in case of matching with contracts is close to the conventional

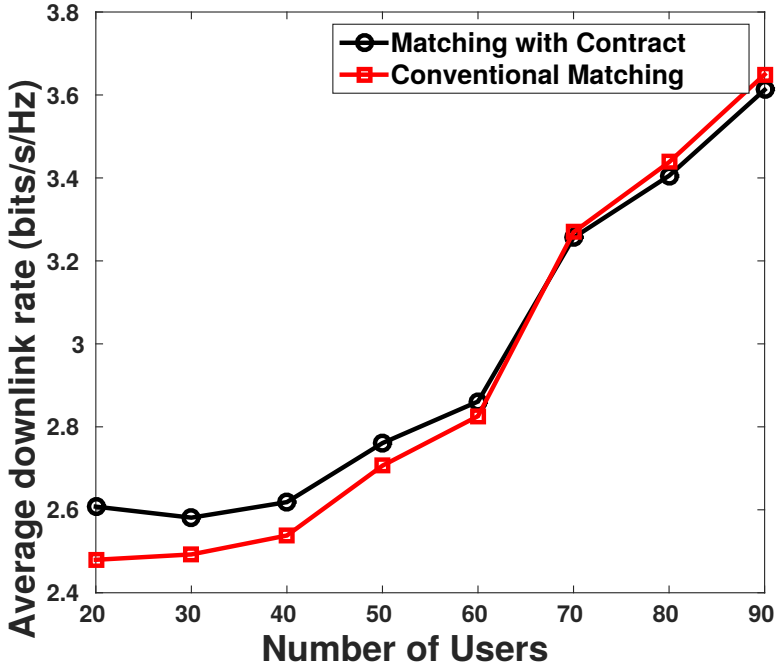

Figure 4.5: Downlink average rate results for different approaches with varying number of users.

matching approach, as shown in Fig. 4.5. This is because both algorithms uses the same max-SINR which is used also in the other approaches (e.g., coupled association and decoupling with $BH_{\text{Awareness}}$). Also note that true performance of $BH_{\text{Awareness}}$ approach is after accounting for the decoupling cost which in fact makes it worse than the baseline coupled association case.

In the third set of evaluations, we studied the question of *which type of matching is more practical: Instantaneous matching or Long-term matching?* The difference between the two types of matching lies in deciding when the mobile user updates its user association (matching decision), whether instantaneously every few milliseconds or relatively infrequently (keeping the association for a longer term) say every few seconds/minutes. We study the conditions where the long-term matching could be better or worse than instantaneous matching. First, we studied the effect of BS density (intensity) on both cases. We find that when BS intensity increases the downlink average rate also decreases in both cases. This is because mobile users suffers more interference compared to lower density conditions, as in Fig. 4.7. On the other hand, both Long-term and Instantaneous matching perform differently in case of uplink average rate when the intensity increases. In Long-term matching the average uplink rate increases when the number of base station increases as mobile users start to find closer

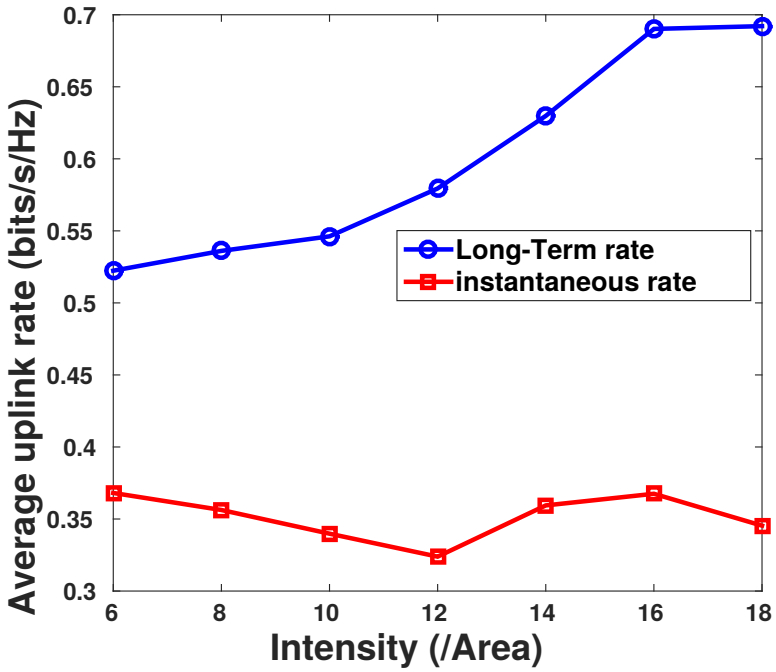

Figure 4.6: Uplink average rate when base station intensity increases.

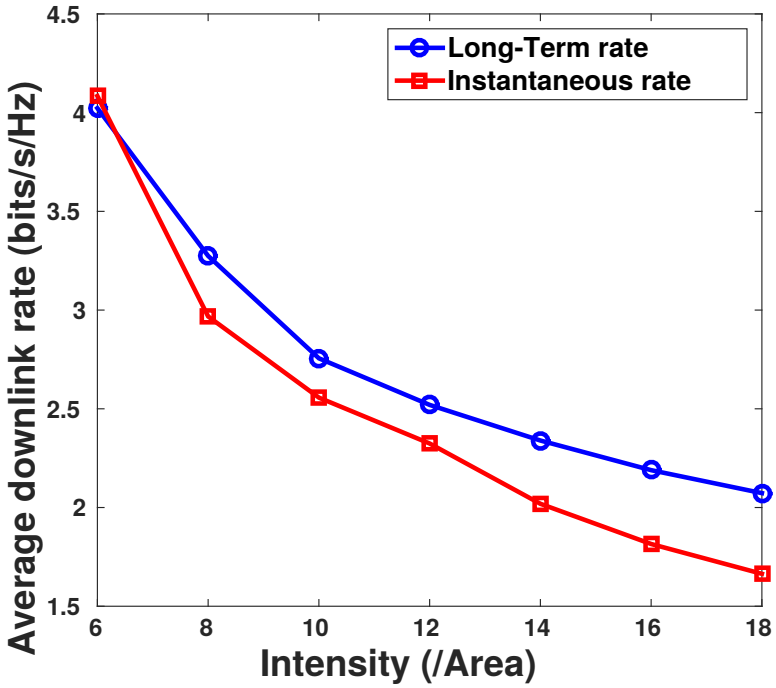

Figure 4.7: Downlink average rate when base station intensity increases.

base station to associate with, however, the average uplink rate in Instantaneous matching is unaffected by base station intensity, as shown in Fig. 4.6. Beside, base station intensity, we study the effect of average fading duration T (Fig. 4.8, 4.9). In both cases of uplink and downlink and when the number of base station equals $B = 20$, it is clear

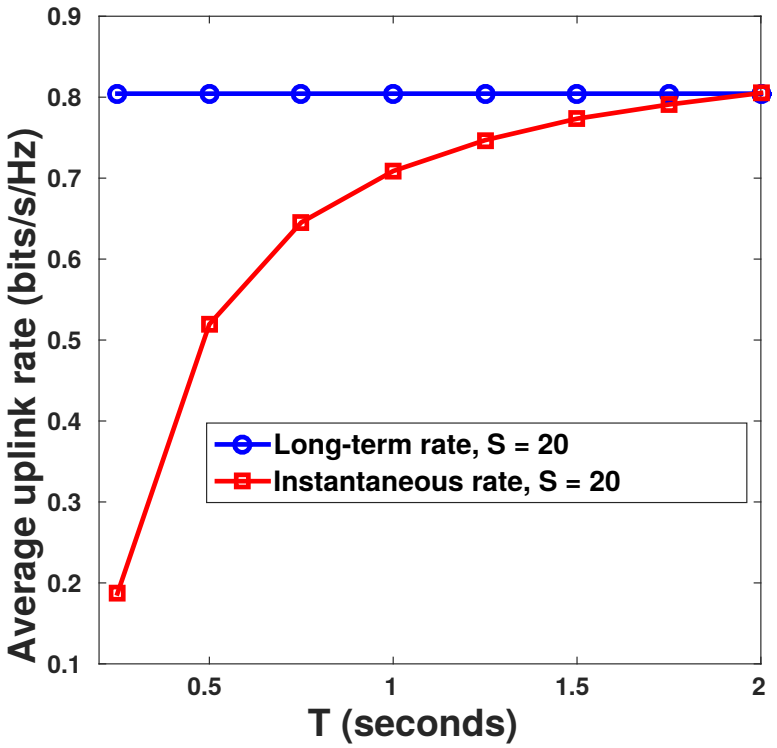

Figure 4.8: The effect of average fading duration on Long-term and Instantaneous matching in uplink direction

that using Long-term matching is better than Instantaneous matching as long as the average fading duration is below *2 seconds* (i.e., fast fading conditions). This is because of the cost of redoing association, in case of instantaneous matching, in response to time-varying channel conditions. In addition, in the case of slow fading conditions ($>$ *2 seconds*), both long-term and instantaneous matching have almost similar performance. Thus, it is very clear that the *Long-term* matching that we adopt becomes more attractive compared to *Instantaneous* matching when the BS density increases and as the channel conditions vary rapidly.

4.6 Proof of Lemma 4.3.1

Case 1: If BS j is a small BS:

$$\theta_{i,j}^{\mathrm{DL}} \triangleq \mathbb{E}\left[\ln\left(1+\mathrm{SINR}_{i,j}^{\mathrm{DL}}\right)\right] = \mathbb{P}\left[\ln\left(1+\mathrm{SINR}_{i,j}^{\mathrm{DL}}\right) < t\right] =$$

$$1-\mathbb{P}\left[\frac{P_j g_{i,j} d_{i,j}^{-\alpha}}{\sum_{k\in S\setminus j} P_s g_{i,k} d_{i,k}^{-\alpha} + P_m g_{i,m} d_{i,m}^{-\alpha} + N_0} > e^t - 1\right]$$

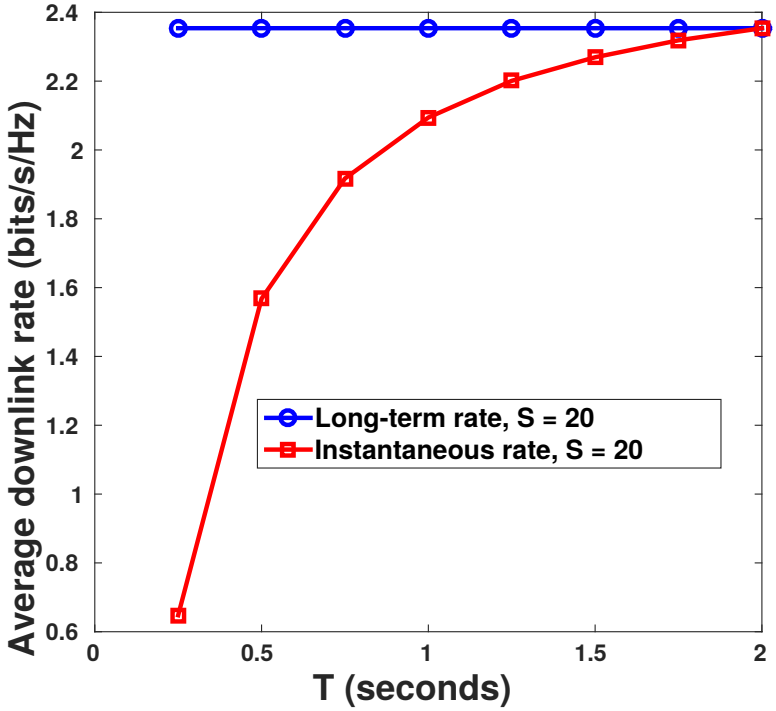

Figure 4.9: The effect of average fading duration on Long-term and Instantaneous matching in downlink direction

$$\mathbb{P}\left[g_{i,j} - \frac{(e^t-1)P_m d_{i,m}^{-\alpha}}{P_s d_{i,j}^{-\alpha}} g_{i,m} > \frac{(e^t-1)(\sum_{k\in S\setminus j} P_s g_{i,k} d_{i,k}^{-\alpha})}{P_s d_{i,j}^{-\alpha}}\right]$$

Let $\chi = g_{i,j} - \frac{(e^t-1)P_m d_{i,m}^{-\alpha}}{P_s d_{i,j}^{-\alpha}} g_{i,m}$ where χ is a difference between two exponentially distributed random variables. Therefore, the PDF $f(\chi)$ and CDF $F(\chi)$ equals:

$$f(\chi) = \frac{P_s d_{i,j}^{-\alpha}}{(e^t-1)P_m d_{i,m}^{-\alpha} + P_s d_{i,j}^{-\alpha}} \begin{cases} e^{-\chi} & \text{if } \chi > 0 \\ e^{(e^t-1)P_m d_{i,m}^{-\alpha}} & \text{if } \chi < 0 \end{cases}$$

$$F(\chi) = \frac{P_s d_{i,j}^{-\alpha}}{(e^t-1)P_m d_{i,m}^{-\alpha} + P_s d_{i,j}^{-\alpha}} \cdot \begin{cases} 1 + \frac{(e^t-1)P_m d_{i,m}^{-\alpha}}{P_s d_{i,j}^{-\alpha}} - e^{-\chi}, & \text{if } \chi > 0 \\ \frac{(e^t-1)P_m d_{i,m}^{-\alpha}}{P_s d_{i,j}^{-\alpha}} e^{(e^t-1)P_m d_{i,m}^{-\alpha}}, & \text{if } \chi < 0 \end{cases}$$

$$\mathbb{P}\left[g_{i,j} - \frac{(e^t-1)P_m d_{i,m}^{-\alpha}}{P_s d_{i,j}^{-\alpha}} g_{i,m} > \frac{(e^t-1)(\sum_{k\in S\setminus j} P_s g_{i,k} d_{i,k}^{-\alpha})}{P_s d_{i,j}^{-\alpha}}\right]$$
$$= \frac{P_s d_{i,j}^{-\alpha}}{(e^t-1)P_m d_{i,m}^{-\alpha} + P_s d_{i,j}^{-\alpha}} \exp\left(-\frac{(e^t-1)N_0}{P_s d_{i,j}^{-\alpha}}\right)$$
$$\cdot \exp\left(-\frac{(e^t-1)}{d_{i,j}^{-\alpha}} \sum_{k\in S\setminus j} g_{i,k} d_{i,k}^{-\alpha}\right)$$

Therefore, the PDF and CDF of the downlink direction can be found as:

$$F^{DL}(t) = 1 - \frac{P_s d_{i,j}^{-\alpha}}{(e^t-1)P_m d_{i,m}^{-\alpha} + P_s d_{i,j}^{-\alpha}} \exp\left(-\frac{(e^t-1)N_0}{P_s d_{i,j}^{-\alpha}}\right)$$
$$\cdot \exp\left(-\lambda_B \pi d_{i,j}^2 (e^t-1)^{2/\alpha} \frac{2\pi/\alpha}{\sin(2\pi/\alpha)}\right)$$
$$f^{DL}(t) = \frac{P_s d_{i,j}^{-\alpha}}{(e^t-1)P_m d_{i,m}^{-\alpha} + P_s d_{i,j}^{-\alpha}}$$
$$\cdot \left(\frac{e^t N_0}{P_s d_{i,j}^{-\alpha}} + \lambda_B \pi d_{i,j}^2 e^t (e^t-1)^{2/\alpha-1} \frac{4\pi/\alpha^2}{\sin(2\pi/\alpha)}\right)$$
$$\cdot \exp\left(-\frac{(e^t-1)N_0}{P_s d_{i,j}^{-\alpha}} - \lambda_B \pi d_{i,j}^2 (e^t-1)^{2/\alpha} \frac{2\pi/\alpha}{\sin(2\pi/\alpha)}\right)$$

Case 2: Similarly, If BS j is the macro BS, we have only on random variable $g_{i,m}$:

$$F^{DL}(t) = 1 - \exp\left(-\frac{(e^t-1)N_0}{P_m d_{i,j}^{-\alpha}}\right)$$
$$\cdot \exp\left(\lambda_B \pi d_{i,j}^2 (e^t-1)^{2/\alpha} \left(\frac{P_s}{P_m}\right)^{2/\alpha} \frac{2\pi/\alpha}{\sin(2\pi/\alpha)}\right)$$
$$f^{DL}(t) =$$
$$\left(\frac{e^t N_0}{P_m d_{i,j}^{-\alpha}} + \lambda_B \pi d_{i,j}^2 e^t (e^t-1)^{2/\alpha-1} \left(\frac{P_s}{P_m}\right)^{2/\alpha} \frac{4\pi/\alpha^2}{\sin(2\pi/\alpha)}\right)$$
$$\cdot \exp\left(-\frac{(e^t-1)N_0}{P_m d_{i,j}^{-\alpha}} - \lambda_B \pi d_{i,j}^2 (e^t-1)^{2/\alpha} \left(\frac{P_s}{P_m}\right)^{2/\alpha} \frac{2\pi/\alpha}{\sin(2\pi/\alpha)}\right)$$

4.7 Discussion

In this work, we studied the decoupled performance in a half-duplex scenario where we assume different uplink and downlink frequencies. The mobile user jointly selects the two base stations to maximize the total throughput (uplink and downlink). On the other hand, the full-duplex coupled user association assumes that the uplink and downlink frequencies are the same; in addition, the mobile user associates to the same base station in both directions. Although the available bandwidth, in the full-duplex, is doubled (compared to the half-duplex scenario); however, the mobile user still experiences

bad performance in the uplink direction. The reason because the mobile user associates with the same base station that is preferred in the downlink direction (i.e., based on DL maximum received signal power criterion). In addition, doubling the bandwidth does not help to boost the uplink performance because the mobile user transmission power is limited. Hence, it might negatively affect UL SINR. Therefore, in terms of uplink performance, the half-duplex decoupled user association might perform better than the full-duplex coupled user association.

On the other hand, the full-duplex coupled user association guarantees better spectral efficiency if the self-interference is significantly mitigated. Several recent studies have focused on the decoupled user association in the full-duplex scenario. They proposed an interference-aware user association utility function in order to maximize the total throughput while avoiding the UL-to-DL or DL-to-UL interference in full-duplex mode [155, 156].

4.8 Summary

In this chapter, we focused on the first use-case of the multi-connectivity paradigm. More specifically, we have studied the problem of decoupled UL/DL user association in a HetNet context, given the diverse objectives, preferences and capabilities of the three types of entities involved: the users, the small-BSs, and the macro BSs. We formulate this problem as a matching with contracts game by drawing an analogy with the doctors-to-hospitals matching problem in the matching literature. Our user-BS matching algorithm results in stable associations and its convergence is comparable to standard (one-to-many) matching. This is also the first time matching with contracts was employed for addressing any wireless resource allocation problem. Through extensive simulation based evaluations, we show that the proposed approach outperforms existing matching based solutions for decoupled user association as well as traditional coupled user association. In addition, our solution also provides close to optimal performance.

As the number of mobile users and base stations increase, the distributed algorithm proposed in this work is considered to be more practical and less complex compared to the centralized optimization approach. Thus, the feasibility of the centralized approach is questionable because of the milliseconds time constraints of the user association problem. On the other hand, our distributed approach guarantees the near-to-optimal performance within reasonable time complexity, as discussed in the evaluation section.

Our distributed user association approach can be integrated into the RRC layer, and during the RACH procedures, the base station decides whether to accept or reject the association request. More specifically, when the mobile user sends the RRCConnectionRequest message, the base station should evaluate the requested mobile user based on the criteria we discussed above and reply with RRCConnectionSetup if it accepts the mobile user request or replies with RRCConnectionRelease if the request is rejected. The key limitation of this approach is that it might require some changes to the RRCConnectionRelease message to include different release cause.

Chapter 5

DIY Mobile Network Deployment Model for Rural and Developing Regions

Mobile phones undoubtedly are an integral part of people's lives in much of the world helping them stay socially connected, have access to information etc. wherever they may be. Their use in the developing world has been rising rapidly and has been innovative too, going beyond these usual benefits to enable better governance, improved citizen engagement in democratic processes, better health monitoring, creating economic opportunities, and so on. In view of their role as Internet end-hosts in modern mobile networks, they can be seen from the perspective of broadband Internet access and associated impact on the economy. According to World Bank estimates, every 10% increase in broadband Internet access translates to 1-2% rise in gross domestic product (GDP). Moreover, next-generation 5G mobile networks, which will start being rolled out in a few years, are expected to have even greater impact on the global GDP, sustained over a longer term period [84].

Yet, we are still quite some distance away from universal data oriented mobile access. Mobile services reach 95% of the world's population today but this is limited to only GSM/2G access (mobile voice and SMS) and even so mobile subscriber penetration is relatively lower at 66% [69]. From an Internet access viewpoint (including via mobile networks), more than half the world's population lacks access, with per capita Internet users in very low income countries even lower than 15%. The major challenge lies in taking the Internet connectivity via traditional means beyond the major urban centers to rural and remote areas [33].

Traditional mobile operators have little economic incentive to expand the reach of their infrastructure to provide high-end 4G and beyond data oriented services for

scattered and sparsely populated areas as well as for low-income regions with small number of prospective subscribers. Universal service obligations included as part of mobile spectrum auctions in developed countries also have not achieved the intended service coverage goals in practice. The traditional approach to mobile service provisioning also lacks the flexibility to cater to the particular requirements of developing region settings such as local services and content delivery. In recent years, a cost-effective alternative approach has emerged in the form of community cellular networks [22, 78, 79, 146, 173, 154], leveraging open source platforms like OpenBTS, minimizing power consumption by adapting to demand and enabling local services. However these efforts only offer voice and SMS type services as with GSM.

In this chapter, we propose a do-it-yourself (DIY) model for deploying mobile networks in under-served regions that is in the spirit of above mentioned community cellular networks but aimed at provisioning high-end (4G and beyond) mobile services. Our proposed model is in tune with the increasing openness (in terms of ecosystem with IT/cloud vendors and verticals, platforms, spectrum types, services, etc.) and cloudification of mobile networks in the run up to 5G. It is meant to enable and ease deployments at low cost by a new set of non-traditional operators (e.g., communities, local small-scale mobile network operators) in areas with market failure and limited availability of mobile services, thereby allowing these areas to leapfrog towards 5G through bottom-up initiatives.

Specifically, the network architecture based on our model consists of three main components. Firstly, the core network component is realized as a commodity and customizable cloud service. Secondly, the access network component is realized via plug-and-play small cell base stations, ideally leveraging open software platforms (e.g., OpenAirInterface [119], srsLTE [1], OpenCellular [61]), software radios and unlicensed/shared spectrum, and commodity end-user devices (smartphones and MiFi devices). Thirdly, the access and core networks are interconnected via a low cost backhaul infrastructure. Depending on the deployment setting this could be realized differently using a different combination of wired/wireless technologies (e.g., fiber, satellite, microwave, long-distance Wi-Fi). We in particular highlight the potential of exploiting TV white space (TVWS) spectrum (given the ample availability of this spectrum and its propagation characteristics) to enable a low-cost backhaul with fewer number of intermediate backhaul relays, especially with aggregation of multiple TVWS channels [93]. To demonstrate the practicality of the above outlined model, we present a

[1] https://github.com/srsLTE/srsLTE

trial deployment of a particular instance of this model in a rural area in the UK with poor conventional market-driven broadband/mobile infrastructure. We should note that our proposed deployment model is complementary to various recent proposals that can be viewed under the umbrella of 5G for universal access, including the use of drones or unmanned aerial vehicles (UAVs) [157, 39]; white space spectrum [97, 136]; millimeter wave (mmWave) spectrum [49, 110, 109]; and Massive MIMO [60].

5.1 Challenges for Deploying Modern Mobile Networks in Under-served Regions

Deploying mobile networks is challenging in rural/developing regions. There are a range of factors that constrain such deployments including the low population density and sparse distribution; affordability; the location of nearest Internet point-of-presence (PoP); the unreliability and limits of the power sources; and the deployment area terrain. These factors have major influence on the deployment cost, architecture (both access and backhaul networks) and reliability. Here we elaborate on some of the key underlying challenges, which especially hinder deployment of data oriented current and emerging mobile networks in such regions.

High Infrastructure and Operational Costs. Deploying mobile infrastructure in rural and developing regions is seen to be economically unattractive for traditional operators to recoup the high (access and backhaul) infrastructure cost and recurring operational expenses from the small number of subscribers that would be served. For non-traditional operators, deployment using licensed spectrum may be prohibitively expensive. Cost of powering base stations is also an issue in developing regions as noted in prior work [78].

Lack of Affordable Backhaul (Middle-Mile) Network Infrastructure. This is a crucial part of the end-to-end connectivity to bridge local access networks with the wider Internet, and also dictates their effective capacity and reliability. Both wired and wireless backhaul solutions have been considered in the rural Internet access context. Wired backhaul solutions such as fiber offer high capacity and reliability but with a high cost that is proportional to the required distance and capacity. Wireless solutions, on the other hand, can be relatively cost-efficient but challenging to match the capacity and reliability of wired approaches as they need to grapple with issues like type and amount of spectrum available; terrain and climatic conditions; power availability;

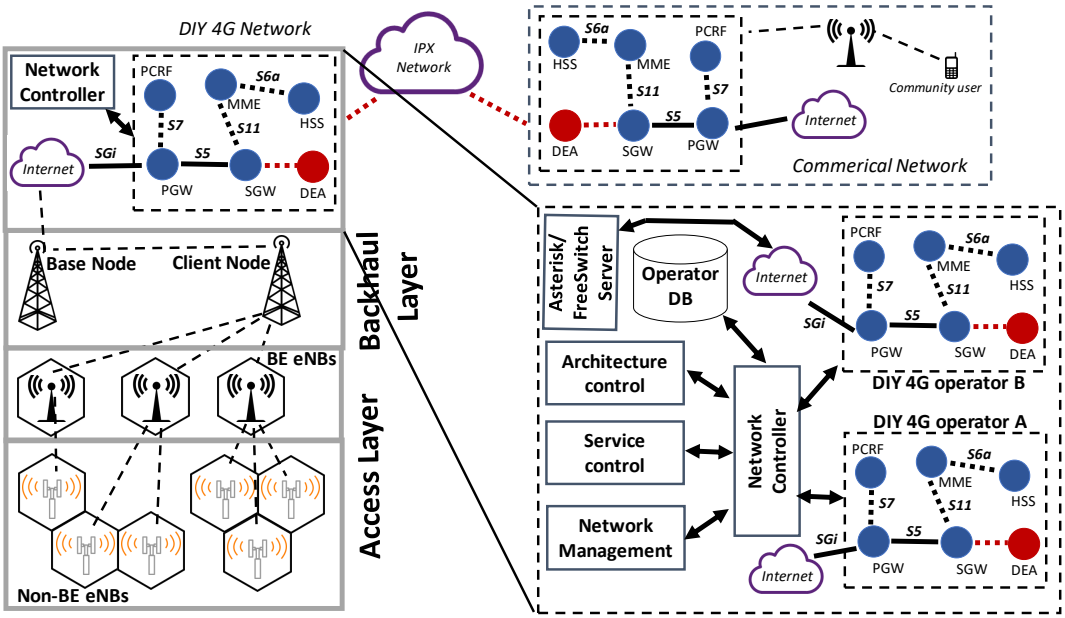

Figure 5.1: Schematic illustration of of DIY xG mobile network architecture considering the case of 4G/LTE.

deployment and maintenance costs.

Limited Flexibility. Proprietary black box solutions employed in conventional mobile network deployments limit the flexibility needed for rural and developing region settings. The market demand is different from one community to another, therefore, a fixed and rigid deployment model may be insufficient to address and handle the diversity of service requirements.

5.2 DIY xG Mobile Network Deployment Model

To better address the aforementioned challenges and accelerate the arrival of high-end and flexible mobile services to under-served regions, we propose an alternative DIY deployment model for such regions. Before elaborating our proposed model, we first outline the design principles that shaped it.

5.2.1 Design Principles

Low Cost. As already stated, high cost can seriously limit the mobile service usage in under-served regions but also their availability in the first place. Therefore being cost-effective is paramount. This could be achieved via the use of unlicensed/shared spectrum, open source software platforms, software radios and virtualized network

functions over commodity hardware and cloud infrastructure.

Ease of Deployment and Operation. Plug-and-play deployment is essential to lower the initial deployment costs and then to organically grow the infrastructure with new users. Equally, automated and flexible network management is key to lower the operational costs, especially in settings with limited technical know-how, and to add/adapt services as per the evolving needs of the target community.

Flexibility. In under-served regions, different communities present different demands and their affordability of mobile services can also be significantly different. For example, agricultural communities would need the cellular data service to boost their farm productivity using different Internet of Things (IoT) applications [164]. The service requirements for such IoT applications can vary from few hundreds of Kbps for basic monitoring applications to multiple Mbps for precision farming or agricultural drones types of application. Another example is the remote healthcare applications that help to increase the quality of care in the remote communities. These eHealth applications have different service requirements (e.g., higher data rates, low latency). This diversity in service requirements leads to differing technical requirements between different deployments in terms of backhaul link capacity, core network processing capability, etc. Thus, flexibility in being able to accommodate such requirements in an affordable manner is desirable.

Interworking with other mobile networks. Most community-driven local mobile networks do not interwork with other mobile networks (commercial or otherwise). This prevents the user of a local mobile network from using the same SIM card when outside the coverage area of that network. It would however be desirable to have users transparently access mobile services no matter where they are and to communicate with mobile users from other networks. There is some recent work addressing such interworking issues, e.g., leveraging VoIP gateways or service providers to allow the mobile users in a local community to connect with external users [85, 19]; and extending the footprint of commercial networks with local cellular networks [153].

5.2.2 Architecture

The proposed deployment model (illustrated in Fig. 5.1) is guided by the above principles. It consists of three main components/layers: access, backhaul and core network layers.

Access Network Layer. Access network infrastructure in our model can comprise

of two types of base stations (eNodeBs/eNBs in 4G/LTE) depending on whether they have direct backhaul connection to the core network. End users in this model either connect via MiFi devices when inside their homes or directly from their smartphones otherwise. Backhaul enabled base stations, in addition to interfacing with the backhaul and serving associated end users, also serve as traffic relay for non-backhaul enabled base stations. Capability of base stations can be realized either with commercial (LTE) small cell base stations or via open source software platforms like OpenCellular, OpenAirInterface or srsLTE along with software radios. Spectrum wise, several different possibilities exist including TVWS spectrum as in [28] and unlicensed/shared spectrum via MulteFire[2] like technology.

Backhaul Network Layer. With cost optimization in mind, we consider wireless backhaul as the suitable option for this layer. Among the various wireless alternatives, we believe TVWS spectrum is particularly attractive as a low cost means for backhaul connectivity in view of its superior range and non-line-of-sight propagation characteristics and given the ample availability of this spectrum in rural and developing regions [93]. Both these in turn translate to lesser amount of backhaul infrastructure (fewer relays) for connectivity over a given distance with TVWS spectrum (and corresponding reduction in deployment costs) as well as the potential for high bandwidth connections like the other expensive alternatives (e.g., fiber) through aggregation of multiple TVWS channels. While in general the backhaul layer can comprise of multiple relays in Point-to-Point (PtP) or Point-to-Multi-Point (PtMP) configurations, the simplest scenario involves a single PtP link with access network end serving as a client to the other Base node (as shown in Fig. 5.1).

Core Network Layer. For reasons of cost, flexibility and ease of management, the core network layer in our model is realized as a virtualized service over a commodity cloud infrastructure. Broadly speaking, this layer is made up of two types of virtual network functions: (i) *Core network functions* that implement the key functions of a mobile core network (e.g., MME, HSS, SGW etc. in 4G/LTE networks); (ii) *Orchestration functions* which generally deal with centralized network management and control including architecture control, service control and network management. The architecture control is responsible for maintaining and controlling the current network architecture and RAN configurations of all the underlying DIY xG networks. This helps the network controller to efficiently manage the underlying access and backhaul networks and adapt their configuration parameters (e.g., operating frequencies). Service con-

[2] https://www.multefire.org/

trol implements the set of functions that are responsible for customizing/expanding the set of services offered within a community, which in turn can impact different network layers (e.g., increasing backhaul capacity, access network bandwidth, the core processing requirements). Network management focuses mainly on monitoring the underlying backhaul and access networks and generates periodic reports to the network controller. The operator database is a key component that maintains all the information about the underlying networks and their statistics such as the number of subscribers and the running services. Note that due to realization of this layer via virtual network functions in the cloud, multiple instances of core network functions corresponding to different deployments can be concurrently supported on different virtual machines (VMs) while at the same time allowing them to customizable with different set of policies and services. The network controller is responsible for applying the orchestration control functions on the respective core network instances.

Roaming capability when the user from the DIY xG network is outside its coverage but within that of another mobile network (e.g., a commercial mobile operator's coverage area) can be supported via a combination of roaming agreement/partnership setup between the cloud based core of the DIY network and other networks, and standard home routing; the latter requires a signaling connection between the visited core network and the home core network to be established to allow the user to authenticate and register under the visited network. Through the S6a interface and using Diameter protocol and diameter edge agent (DEA), this signaling is carried over an IP exchange (IPX) network between the visited network and home network.

5.3 Trial Deployment

To demonstrate the feasibility of the proposed deployment model in practice, we did a trial deployment of a particular instance of this model in Balquhidder area in rural Scotland with a cohesive and vibrant community of 200 households and supporting more than 95 diverse businesses. Due to the poor broadband and mobile infrastructure in this area, an initiative driven by the community is in process to bring fiber connectivity to majority of the properties but about 15% of them would be too expensive to reach through community fiber roll out initiative so we target those households through this trial deployment in a partnership involving the University of Edinburgh, the Balquhidder community, Microsoft Research (Cambridge) and WhitespaceUK[3].

[3] https://www.whitespaceuk.com/

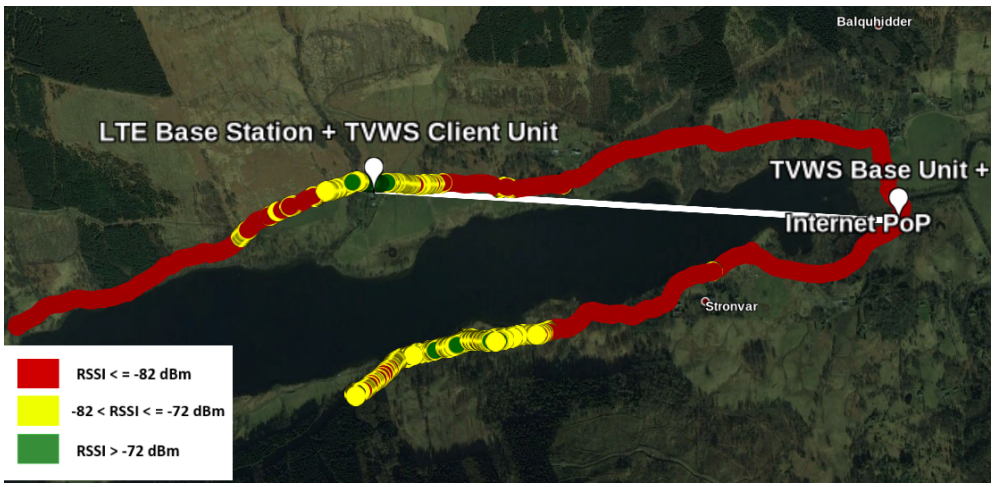

Figure 5.2: Measurement based base station coverage map of the deployment area

The deployment (as in Fig. 5.3) consists of a single LTE base station connected to the core network in the cloud via a TVWS backhaul link to the Internet POP with fiber connectivity, as shown in Fig. 5.2. For the access layer, we use IP Access [86] E40 small cell LTE base station and Novatel 6620 MiFi devices as end-user devices. The access layer is configured to use a 5MHz channel in LTE band 13 in the 700MHz supported by a non-operation development licence from Ofcom and after consulting an Ofcom-endorsed TV white space database. For the 1.6Km PtP backhaul link across the lake (Loch Voil) with considerable foliage, we use Adaptrum [1] TVWS hardware equipped with 11dBi Yagi antennas on 2m poles on each end and operating on one 8 MHz TVWS channel around 500MHz, supporting a link data rate of 12Mbps. For the core network, we leverage the ECHO core network service instantiated on Azure cloud [118]; each of the core network layer components in the cloud is a Standard-DS3 VM with 4 cores.

To assess the coverage and throughput performance with this deployment, we conducted a systematic measurement campaign in the area around the base station with an Android smartphone connected via a MiFi device to the base station. Fig. 5.2 shows the coverage map from the RSSI measurements. The green and yellow colored points represent good to moderate coverage (with an average RSSI level of -75dBm) due to them falling in the main beam of the 120 degree sector antenna used at the base station, including several locations on the other side of the lake from the base station. The distance between the base station and the moderate coverage location on the other side of the lake ranges from 500 to 700 meters. Points outside of the main beam shown in red color exhibit poor coverage with an average RSSI level of -88dBm. This indi-

Figure 5.3: TVWS client node (on the right) and LTE small cell (on the left)

cates the role of choosing the appropriate antenna and its orientation depending on the deployment setting to ensure good coverage.

In addition to coverage, we also measured uplink/downlink throughputs seen at 15 different locations from among those where RSSI levels are sampled for the coverage map. Distribution of these throughputs is shown in the form of CDFs in Fig. 5.4. While the maximum downlink throughput is almost the same as the backhaul link rate, median uplink and downlink throughputs are around 3 and 7Mbps, respectively. For those locations falling in the main beam of the base station antenna, the average throughput values are higher (8.5Mbps in the downlink and 4.4Mbps in the uplink). Even when a location is outside of the main beam but has sufficient coverage to be associated with the base station, the average throughputs are reasonable at 3.7Mbps (downlink) and 0.74Mbps (uplink). Overall these results show that mobile data services from commodity smartphones can be supported with the proposed model. With modern small cells capable of handling up to 64 devices, by scaling the channel bandwidth of the access base station and backhaul link capacity, per user and system throughputs can be correspondingly scaled up to support even more bandwidth hungry services.

We close with a brief discussion on the deployment and operational costs with

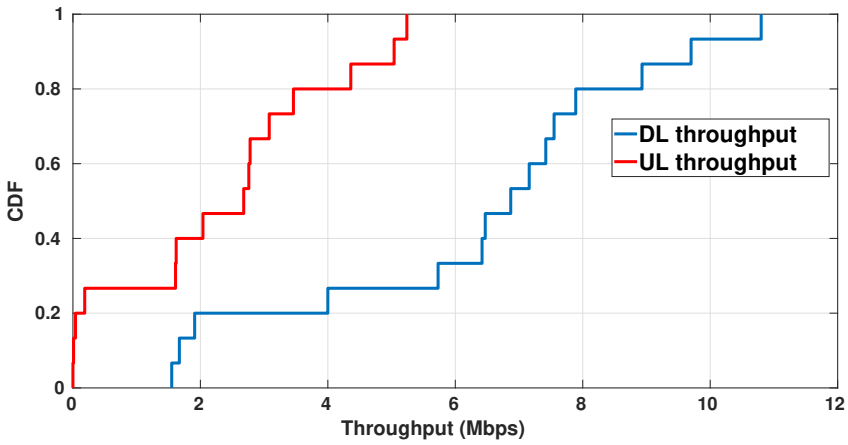

Figure 5.4: CDF of uplink/downlink throughput measured at 15 different locations across the coverage measurement survey path.

Table 5.1: Capital Expenditures (CAPEX) which is the up-front cost to construct the site and the Operational Expenditures (OPEX) represents the monthly operational costs

CAPEX	Cost (USD)	OPEX	Cost (USD)
1 eNB	1000	Cloud based core service	0.087 per GB
TVWS Backhaul	5000	Power	0.35 per kWh
1 Mi-Fi	30	**Total Monthly**	**1 USD/subscriber/month**
2 Yagi Antenna	160		
1 LTE Antennas	200		
4 N-Type Cables	156		
Total Installation	**6546**		

our proposed model. Generally speaking, these costs are highly dependent on the deployment setting, number of users and their service requirements. Although we used commercial small cell and TVWS hardware not optimized for this use case, we expect the deployment cost (CAPEX) can be brought down to within few thousand dollars at most, especially with open source platforms. Table.5.1 provides a breakdown of our CAPEX cost, which is below 7,000 USD. OPEX on the other hand is dependent largely on two factors. (1) the energy cost and (2) the cloud based service cost. The energy cost is relatively small because the TVWS backhaul solution uses Power-over-Ethernet and the LTE small cell has maximum energy consumption of 20 Watts. Therefore, the total energy consumption per month for the LTE small cell can be roughly around $14.4kWh$.

The second component in the OPEX cost is the cost of cloud based core service

and optionally the cost of accessing the TVWS database (i.e., it is negligible). As core related cost is linked with the amount of traffic handled by the cloud, it can be significantly reduced by limiting only the signaling traffic to go to the cloud and rest via a local breakout. With such optimizations, we expect the recurring costs can be reduced to well below 1 USD per subscriber per month.

5.4 Summary

In this chapter, we presented our do-it-yourself (DIY) model for deploying mobile networks in rural and remote regions that is in the spirit of earlier community cellular networks but aimed at provisioning high-end (4G and beyond) mobile services. We showcased a particular instance of the proposed deployment model through a trial deployment in rural UK to demonstrate its practical feasibility. The key observation of this study is the fact that high capacity backhauling link is crucial in order to enable 4G/5G mobile services in the rural areas. That motivates us to propose WhiteHaul system in Chapter.7. One of the limitations of this work is that it has not been deployed on large scale. Although, the proposed deployment model is scalable, in nature, however, large scale deployment will give us more insight on the user behavior in such a model.

Chapter 6

On the Potential of TVWS Spectrum to Enable a Low Cost Middle Mile Network Infrastructure

In this chapter we analytically study the nature of the TVWS spectrum in the rural area to better understand the key requirements for the backhauling system. We examine the potential for leveraging TVWS spectrum for middle mile connectivity through analysis of TVWS spectrum that could be used for this purpose, considering a representative rural region in the UK. Unlike the several previous studies on TVWS spectrum availability (e.g., [81]), we focus on the *quality* of the available TVWS spectrum to be able to enable middle mile links by accounting for not only the topography of the region but also the aggregate interference from nearby TV transmitters and relays. To this end, we introduce a novel TVWS receiver oriented notion of "usable" TVWS spectrum that differs from the commonly used TVWS transmitter side perspective on spectum availability. Our analysis shows that aggregate interference from nearby TV transmitters can in fact have a significant negative impact on the usable TVWS spectrum for establishing middle mile links. Use of directional antennas, however, can counter much of this effect and thus is crucial for the TVWS backhaul case. Our analysis also sheds light on the nature of TVWS spectrum fragmentation for this use case and this in turn poses requirements for the design of spectrum aggregation systems for TVWS backhaul.

Figure 6.1: Representative rural region in the UK considered in our analysis.

6.1 Methodology

This section describes the methodology we used for our analysis along with the newly introduced notion of "usable" TVWS spectrum. Regarding the TVWS spectrum, although it currently ranges from 490 – 790 MHz as per UK regulations [132], there is a plan to clear the 700 MHz band (694–790MHz) and allocate it to mobile operators [92]. Nevertheless, we consider the whole range as it is today.

Area and backhaul links considered. As noted at the outset, we are interested in examining the potential of TVWS spectrum for enabling middle mile connectivity in rural and developing regions. To this end, consulting the Urban-Rural Classification data [10], we select as a representative setting the rural region in the UK shown in Fig. 6.1 with dimensions 60 Kms × 60 Kms. To guide the placement of TVWS backhaul transmitters and receivers in this large area, we divide it into smaller and equal sized pixels ($0.67 Km^2$ for results in this chapter). Each of these pixels is a potential location for TVWS transmitter/receiver.

While the placement of backhaul link transmitters and receivers[1] in practice need

[1]Depending on the deployment scenario and location of the Internet PoP, there could be a sequence of TVWS links with relays connecting them that make up the TVWS backhaul. But for the sake of simplicity, we focus on each such individual links in the backhaul path.

to also consider population distribution, access to grid power and other such factors, we take a general approach considering a wide range of backhaul links only taking into account the terrain/topography and its influence on radio signal propagation. To realistically model the radio wave propagation between a transmitter/interferer and receiver, we use the new Irregular Terrain With Obstructions (ITWOM v3.0) model implemented in the SPLAT! software package [6]. Concerning the length of a TVWS backhaul link, this could vary in practice from several Kms to few tens of Kms, we consider a fixed 10Km length to limit the number of variables in our analysis. It is straightforward to repeat our analysis for other link lengths. Now to address the question of selecting the set of potential backhaul links considered in the selected area, we place a TVWS receiver in each pixel and pick a transmitter pixel location 10Kms away in the direction with least path loss (as determined by the above mentioned terrain based propagation model).

Interference calculation. At each pixel (i.e., TVWS receiver location) in Fig. 6.1, we calculate the signal-to-interference ratio (SINR) values as the ratio between the received power at the TVWS receiver (from its corresponding TVWS backhaul transmitter) and the sum of interfering power from all surrounding digital terrestrial TV (DTT) transmitters. We express the SINR value at a location κ as $\frac{P}{\sum_{i \in N} I_i + noise}$, where P is the received power from TVWS transmitter, N is number of DTT interferers. We obtained the information on location, transmission power, operating frequencies and antenna heights for all DTT stations from [9] maintained by Ofcom (the UK regulator). This information combined with the path loss calculated using the propagation model yields interference power from each DTT transmitter. To calculate the received power from the TVWS transmitter in question, we query the geolocation database with transmitter location to retrieve the list of available TV channels and their corresponding allowed transmission power in terms of Equivalent Isotropically Radiated Power (EIRP). As with interference power calculation, TVWS transmitter power discounted by the propagation related path loss gives the received power at TVWS receiver; we ignore cable related losses in our analysis. Note that as per Ofcom TVWS regulations, white space devices can fall in one of five classes, differing in their power leakage into adjacent channels [132]. We assume Class 1 devices with least power leakage in our analysis.

Usable TVWS channel. We now introduce the receiver oriented notion of a usable TVWS channel in the context of PTP TVWS backhaul links. Specifically, a TVWS channel at a location κ is considered usable if SINR exceeds a threshold ρ at that

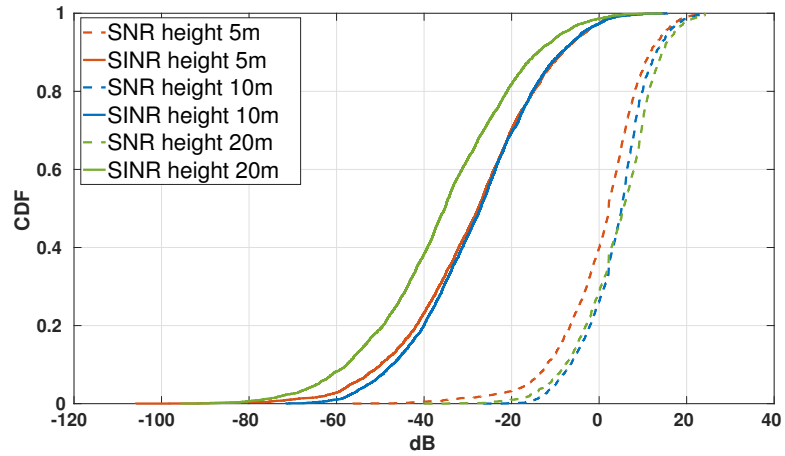

Figure 6.2: Degradation in link quality (SINR) at TVWS backhaul receivers due to aggregate DTT interference for different TVWS device antenna heights.

location. Denoting usability of a TVWS channel ch at location κ as $\Theta_{ch}(\kappa)$, we have:

$$\Theta_{ch}(\kappa) = \begin{cases} 1, & \text{if } SINR_{ch}(\kappa) \geq \rho \\ 0, & \text{otherwise.} \end{cases} \tag{6.1}$$

Where $SINR_{ch}(\kappa)$ is the SINR value on channel ch at location κ and ρ is the usability threshold parameter. Depending on this threshold parameter, received power from TVWS transmitter and cumulative interference from nearby DTT transmitters, a channel that is considered available by the geolocation database at the transmitter may not be usable at the receiver. To study the impact of this parameter, we consider three different values for the threshold in our analysis: $5, 10$, and 15 dB. Besides we also study the effect of TVWS transmitter/receiver antenna heights considering three different values: $5, 10$ and 20 meters.

6.2 Negative Impact of Aggregate Interference from DTT Transmitters

Contrary to common perception, the *effectively* available TVWS spectrum in rural areas can also be low just as in outdoor locations of urban areas due to the aggregate interference from multiple DTT transmitters. This would especially be the case when a TVWS receiver lies at the intersection coverage region of multiple surrounding DTT stations.

To better understand and quantify this effect, in Fig. 6.2 we compare the SNR and SINR at different TVWS receiver locations (pixels) in the area shown in Fig. 6.1, con-

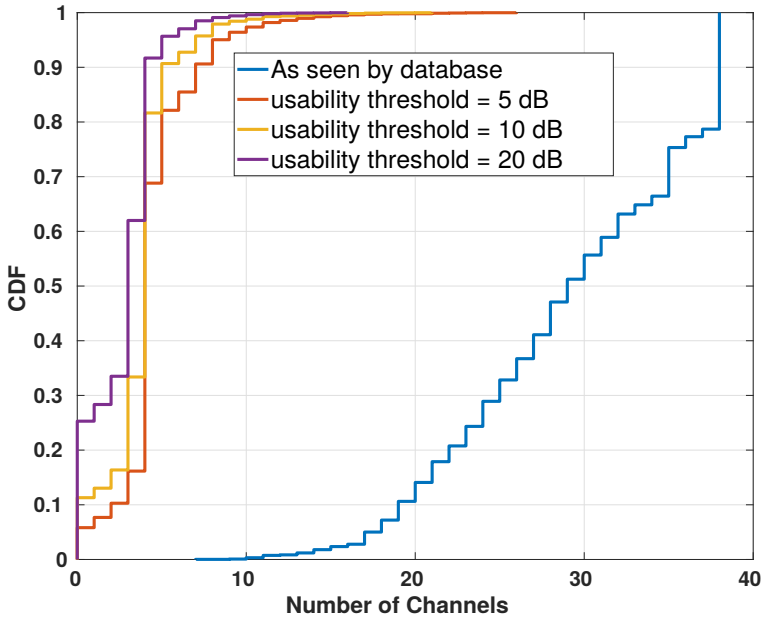

Figure 6.3: CDFs of the number of usable channels at the TVWS receiver with different usability thresholds in SINR levels compared to the number of available channels on the transmitter side as per the geolocation database for TVWS device antenna height of 20m.

sidering omni-directional antennas and at different antenna heights. Note that SINR values here capture the effect of aggregate DTT interference while SNR values indicate the receiver perceived link quality ignoring this interference. Whereas median SNR is over 0dB, the median SINR values are lower than -30dB, more than 30dB drop in receiver signal quality solely due to DTT interference. Although increased antenna heights are expected to make this effect more pronounced and is the case for some antenna heights (e.g., 20m), it is not always the case (e.g., 5m). The reason is lowering the antenna height also increases the number of locations with non-line-of-sight (NLOS) links making the weak received power a bigger concern than DTT interference.

We now look at the question of how the degradation in receiver signal quality due to aggregate DTT interference manifests in terms of the number of channels that become unusable. To this end, Fig. 6.3 presents the results for number of available/usable channels as CDFs considering different usability thresholds and a fixed TVWS device antenna height of 20m. As expected, given the rural region under consideration, the number of channels (the amount of TVWS spectrum) considered available at the transmitter side as per the geolocation database is quite high – above 20 channels (160

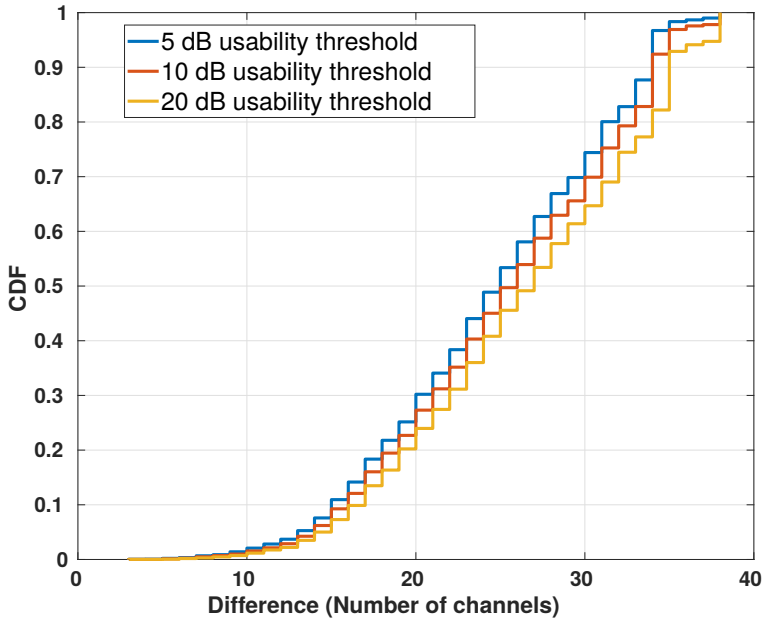

Figure 6.4: Same results shown as CDFs of difference in number of usable and available channels with different thresholds.

MHz in spectrum) in 90% of the locations and median number of available channels is around 30 (240MHz). However the number usable channels as per the TVWS receiver accounting for aggregate DTT interference drops significantly to less than 5 (40MHz) in 80% of the locations using any of the three reasonable link quality (SINR) thresholds considered. The difference in usable and available channels at different locations with different SINR thresholds is clearly shown in Fig. 6.4 . From this figure, we can observe that median drop in the number of usable channels (compared to available) is in the region of 25 (200MHz), a very significant reduction.

6.3 Benefit with Directional Antennas

Results from the last section highlight the severe reduction in the number of usable channels due to aggregate DTT interference when TVWS backhaul link devices use omni-directional antennas. In this section, we study the potential for mitigating this effect with directional antennas. Even without DTT interference, using directional antennas would clearly be a natural choice for P2P TVWS backhaul links as they have a signal amplification effect on both ends of the link due to gain of the antennas and this in turn results in range improvement for a given SINR threshold or improved

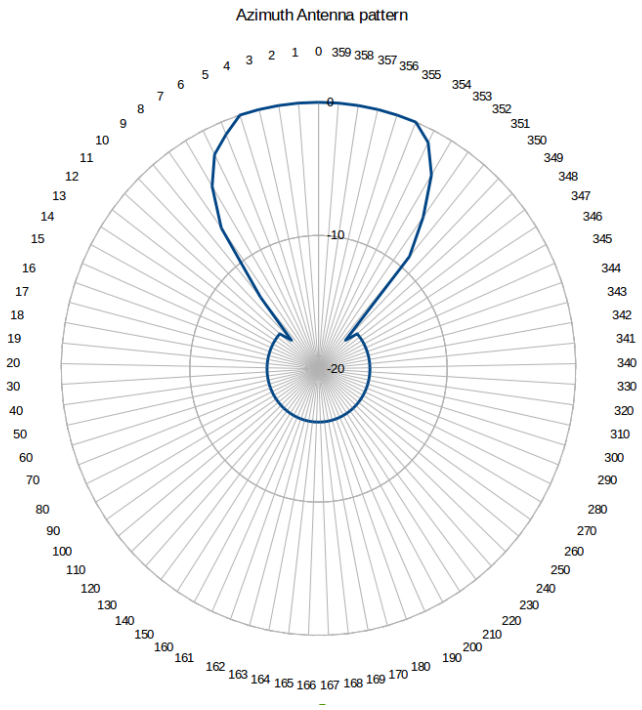

Figure 6.5: Azimuthal antenna pattern for the directional antenna (with gain = 16 dBi) used in the analysis.

SINR for a specified range due to higher received signal power. But our intention is to also consider the potential level of immunity to DTT interference that comes with the use of directional antennas, i.e., suppression of interference from directions other than the main lobe of the antenna radiation pattern; this then would result in lowering the effective interference seen by the receiver and thus also contributes to a higher SINR.

To study the benefit from employing directional antennas at the TVWS devices, we consider a directional antenna with about 10 degree beam width and radiation pattern as shown in Fig. 6.5. To make a fair comparison with the previously considered omni-directional antenna case, we keep the EIRP level at transmitter side on every available TVWS channel identical in both cases, as prescribed by the geolocation database; this essentially means the use of a lower transmit power in the directional antenna case.

Figs. 6.6, 6.7, 6.8 show the results comparing the number of usable channels between omni-directional and directional antenna cases for different channel usability thresholds (ρ values) and at different TVWS device antenna heights. With all thresholds, there is a significant improvement in the number of usable channels with directional antennas. Whereas the median number of usable channels with omni-directional antennas is around 5 (40MHz) as seen before, this number increases with directional

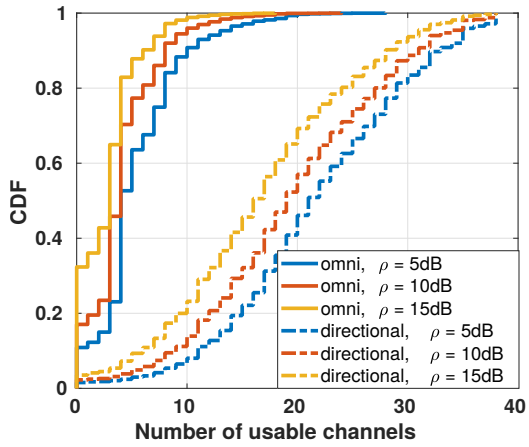

Figure 6.6: Improvement in the number of usable TVWS channels using directional antennas compared to omni-directional antennas for different usability thresholds (5/10/15dB) and antenna height of 5m.

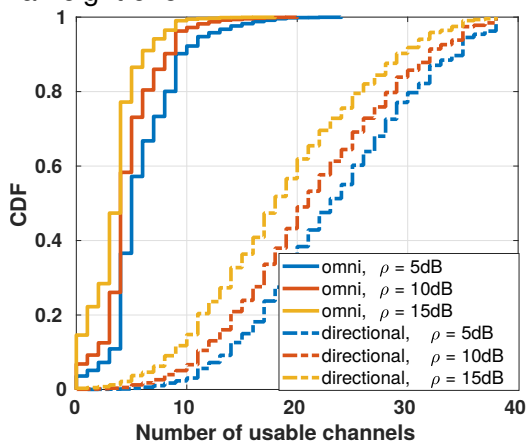

Figure 6.7: Improvement in the number of usable TVWS channels using directional antennas compared to omni-directional antennas for different usability thresholds (5/10/15dB) and antenna heights of 10m.

antennas to fall in the range of 15 – 25 (120 – 200MHz) depending on the ρ value. While this same conclusion across all different antenna heights considered, we can also observe that antenna directionality brings in a bigger advantage than lowering the antenna height. Overall these results clearly show that use of directional antennas at TVWS devices counter the negative effect of aggregate interference from nearby DTT transmitters to a large extent.

6.4 Nature of TVWS Spectrum Fragmentation

So far in our analysis, we focused only on the number of available/usable channels and the corresponding amount of spectrum without considering how this spectrum is

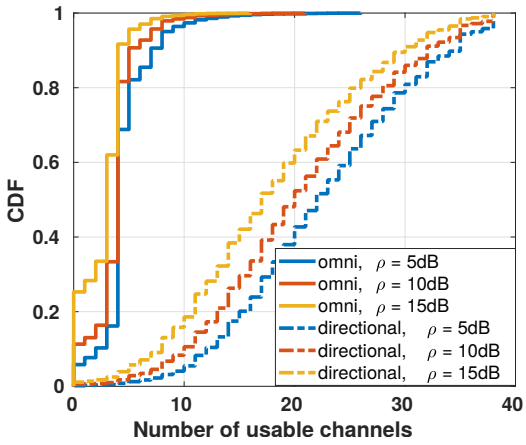

Figure 6.8: Improvement in the number of usable TVWS channels using directional antennas compared to omni-directional antennas for different usability thresholds (5/10/15dB) and antenna heights of 20m.

distributed – contiguous versus highly fragmented. This is a key issue to understand in order to exploit the TVWS spectrum for enabling middle-mile connectivity by aggregating multiple TVWS channels; individual TVWS channels by themselves are small[2] and insufficient for this purpose. Generally speaking, non-contiguous spectrum in the same band is relatively harder to aggregate and fully exploit compared to the case where spectrum is available as a single chunk.

In order to better understand the nature of TVWS spectrum fragmentation for the rural middle mile use case, we consider three metrics: (i) number of TVWS spectrum fragments where each fragment is a contiguous chunk of usable spectrum that is at least the size of a single TVWS channel (i.e., minimum fragment size is 1); (ii) maximum fragment size (in terms of number of channels contiguously usable); (iii) percentage of fragmentation which is defined as $\Omega(\kappa)$ for a location κ:

$$\Omega(\kappa) = (1 - \frac{\text{Maximum fragment size}_{\kappa}}{\text{Total number of usable channels}_{\kappa}}) \times 100 \tag{6.2}$$

Note that $\Omega(\kappa) = 0\%$ is ideal as it means that all the usable spectrum is contiguous in one chunk. Higher values of this metric are less desirable and a value closer to 100 indicates a very high degree of fragmentation.

Figs. 6.9 to 6.17 show the results for the above three metrics, respectively, for different usability thresholds and antenna heights. Results for the omni-directional antenna case are included for completeness and as a baseline but our discussion of these

[2]Specific channel widths vary between regulatory regimes – 6MHz in the US, 8MHz in the UK and most African countries. But the fact that they are relatively much smaller compared to other bands (e.g., up to 160MHz in the 5GHz band) is clear.

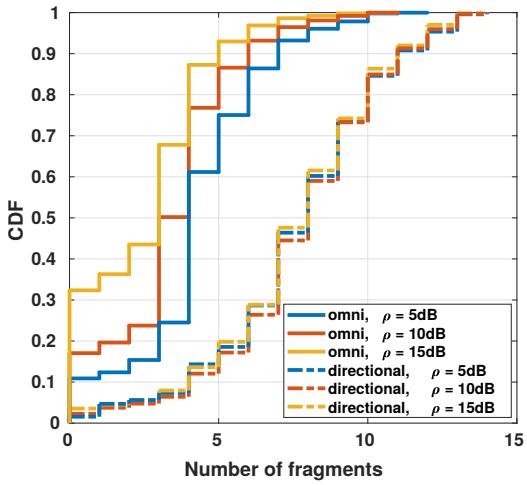

Figure 6.9: Number of fragments of usable TVWS spectrum with different antenna types, usability thresholds (ρ) and TVWS device antenna height is 5m.

results focuses on the directional antenna case based on the conclusion from the last section. Starting with the results for the number of fragments metric (Figs. 6.9, 6.10, 6.11), we can observe that, regardless of the usability threshold and antenna height settings, the overall usable spectrum is divided into 8 or more fragments in half the locations. In over 90% of the locations, the number of fragments is at least 5. This indicates the aggregation of non-contiguous spectrum in the same band is inevitable in order to exploit all the usable TVWS spectrum.

Turning attention to the maximum fragment size (Figs. 6.12, 6.14, 6.14), the median value of this metric ranges from 3 to 10 channels depending on the usability threshold – higher the threshold, lower the maximum fragment size. Taken together with the above discussed number of fragments metric, these results suggest that exploiting all the usable spectrum at a typical location translates to aggregating 5 or more fragments, spanning over a wide range in size from 8MHz to around 160MHz.

Results on the percentage of fragmentation in Figs. 6.15, 6.16, 6.17 indicate that the level of fragmentation is quite high in general, consistent with the above observations – in 80% of the locations the overall usable amount of spectrum is 50% fragmented and the fragmentation level is above 70% in half the locations. In summary, these results suggest that TVWS spectrum is quite fragmented and using it for the rural middle mile case may in practice mean focusing on and aggregating the few biggest fragments.

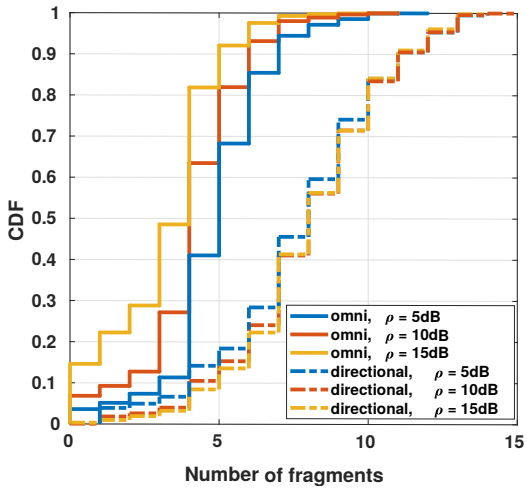

Figure 6.10: Number of fragments of usable TVWS spectrum with different antenna types, usability thresholds (ρ) and TVWS device antenna height is 10m.

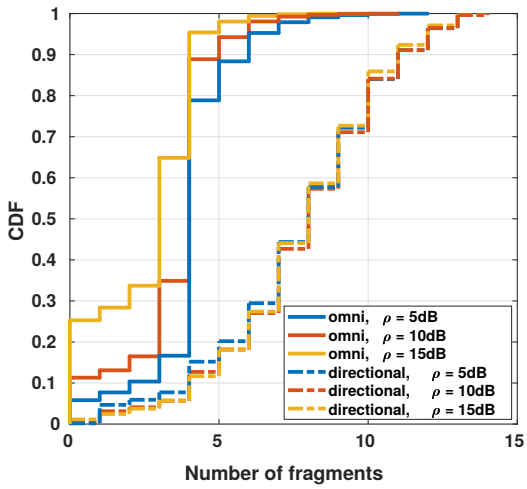

Figure 6.11: Number of fragments of usable TVWS spectrum with different antenna types, usability thresholds (ρ) and TVWS device antenna height is 20m.

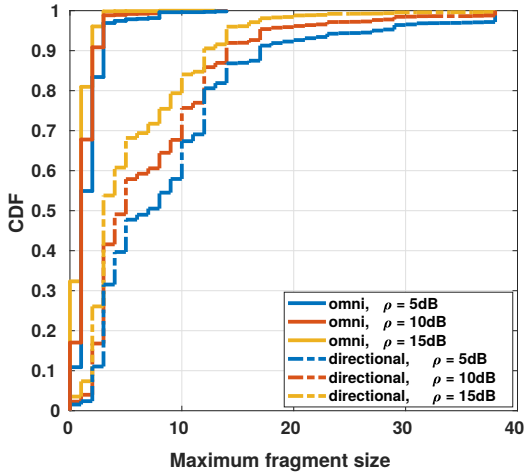

Figure 6.12: Maximum fragment size of usable TVWS spectrum with different antenna types, usability thresholds (ρ) and TVWS device antenna height is 5m.

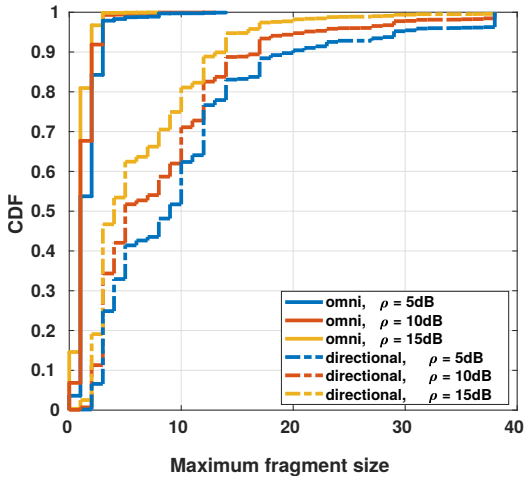

Figure 6.13: Maximum fragment size of usable TVWS spectrum with different antenna types, usability thresholds (ρ) and TVWS device antenna height is 10m.

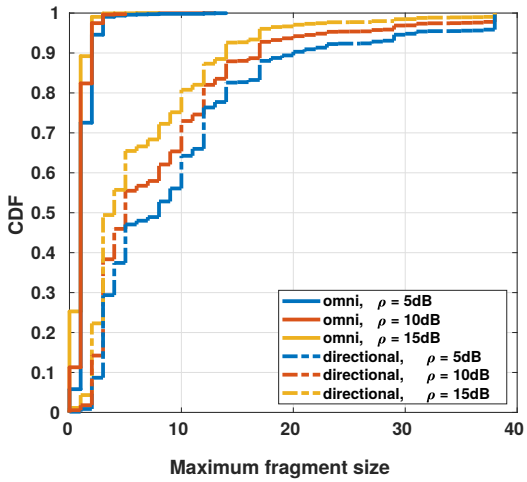

Figure 6.14: Maximum fragment size of usable TVWS spectrum with different antenna types, usability thresholds (ρ) and TVWS device antenna height is 20m.

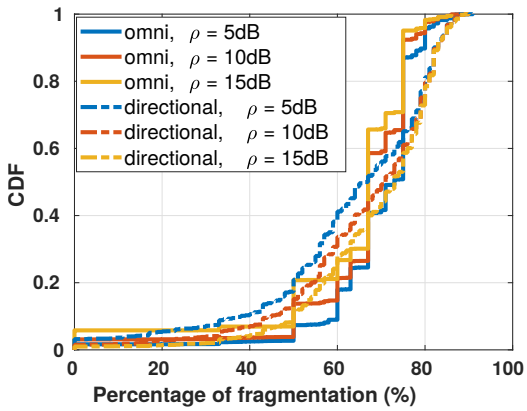

Figure 6.15: Percentage of fragmentation of usable TVWS spectrum with different antenna types, usability thresholds (ρ) and TVWS device antenna height is 5m.

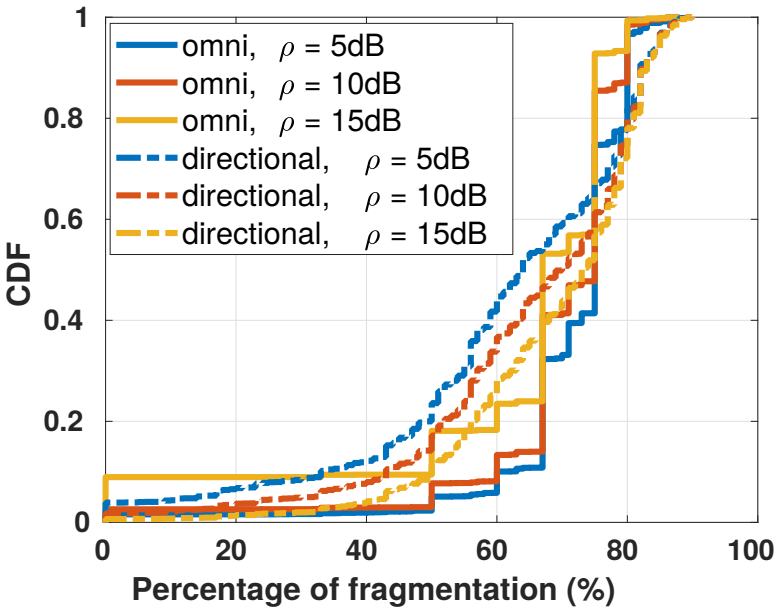

Figure 6.16: Percentage of fragmentation of usable TVWS spectrum with different antenna types, usability thresholds (ρ) and TVWS device antenna height is 10m.

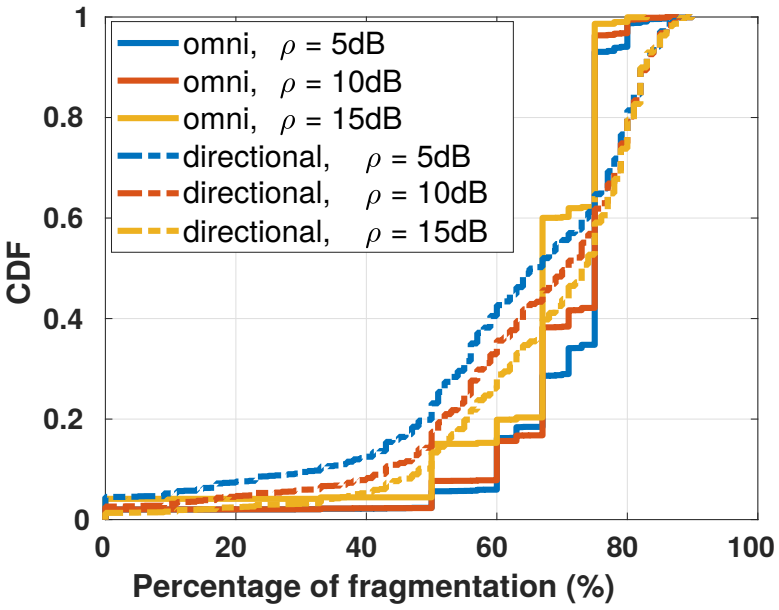

Figure 6.17: Percentage of fragmentation of usable TVWS spectrum with different antenna types, usability thresholds (ρ) and TVWS device antenna height 20m.

6.5 Discussion

Our analysis results indicate that aggregated interference from multiple DTT stations can have a detrimental impact on the amount of usable TVWS spectrum in outdoor rural settings and also that this usable spectrum can be highly fragmented. To put these results into perspective, they reflect the situation in rural areas of developed countries with TVWS regulations like in the UK and substantial over-the-air TV use. In other regions with little or no terrestrial TV use, these effects would be relatively weaker and thus more amount of contiguous spectrum would be actually available to use for TVWS middle mile solutions. In that sense, the setting considered by the analysis in this chapter is a relatively challenging one for TVWS based middle mile connectivity.

Concerning TVWS spectrum aggregation, which is shown to be essential to realize high-bandwidth backhaul links, there is no practical and low cost existing solution in the literature. Commercial solutions (e.g., newer generation of Carlson TVWS devices [3]) support limited aggregation up to three 8MHz TVWS channels. Although in unlicensed 5GHz band used, more recent WiFi standards support bonded contiguous channels up to 160MHz wide, such solutions are insufficient when spectrum is highly fragmented like our results show. LTE-Advanced carrier aggregation (CA) feature that in theory supports aggregation of intra-band non-contiguous spectrum is potentially a relevant approach although in practice only aggregation across different bands is currently supported. Aggregation of non-contiguous spectrum within a band requires the use of sophisticated and expensive filters to mitigate the interference among concurrent transmissions on adjacent chunks of the spectrum.

6.6 Summary

TV white space (TVWS) spectrum has the potential to be a significantly lower cost alternative for middle mile connectivity. TV white spaces at any given location and time refer to the portions of spectrum in the UHF TV bands (e.g., 470 - 790 MHz in the UK) which are not used by TV transmitters and wireless microphone users (the primary users of this spectrum). Led by the U.S. FCC in 2008, several countries including the UK have made the TVWS spectrum unlicensed (like with WiFi devices) subject to interference protection for primary users (e.g., TV receivers) by consulting a geo-location database for available spectrum at a given location and time. TVWS spectrum is attractive for rural and middle mile connectivity for two reasons. First, it

has superior propagation characteristics compared to other higher frequency bands in terms of range and non-line-of-sight (NLOS) propagation in presence of foliage and obstructions. For example, measurement studies confirm that it is possible to get 4 times greater range with TVWS spectrum compared to 2.4GHz unlicensed spectrum used by WiFi [37]. This means lesser amount of infrastructure (fewer base stations) for connectivity over a given distance with TVWS spectrum and corresponding reduction in deployment costs. Second, there is a large amount of TVWS spectrum likely available in rural areas (in the region of 200+ MHz) with fewer TV transmitters and rare wireless microphone use. In developing countries, almost all of the UHF band is available as white space due to non-existent or limited presence of over-the-air TV. This aspect is also beneficial for middle mile connectivity as it allows high bandwidth connections like the other expensive alternatives (e.g., fiber). In this chapter, we examined the potential of exploiting TVWS spectrum for middle mile solutions. Different from the existing works in literature, we study the quality of available TVWS channels and how the available spectrum is fragmented. We show that the aggregated interference, observed at a TVWS receiver, coming from of multiple DTT stations is the main reason that risks making much of the available TVWS spectrum unusable even in rural outdoors. We have also shown that using directional antennas is key to mitigating this effect. Even though directional antennas can help recover some of unusable spectrum but TVWS spectrum is still quite fragmented. Thus, new cost-effective spectrum aggregation solutions are needed to efficiently exploit the fragmented spectrum towards enabling high-speed TVWS middle mile infrastructure.

Chapter 7

WhiteHaul: Flexible and Efficient Backhauling System over TVWS Spectrum

As presented in Chapter 5 and 6, the low cost and high capacity backhauling link is crucial and is considered to be the vital element in any system that aims to enable Universal Internet Access. Motivated by that, in this chapter, we present WhiteHaul, a flexible and efficient system for high capacity backhaul over TVWS spectrum. We start first by analyzing the constraints in TVWS spectrum through an analytical study that helps to identify the three main system requirements including the need to handle the diversity of available spectrum, a spectrum aggregation technique that fully utilize the fragmented TVWS spectrum (i.e., motivated by the study in Chapter. 6) and the orchestration software layer that distributes the asymmetric traffic between the different interfaces. The analytical study in this chapter complements the study presented in Chapter. 6; yet from different perspective. While the study in Chapter. 6 sheds the light on the affect of the aggregate interference on the TVWS availability, the study in this chapter aims at highlighting the diversity in TVWS spectrum that can be observed in the amount of available spectrum, the allowed transmit power and the channel conditions in which all these variables significantly affect the performance of the backhaul link. Following the analytical study, we describe our system architecture and its detailed components. We then present the thorough evaluation of WhiteHaul system in our lab environment. Finally, we provide a brief analysis on the trade-off between the link distance and the size of aggregated spectrum.

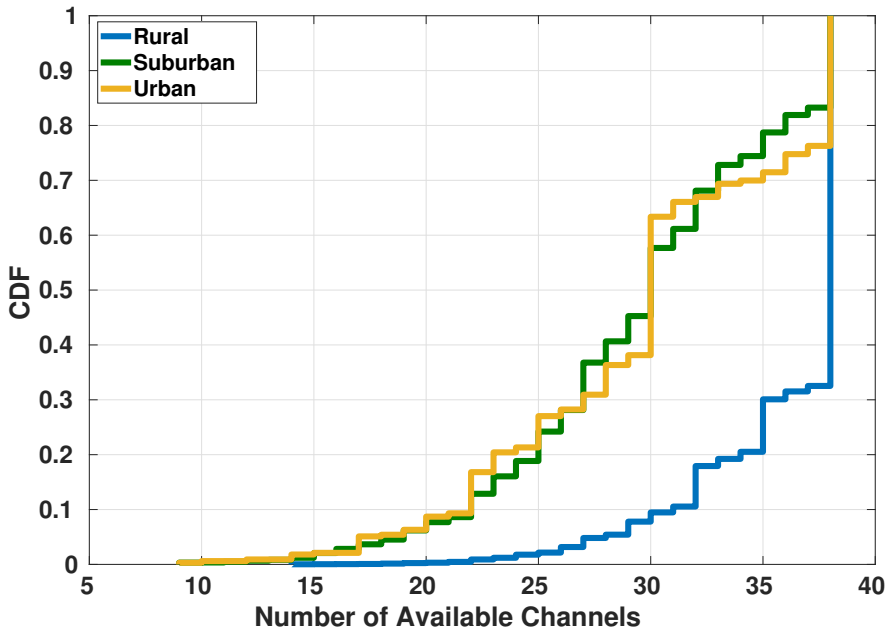

Figure 7.1: TVWS spectrum availability CDF distribution in different types of areas in Scotland.

7.1 TVWS Backhaul Links: Characteristics and Challenges

As a way to substantiate the challenges associated with using TVWS spectrum for backhaul links in underserved regions, this section presents a case study considering a representative European country and examine the nature of TVWS spectrum in the 470-790MHz TV band as per the ETSI Harmonised Standard for White Space Devices [58]. To this end, we represent the country as a set of pixels, each corresponding roughly to a square of size 6km^2(corresponding to the intersection of three degrees in latitude and three degrees in longitude). For the center location of each such pixel, we query a commercial geolocation database to obtain the available TV channels at that location along with allowed power levels. The TVWS spectrum availability results in Fig. 7.1, 7.2 for different area types, corresponding to area classification in the case study country based on population density, confirm the ample availability in rural areas (e.g., 38 8MHz wide TV channels available in 70% of rural locations), broadly in agreement with prior studies (e.g., [74, 163]). Our focus in the rest of this section is to shed light on several salient issues that need to be accounted for when designing TVWS based backhaul links.

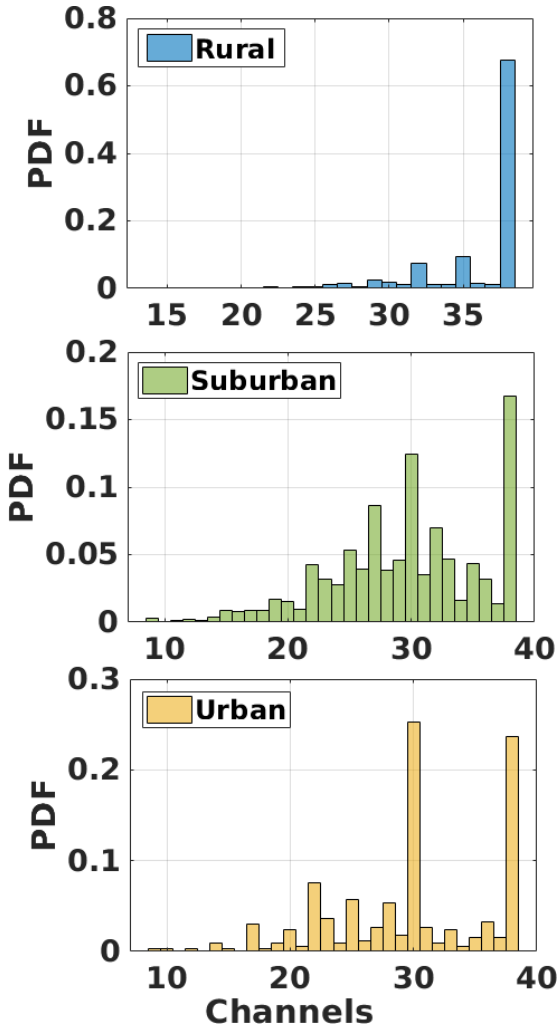

Figure 7.2: TVWS spectrum availability PDF distribution in different types of areas in Scotland.

7.1.1 Spectrum fragmentation

We now focus on the inhabited rural areas to understand their TVWS spectrum characteristics.

We first look into the extent to which the available TVWS spectrum is fragmented. For this, we define a *spectrum chunk* as a set of contiguous TVWS channels available at a given location. Fig. 7.3 quantifies the extent to which TVWS is fragmented in rural areas. For example, in 60% of the locations, the spectrum is fragmented into at least 6 chunks and in only 20% of the locations is the spectrum available in 4 or fewer chunks. Such a high degree of spectrum fragmentation is due to the presence of multiple lower power TV relays/amplifiers needed to extend the coverage of the primary DTT transmitters. This creates gaps in available TVWS spectrum as access to channels amplified by such relays are restricted by the geolocation database.

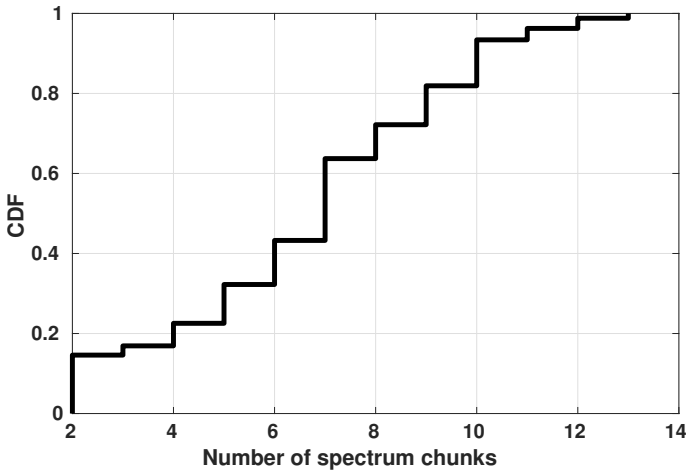

Figure 7.3: The CDF of number of spectrum chunks across different locations.

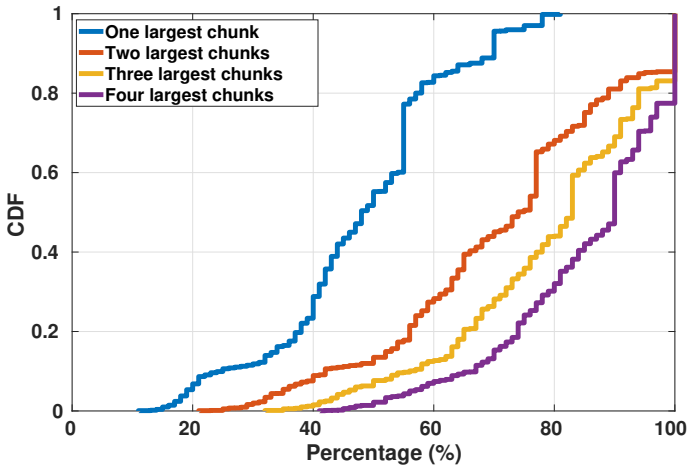

Figure 7.4: The percentage of largest 4 chunks of the spectrum to the total amount of available spectrum.

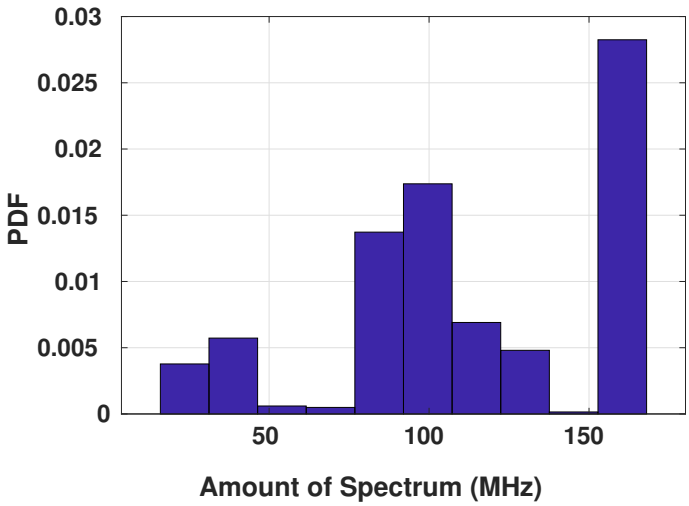

Figure 7.5: The distribution of the size of the first largest spectrum chunks.

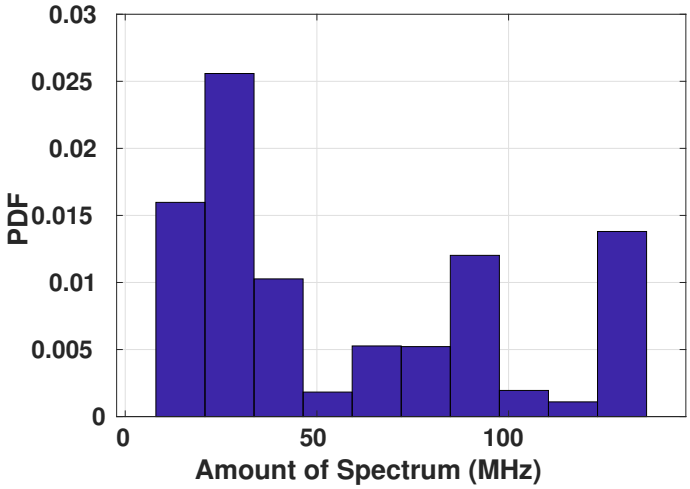

Figure 7.6: The distribution of the size of the second largest spectrum chunks.

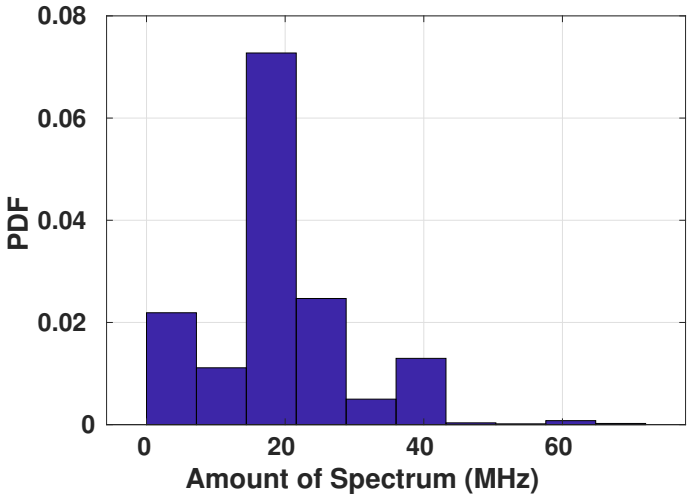

Figure 7.7: The distribution of the size of the third largest spectrum chunks.

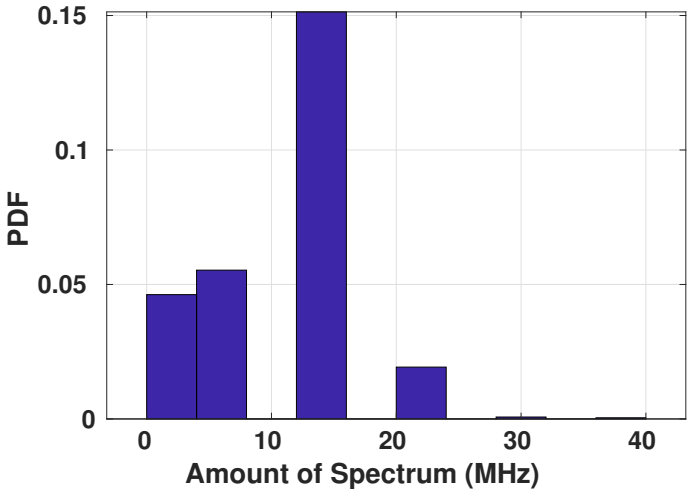

Figure 7.8: The distribution of the size of the fourth largest spectrum chunks.

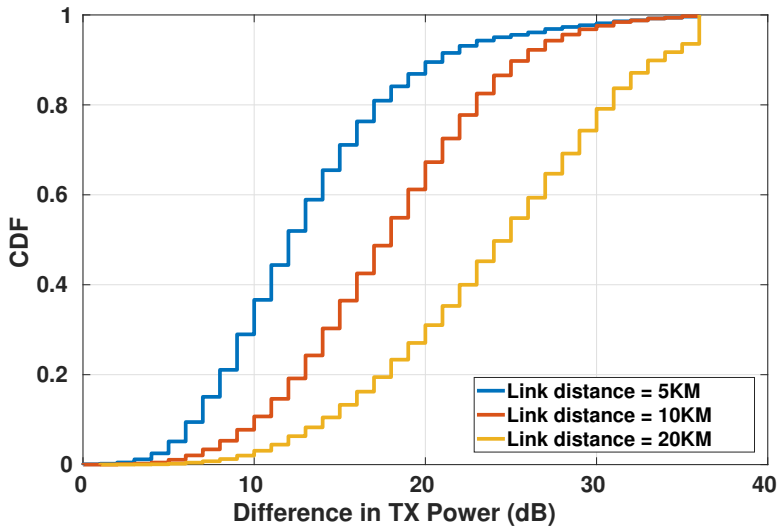

Figure 7.9: Power asymmetry effect at different link distances (5-20Km).

7.1.2 Spectrum chunk size diversity.

Fig. 7.4 shows how the spectrum is distributed across chunks through CDFs of the percentage of total available spectrum that is covered by the one, two, three and four largest chunks. We observe that only about half the available spectrum is covered by the largest chunk (red solid curve) in half the locations, and that even top four chunks combined cannot cover all the available spectrum in 80% of the locations. Distribution of chunk sizes within each of the four largest sized chunks is shown in Fig. 7.5, 7.6, 7.7 and 7.8. These results demonstrate *the significant diversity in chunk sizes*, which adds further complexity to the problem of aggregating TVWS spectrum in that traffic should be distributed across chunks accounting for this diversity.

7.1.3 Power asymmetry.

With the TVWS spectrum, the geolocation database needs to be queried to determine the available set of channels and power levels at a location, and it is possible that these could be substantially different between link endpoints that are some distance apart. We examine the potential power asymmetry resulting from this issue in Figs. 7.9, 7.10 for our case study country. Fig. 7.9 shows the allowed power level differences for different point-to-point (PtP) link distances for each channel in the common set of channels available at both ends of the link. We observe that the power differences can be quite significant for longer (20Km) links with a median around 25dB. This effect is

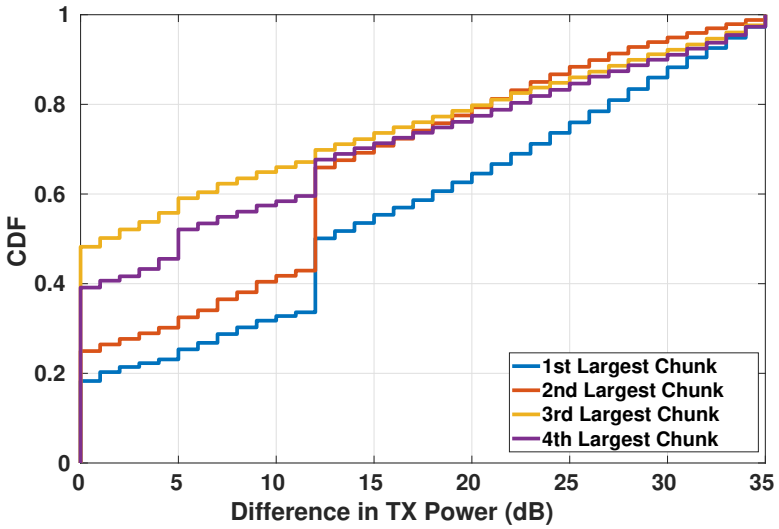

Figure 7.10: Power asymmetry effect between channels within individual spectrum chunks.

also seen for shorter (5Km) links where only in 10% of the cases is the transmit power difference less than 6dB. Note that this power asymmetry effect is unique to TVWS based backhaul setting and not present in other approaches used in the literature for low-cost backhaul such as long-distance Wi-Fi [140, 159, 64, 52, 137, 145].

Power differences can also occur between different channels available at a link end-point. This effect is quantified in Fig.7.10, where maximum power differences between channels within each of the four largest chunks is shown. We see that channels within a chunk can have quite different power levels; for example, the median power difference within 1st and 2nd chunks is around 12dB. As such, the set of chunks and their size need to be carefully chosen to minimize these above highlighted power asymmetry effects. Moreover, time allocation for each end of a backhaul link needs to account for the effective capacity of the link and the traffic demand from each direction, the former being affected by transmit power used for each of the chunks. We factor these observations in our design (§7.3.2).

7.1.4 Interference

While consulting the geolocation database is mandatory to access the TVWS spectrum, it cannot capture *receiver-side interference* characteristics that could affect the quality of TVWS transmission from a distant transmitter. To illustrate this point, we suppose a TVWS receiver at the rooftop of our office building and consider a transmitter on top

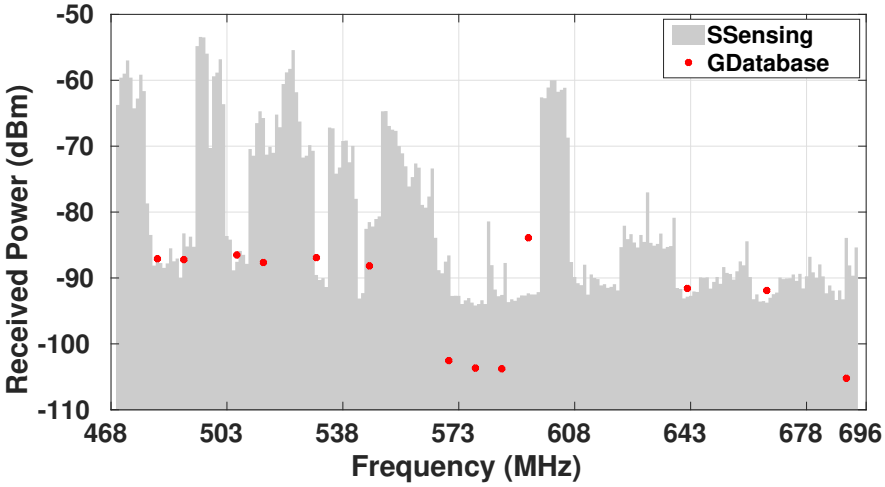

Figure 7.11: Spectrum occupancy (reflecting interference levels) as measured by a spectrum analyzer at a receiver. The red points are the estimated received power from a remote TVWS transmitter on available channels at the latter

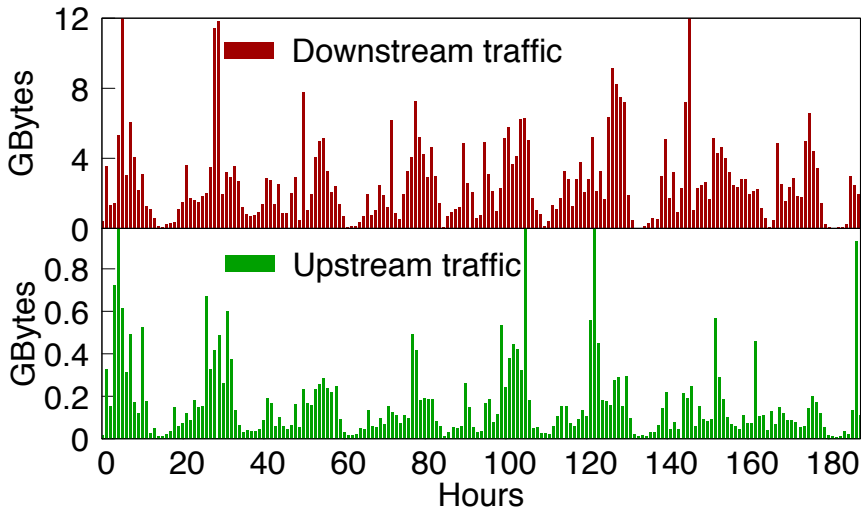

Figure 7.12: Weekly backhaul traffic volumes for a rural community wireless network: (top) downstream and (bottom) upstream.

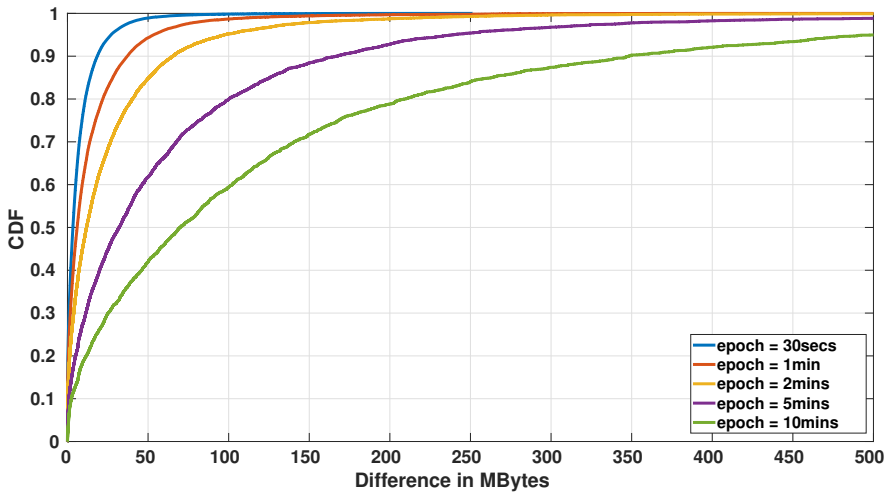

Figure 7.13: Downstream traffic volume variation (in MBytes) between consecutive epochs for different epoch lengths.

of another building 3km away. Based on available TVWS channels and allowed power levels at the transmitter location by querying the geolocation database, then accounting for path loss (calculated using the SPLAT! RF planning tool [6]) and antenna gains, we obtain expected signal power at the receiver on channels available at transmitter side as shown in Fig. 7.11 (the red dots). At the receiver side, we use a spectrum analyzer to estimate the level of interference on different channels across the whole TV band, overlaid in the same figure. We see that the channels available at transmitter side can be very different from each other on the receiver side in terms of received signal power and interference levels. This highlights the importance of measuring and considering receiver-side perspective in choosing spectrum chunks, which we do in our design (§7.2 and §7.3.2.1).

7.1.5 Traffic characteristics

Effective backhaul network design requires a good understanding of the characteristics of traffic it is expected to carry. To this end, we collected trace of traffic from a long-running rural community wireless access network in our case study country as seen by its leased fiber backhaul link (with 200Mbps symmetric upstream and downstream bandwidth limit). This network serves at least 250 households and local businesses. Fig. 7.12 shows a week long backhaul traffic profile in the downstream (towards access network) and upstream directions. We observe a high degree of asymmetry with average daily downstream traffic much higher, around 63GBytes, compared to average upstream traffic each day (only about 4GBytes). We also notice that, although there

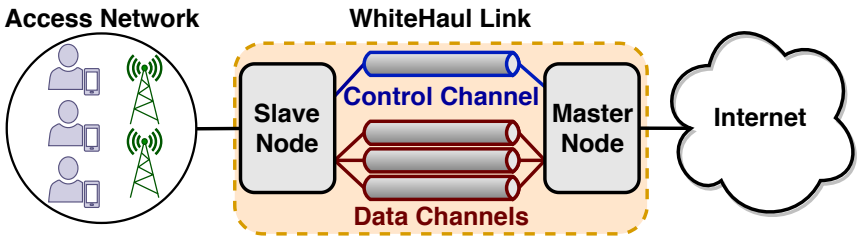

Figure 7.14: High-level schematic of WhiteHaul system in an end-to-end application scenario.

is some apparent diurnal pattern, traffic in both directions fluctuates substantially over time. To understand the degree of fluctuation at different time granularities (epochs), Fig. 7.13 shows the CDF of variation in downstream traffic from one epoch to the next for different epoch lengths. These results indicate considerable degree of traffic variation for longer epochs but marginal variation with the smallest epoch size we could obtain for this trace, which is based on data collected every 30s.

7.2 WhiteHaul Overview

WhiteHaul is a system to realize point-to-point (PtP) TVWS based backhaul links, meaning a WhiteHaul node forms the endpoint of such a link. Fig. 7.14 shows a basic application scenario where a WhiteHaul link connects an access network (serving end-user devices) and the Internet. We do not make any assumptions on the nature of the access network, which could take several forms including a community cellular network (e.g., [158]). While it is fairly straightforward to go from the case of one WhiteHaul link to a path or mesh network with multiple WhiteHaul links with suitable spectrum usage coordination amongst them, we focus on the single link case in this work. Also, as shown in Fig. 7.14, we adopt a master-slave model in that one end of a WhiteHaul link acts as the `Master Node` and the other as the `Slave Node` with the former responsible for link configuration decisions (e.g., spectrum to use for interfaces on both sides). The `Master` and `Slave` coordinate over an *out-of-band control channel* while carrying user traffic over *multiple data channels that each operate on a separate TVWS spectrum chunk*. There are as many data channels as the number of interfaces at WhiteHaul end nodes making up the link. For reasons elaborated later in section 7.3.2, WhiteHaul links operate in time-division duplexing (TDD) mode, meaning the `Master` and `Slave` take turns in time, possibly of different slot durations in each direction, to

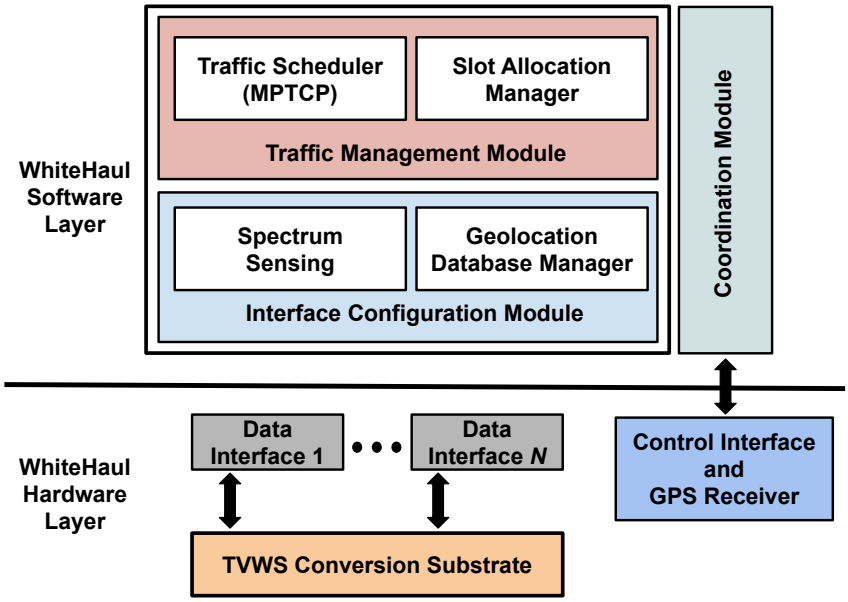

Figure 7.15: WhiteHaul node architecture.

communicate over their respective data interfaces. Fig. 7.15 shows the schematic of the WhiteHaul node architecture, that consists of two layers: the *Hardware Layer* and the *Software Layer*. The hardware layer is composed of the physical wireless interfaces used for both control and data communication as well as the TVWS conversion substrate for the data interfaces. For the data interfaces, we use commodity off-the-shelf (COTS) 802.11n/ac Wi-Fi cards operating in 5GHz band. The conversion substrate is responsible for frequency up/down conversion between available TVWS spectrum chunks and 5GHz Wi-Fi channels. For the control interface, we use LoRa [144], a low-power wide area network (LPWAN) technology, that costs a few dollars a piece, operates in unlicensed sub-GHz bands, and provides data rates of few tens of Kbps over long distances up to 40Km.

The WhiteHaul software layer orchestrates the underlying interfaces to maximize the overall system performance. It is made up of three modules: (i) the *Coordination Module* facilitates communication between the `Master` and `Slave` nodes via the underlying LoRa control interface. (ii) the *Interface Configuration Module* configures the TVWS spectrum chunks and transmit power of data interfaces as decided by the `Master` node. These configurations are based on the TVWS spectrum availability information obtained from the geolocation database and local low-cost spectrum sensing from both ends of the WhiteHaul link. (iii) the *Traffic Management Module* performs two functions. One, by the *Slot Allocation Manager*, is to adapt the time slot duration

for `Master-Slave` (*forward*) and `Slave-Master` (*reverse*) directions, every *epoch*, depending on the effective capacity and traffic demand of forward and reverse links. The *Traffic Scheduler* is responsible for the other function to efficiently schedule the traffic among the underlying data interfaces using a modified variant of MPTCP, aided by advisory signals from the *Slot Allocation Manager*.

7.3 System Design & Implementation

In this section, we describe the WhiteHaul design and implementation in detail.

7.3.1 Hardware Layer

7.3.1.1 TVWS Conversion Substrate

As previously stated, this part of the hardware layer converts between 5GHz and TVWS spectrum. Fig. 7.16 shows the schematic of its design for the case of two 802.11n/ac data interfaces. As shown, data interfaces as well as the substrate, specifically the local oscillator (LO), are dynamically controlled by the *Interface Configuration Module* to set parameters such as oscillator frequencies, channel bandwidths and power levels while ensuring compliance with TVWS spectrum regulations. In general, we target a flexible and modular design for the substrate to allow its realization with replaceable/configurable components as per link requirements and cost considerations (e.g., trade off between noise and linearity). Our implementation consists of a desktop (running Ubuntu Linux 14.04) connected to a set of Mikrotik RB922UAGS-5HPacD Router-Boards with 802.11n/ac cards, acting as data interfaces, via Gigabit Ethernet. The desktop also hosts a USRP B210 [11] per data interface for use as a LO, as described below.

SDR based Local Oscillator. The LO component plays the key role of translating RF/IF signal up/down to a different frequency band by multiplying it with the sinusoidal signal it generates. Previous works employing the frequency conversion concept (e.g., [25, 116]) have relied on Voltage Controlled Oscillators (VCOs) to generate the LO signal; specifically, these VCOs take a control voltage as input to determine the frequency of output LO signal. As VCOs operate under high non-linearity and produce unwanted emissions, they cause frequency fluctuations (harmonics and phase noise) of the output signal that blur the output IF signal when used in down-conversion and degrade its Signal-to-Noise Ratio (SNR). Our experiments validate this effect and

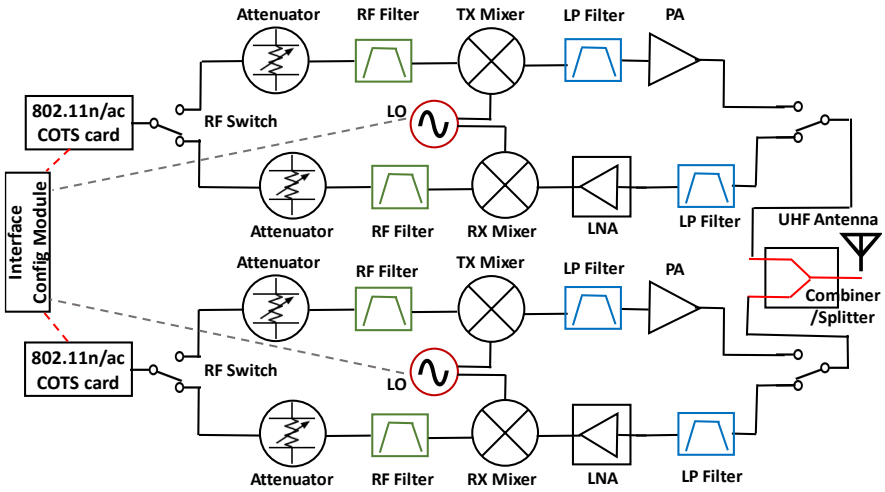

Figure 7.16: WhiteHaul TVWS conversion substrate schematic.

show, for instance, that a VCO oscillator (with $-69dBc/Hz$ phase noise at 1kHz offset frequency) used to down-convert from 5GHz to UHF band can degrade the SNR value of the output IF signal by 5dB (Fig. 7.17). Having two of these VCOs, one in the transmit chain and another in receive chain, can reduce the overall SNR level of the system by 10dB.

So to avoid such degradation, we take a different approach and use a SDR board (USRP B210 in our prototype) to generate a sinusoidal signal without any distortion or phase noise. The SDR-generated LO signal can then be fed to the mixer (see Fig. 7.16) to generate the up/down converted signal. Our approach not only results in a higher-SNR signal compared to VCO oscillators by 4dB (Fig. 7.18) but also provides high flexibility in (re-)configuring the center frequency of the generated signal by the Interface Configuration Module. On the other hand, lack of such flexibility with the VCO due to the low granularity of the tuner voltage (steps of 0.25V which maps to steps of 20MHz in the generated LO signal) leads to misalignment in center frequency (as indicated by the red arrow in Fig. 7.17).

Separate Transmit and Receive Paths. Our design is also distinct from prior work in that it uses two separate transmit and receive paths, which allows for fine-grained configuration for RF components to optimize signal quality of each path. To realize this separation, we make use of two fast Single Pole Double Throw (SPDT) RF switches with 35ns switching time, one interfacing with the 802.11 card and the other before combiner/splitter and UHF antenna. These switches have a wide bandwidth range from 500 to 6000 MHz, allowing operation in both 5 GHz and UHF bands.

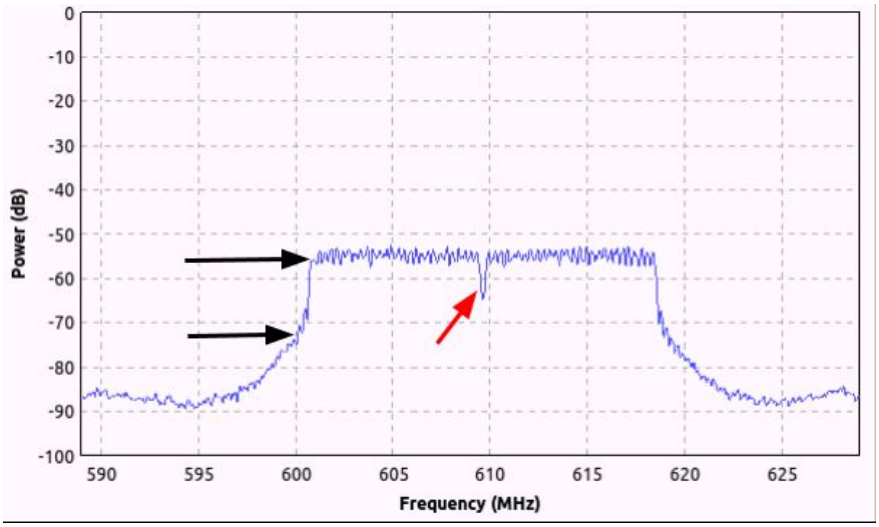

Figure 7.17: The down-converted signal using VCO.

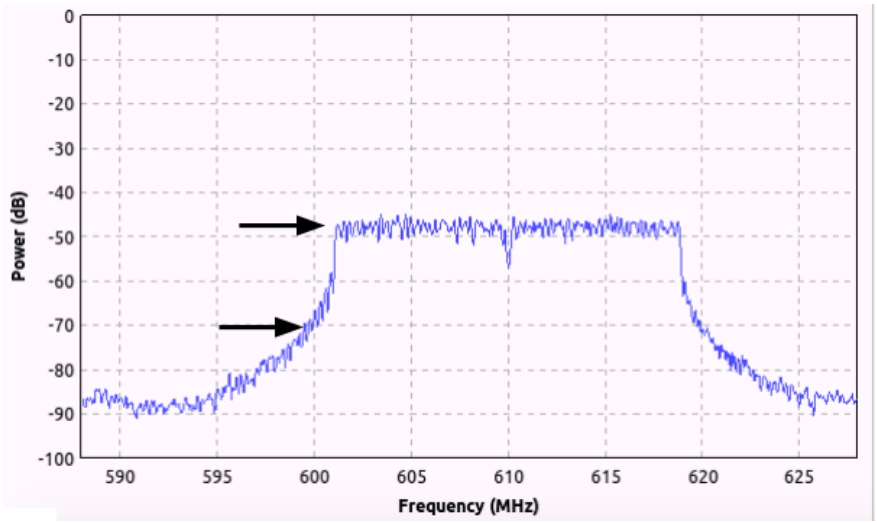

Figure 7.18: The down-converted signal using our SDR-based LO approach

The transmit path has a configurable RF attenuator to start with followed by a high-pass filter to cut out spurious emissions from the 802.11 interface. Next is a highly linear down-conversion mixer that supports wide range of frequencies from 3700 to 7000 MHz and is driven by the SDR based LO as described above. The resulting IF signal goes through a low pass filter to remove mixer related non-linearities. Then a low noise power amplifier (PA), capable of 27dBm output power and with a low noise figure of 1.2dB, is used. This is a voltage-controlled amplifier which can be adjusted (by changing the voltage level) to stay within the allowed transmit power. The amplified signal so generated is then fed to combiner/splitter through another RF switch.

On the receive path, we have a low-pass filter to start with to eliminate unwanted signals before going through a low noise amplifier (LNA), which in our prototype has a high gain of 22.5dB, ultra low noise figure of 0.5dB and wide operational bandwidth range from 50 to 3000MHz. The up-conversion mixer translates the received UHF signal into the 5GHz band with help of LO, as above. We only use one LO for a pair of transmit and receive paths to make sure that the center frequency of the up-converted signal is the same as that of the RF signal down-converted in the transmit path. Following the mixer, we have a high pass filter to remove the unwanted signal from the mixer. Finally, a configurable attenuator to avoid saturating the receive chain on the 802.11 interface.

Combiner/Splitter. To satisfy our design constraint of using a single antenna, while using multiple interfaces towards a high capacity backhaul link, we have a RF power combiner/splitter in the design that can combine different transmit paths (from different 802.11 interfaces) into one output that is fed to the antenna or split the received UHF signal into multiple receive paths. In our prototype, we use a combiner/splitter with high isolation (25 dB typical) to prevent leakage between paths. Moreover, it can handle high transmit power up to 10W (aggregated), and has 5 input ports (for combining up to 5 different 802.11 cards) with a total bandwidth of 320MHz that can span the whole TV band.

7.3.1.2 Coordination and Synchronization

The control interface (see Fig. 7.15) enables the coordination between the `Master` and `Slave` ends of a WhiteHaul link, which is useful for two purposes. First, for the `Slave` node to notify the `Master` about the spectrum sensing information at its location as well as its traffic demand every epoch (30 seconds in our implementation). Second, for the `Master` to notify the `Slave` about the set of TVWS spectrum chunks to use for its interfaces as well as the time slot duration in the reverse direction. In our implementation, we realize this control communication channel using low-cost Pycom LoRa gateways [4] that operate on very narrow channels (7.8 - 500KHz) in 868MHz spectrum band and are capable of achieving few tens of Kbps data rate over long distances, up to 40Km. Along with a control interface, each WhiteHaul node is also equipped with a GPS receiver to facilitate localization and time synchronization, latter for TDD operation.

7.3.2 Software Layer

7.3.2.1 Interface Configuration

This module is responsible for the configuration of data interfaces at WhiteHaul link endpoints with spectrum chunks and power levels via coordination over the control interface. As a basic step, the `Master` periodically checks with the geolocation database (as required by the regulator) about TVWS spectrum availability and allowed power levels at both `Master` and `Slave` node locations. In addition, we equip each WhiteHaul node with a low cost spectrum analyzer (RF Explorer [5] in our implementation) to estimate the interference in available TVWS channels. This is motivated by the observation made in §7.1 about interference and recent work (e.g., [81]) that observes that aggregate interference from multiple nearby transmitters can impact the quality of available channels. So, using the spectrum analyzer, each WhiteHaul node sweeps the whole TV band periodically to obtain the signal level on all the available TVWS channels as an estimate of interference on those channels. The `Slave` node then syncs all its sensing information with the `Master` node.

Using this information, the `Master` then estimates the SINR for each of the TVWS channels commonly available between the endpoints in both forward and reverse directions. This involves estimating the received signal power on the available TVWS channels common to both endpoints. For this, we use the SPLAT! RF planning tool [6] to estimate the path loss in each direction along with allowed transmit power and antenna gains. Based on the above, the link SINR for each TVWS channel is estimated as the lower of the two values for forward and reverse directions. With this channel-level SINR for the link in hand, the question is to decide on the TVWS spectrum chunks for the node interfaces. For this, we start with identifying the potential spectrum chunks considering contiguous set of available channels on both ends. Then, keeping in mind the number of data interfaces available, a subset of chunks (with center frequencies and chunk sizes that are greater or equal to 802.11ac channel widths (20/40/80 MHz)) are selected from all possibilities with the aim of maximizing the minimum channel-level SINR for each chunk. This may result in picking smaller sized chunks (with higher SINR yielding TVWS channels) instead of larger chunks with lower average SINR. Note that the power level chosen for a chunk is limited by the lowest power allowed among the constituent TVWS channels. So by maximizing the minimum SINR within a chunk and across both link directions, we address the power asymmetry effect highlighted in §7.1. We let the modulation and coding scheme (MCS) be automatically

adapted by the 802.11 interfaces via the default built-in mechanism.

7.3.2.2 Slot Allocation

As noted earlier, we design WhiteHaul links to operate in TDD mode. This not only provides more flexibility and control for traffic scheduling across interfaces but also is essential given our choice to use to low-cost COTS 802.11 cards based on CSMA. Concerning the latter, the root of the issue is that in 802.11 each node senses the spectrum for a certain time period given by DIFS (34μs) before attempting to transmit. When the link distance is longer than 10.2Km, one end of the link cannot hear the other within this period, which then leads to collisions from potential simultaneous transmissions by both ends. Indeed, this observation has motivated the shift to using time division multiplexing (TDM) based MAC protocols in the literature for long-distance wireless communications such as for backhaul (e.g., [140]).

While our TVWS conversion substrate with separate transmit and receive paths allows for fast switching between the transmit and receive modes (35ns), the key issue with TDD is deciding on the time slot duration for each direction (forward/reverse). The long-distance Wi-Fi literature (e.g., [140, 52, 137]) has taken the simplest approach to this issue by using static equal time share in both directions but we observe this is not an efficient approach for backhaul and TVWS settings. First, as shown earlier in §7.1, backhaul traffic can be highly asymmetric, with more traffic in the downstream (access network) direction, and also varies over time. Second, with TVWS spectrum, power asymmetry and interference effects may result in different effective capacities between forward and reverse directions. The above suggests an adaptive time split to counter these effects.

In view of the above, we seek a dynamic time slot duration selection for forward and reverse link directions, driven by traffic demand and effective sub-link capacities (latter obtained via the Interface Configuration module). Note that each sub-link here corresponds to each of the underlying data interfaces. We adapt the time slot durations at a coarser time granularity of *epochs* (30s in our implementation) to match with traffic variability; effective capacities of sub-links vary less frequently in our setting. But to avoid undesirable TCP effects, we switch the use of the link between forward and reverse directions at a finer time granularity (20ms in our implementation as per [140], proportional to the relative slot durations at the epoch level.

The decision on relative slot durations between forward and reverse directions is made at the `Master` based on locally available information and that obtained from

the `Slave` over the control interface. The key idea behind our approach is to choose forward and reverse time slot durations (equivalently, fractions within a time unit) so that they minimize the total backlogged traffic in both directions. More precisely, at the start of each epoch t, the `Master` solves the following optimization problem:

$$\max_{t_F, t_R} \left(\frac{\sum_{i \in F} \theta_i(t) \times t_F + \sum_{j \in R} \theta_j(t) \times t_R}{V_F(t) + V_R(t)} \right) \text{ s. t.}$$

$$\sum_{i \in F} \theta_i(t) \times t_F \leq V_F(t) \quad \forall i \in F$$

$$\sum_{j \in R} \theta_j(t) \times t_R \leq V_R(t) \quad \forall j \in R$$

$$t_F + t_R = 1 \qquad AND \qquad t_F, t_R > 0 \tag{7.1}$$

Where $\theta_i(t)$ is the effective sub-link capacity via interface i at the start of epoch t. t_F and t_R are the fractions of time within a 20ms time unit allocated for the forward (`Master-Slave`) and reverse (`Slave-Master`) directions respectively. $V_F(t)$ and $V_R(t)$ are, respectively, traffic volumes in forward and reverse directions for the upcoming epoch t. Each of these traffic volumes are the sum of forecasted traffic demand in the coming epoch t and backlogged traffic carrying over from the previous epoch. We consider a simple forecasting approach of assuming that the demand in the coming epoch will be same as in previous epoch, which is justified from the results in §7.1 for small epoch durations (30s in our case).

7.3.2.3 Traffic Scheduling

The TVWS conversion substrate in the WhiteHaul hardware layer described earlier in this section provides the physical capability to aggregate TVWS spectrum across multiple spectrum chunks over different interfaces. But translating this capability to higher layer aggregated data rates requires a way to concurrently use multiple interfaces and distribute backhaul traffic among them. Not only that, we seek to realize this aggregation in a transparent manner to end-user traffic so as to give the *abstraction of a high-speed link-level tunnel* through which user traffic is transported across. We find Multipath TCP (MPTCP) a natural fit for our use case to meet the above mentioned requirements. Moreover, it offers a reliable bit pipe like TCP while also handling packet reordering from striping user traffic across multiple interfaces. It also automatically adapts to any changes to underlying sub-link capacities or slot durations.

However the default MPTCP with a coupled congestion control algorithm (e.g., LIA [73], OLIA [142]) is not suitable for our purpose as its main focus is on shifting traffic from congested to less congested paths to preserve network fairness among competing TCP flows. We have a single logical flow that needs to efficiently utilize the available capacity to maximize aggregate link data rate. Even the uncoupled variant with the commonly used CUBIC congestion control algorithm [71] fails to quickly and accurately track the changes in slot durations, sub-link capacities and/or losses, as we demonstrate in our evaluation results in §7.4.

Motivated by the above, we propose a new cross-layer and uncoupled congestion control algorithm that is tailored for MPTCP use in WhiteHaul . Information from the Slot Allocation Manager is used to dynamically adjust the congestion window () size of each individual subflow (bound to a different interface) according to its current effective capacity. This allows WhiteHaul MPTCP to exploit the available capacity of each subflow even as it varies over time. At the start of each epoch, the *Slot Allocation Manager* sends an advisory signal to the MPTCP congestion control module indicating the estimated effective capacity of each subflow, determined as the product of corresponding sub-link's effective capacity and the fraction of time allocated to the endpoint in question. MPTCP then calculates a *target value for each subflow* by multiplying the advertised effective capacity and minimum RTT estimate it holds. WhiteHaul then increases rapidly and largely (100 packets per RTT in our implementation) until it reaches the target value. Thereafter, WhiteHaul keeps increasing linearly (one packet per RTT) while monitoring the queuing delay. When the queuing delay exceeds a certain delay budget, is reduced back to the target value. In this way, WhiteHaul prevents self-inflicted packet losses by controlling the queue occupancy of network interfaces. Additionally, even when a packet is dropped for any reason (low SINR or buffer overflow) WhiteHaul is designed to quickly return back to its target, ensuring that the subflow capacity is fully used.

Algorithm 2 highlights the key part of our algorithm that we implemented in the Linux Kernel. In short, when a new ACK is received on subflow (i), which begins a new window of data, the average queuing delay (`aqd`) is computed (lines 2-3). Thereafter, the weight factor (α_i), which dictates the increase rate of $_i$, is updated (lines 4-12). The value of α_i becomes large when $_i$ is lower than the target window (Ω_i) and also the average queuing delay is smaller than the queuing budget (λ_i), ensuring that during the congestion avoidance phase (lines 18-19) $_i$ is increased aggressively until it reaches Ω_i.

Algorithm 2: WhiteHaul MPTCP Congestion Control

input: Ω_i, is the target window for $subflow_i$

input: λ_i, is the delay budget for $subflow_i$

input: α_i, is the increase weight for $_i$

```
1  CongestionAvoidance(subflow_i)
2      if A new window of data begins then
3          aqd ← AvgQueueingDelay(subflow_i)
           /* Update α_i                                   */
4          if aqd ≤ λ_i then
5              if cwnd_i ≥ Ω_i then
6                  α_i ← 1
7              else
8                  α_i ← 100
9              end
10         else
11             α_i ← 1
12         end
           /* Periodic reduction                           */
13         if aqd > λ_i & cwnd_i > Ω_i then
14             cwnd_i ← Ω_i
15             ssthresh_i ← cwnd_i
16         end
17     end
       /* Response to new ACKs                             */
18     if cwnd_i ≥ ssthresh_i then
19         cwnd_i ← cwnd_i + α_i/cwnd_i
20     else
21         tcpInSlowStart ()
22     end
   /* Response to 3 duplicate ACKs                         */
23 DecreaseCWND(subflow_i)
24     cwnd_i ← max(cwnd_i − (cwnd_i ∗ 0.1), 2)
```

Otherwise, $_i$ is increased linearly (similar to standard TCP). At the beginning of every window of data, WhiteHaul examines whether it is allowed to reset $_i$ to Ω_i (lines 13-

16), making sure that the queue occupancy of underlying wireless interface of subflow (i) is not exceeding a certain threshold. Finally, when a lost packet is detected on a subflow, by receiving at least three duplicate ACKs, WhiteHaul reduces very gently (lines 23-24).

7.4 Evaluation

In this section, we present a wide ranging evaluation of WhiteHaul, assessing all aspects of its design. This includes: (i) benchmarking its spectrum aggregation and conversion efficiency relative to the ideal case using our prototype implementation; (ii) experimentally evaluating WhiteHaul MPTCP using our Linux kernel implementation to compare its congestion control algorithm with respect to both commonly used OLIA (coupled) and CUBIC (uncoupled) congestion control algorithms; (iii) additional measurement based and simulation studies (some driven by real-world traffic traces) to evaluate other aspects of WhiteHaul .

Compliance with regulations. Besides having to periodically query a geolocation database for available TVWS channels and their allowed power levels at the operating location, another key requirement for white space devices is to comply with the transmit spectrum mask related regulations. The latter is to ensure power leakage into adjacent channels under the prescribed limit so as not to cause interference to incumbents. To verify that our WhiteHaul prototype meets this requirement, we measured its out-of-band (OOB) emissions at different 802.11ac channel widths it can be configured to (20/40/80 MHz) using a spectrum analyzer (from Keysight) and find that OOB from our prototype is well within the limit specified by ETSI [58] for Class 1 TVWS devices (the relevant class for our outdoor and backhaul use case). For instance, with 80MHz channel, the OOB EIRP spectral density (P_{OOB}) with WhiteHaul is -103.8 dBm/Hz for the adjacent 100 KHz spectrum, which is as per Class 1 device requirements.

Spectrum conversion and aggregation efficiency. We now study aggregate TCP throughput obtained with WhiteHaul in all possible two and three interface combinations of 802.11ac channel widths supported by our interface cards (20, 40 and 80MHz). The flexibility with WhiteHaul allows us to down-convert any 5GHz channel to TV band by appropriately configuring frequency of the SDR based LO. We use unoccupied 5GHz Wi-Fi spectrum in our environment in the range of 5500-5750MHz. We use our implementation of WhiteHaul as described in the previous section including its MPTCP Linux kernel implementation. To generate TCP traffic we use the iPerf tool.

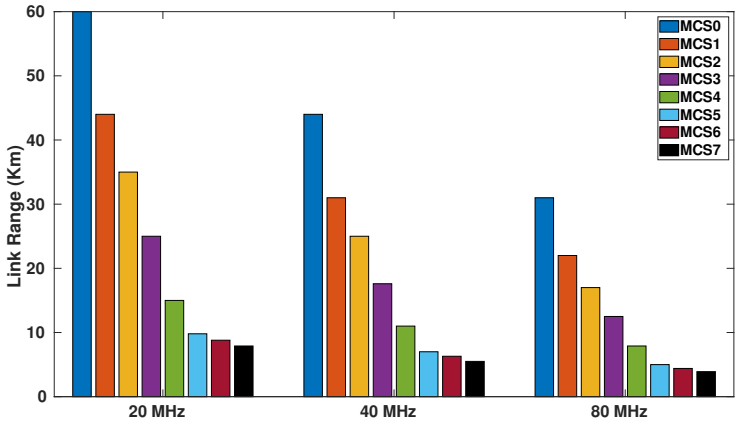

Figure 7.19: Relationship between link range and MCS for different channel widths assuming free-space pathloss and receive sensitivity values with commodity 802.11ac cards.

In each of the two and three interface scenarios, MPTCP throughput achieved with WhiteHaul after down conversion and aggregation is reported. In effect, each interface ends up using a TVWS spectrum chunk of the specified width. Figs. 7.20 and 7.21, respectively, show the throughput results with WhiteHaul for two and three interface scenarios. We see that WhiteHaul can provide maximum throughput up to 446Mbps when using two 80MHz channels. And with three interfaces using three 80MHz channels packed together with little channel spacing (aggregation of 240MHz spectrum), it provides up to 590Mbps aggregated throughput; and up to 640Mbps with adequate channel separation (not shown here). To put these results into perspective, we show in Fig. 7.19 the relation estimated link range (in Kms) and MCS, based on receive sensitivity values for the 802.11ac cards in our prototype and assuming a free space pathloss, reflecting a best case deployment scenario.

We benchmark these throughput results against the best case overall throughput, which is computed as the sum of maximum TCP throughputs achievable per interface for a given channel width and MCS in 5GHz band without any frequency conversion or aggregation. The corresponding throughputs as a percentage of the best case overall throughput, referred to as "Conversion Efficiency", are shown in Figs. 7.22 and 7.23. We observe that in all combinations of 20 and 40MHz channels, WhiteHaul TVWS conversion substrate and aggregation technique achieves 99% efficiency across all MCS values. This is because of almost perfect down-conversion without any signal distortion. When using even wider 80MHz channels with reduced inter-channel spacing,

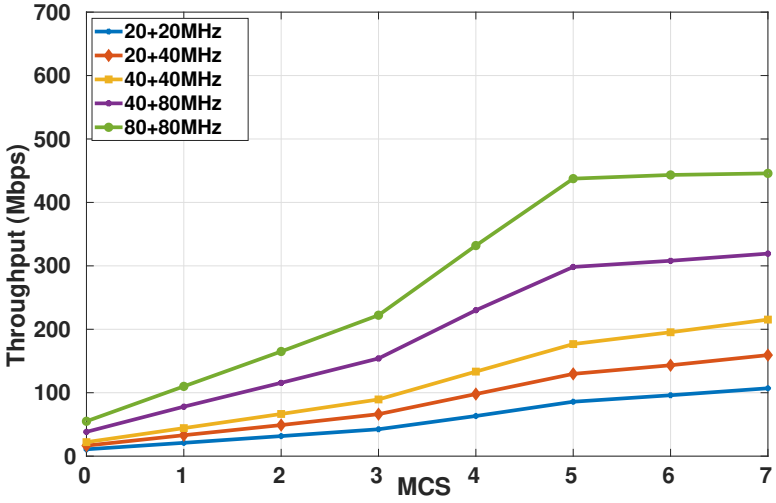

Figure 7.20: WhiteHaul aggregate TCP throughput performance in all two scenarios

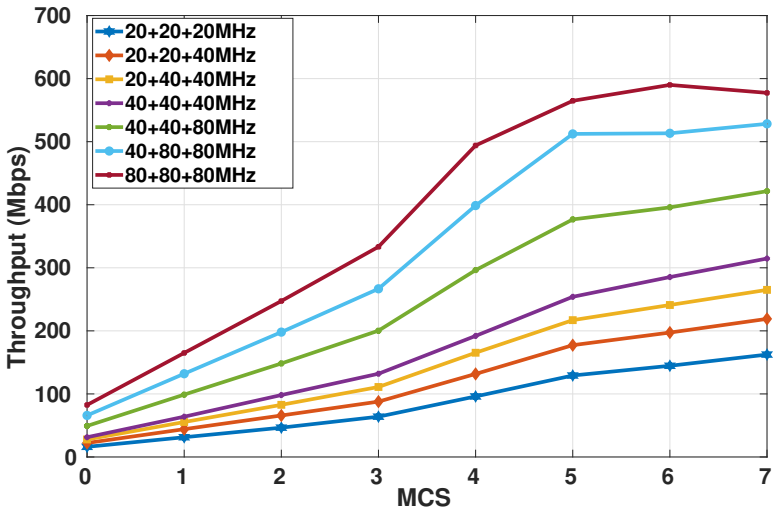

Figure 7.21: WhiteHaul aggregate TCP throughput performance in all three scenarios

however, higher adjacent channel leakage lowers the efficiency. For low MCS values (up to MCS5), WhiteHaul is still able to achieve close to best performance with average efficiency of 98% (as shown in 80MHz scenarios of Figs. 7.20 and 7.21). But the average efficiency drops down to 89% for higher MCS values (MCS6 and MCS7) and to the lowest level of 80% in the case of 3 immediately adjacent 80MHz channels. However, as noted above, with adequate inter-channel separation, as would be the case in a practical deployment, leads to higher throughput and efficiency. Equally, more number of interfaces and smaller widths can provide high efficiencies (results not shown here).

Impact of using 802.11ac channel widths. As we rely on 802.11ac interfaces in WhiteHaul, the set of channel widths we can use are limited to those come with 802.11ac (which in practice are 20/40/80MHz). We now examine the impact of restricting to

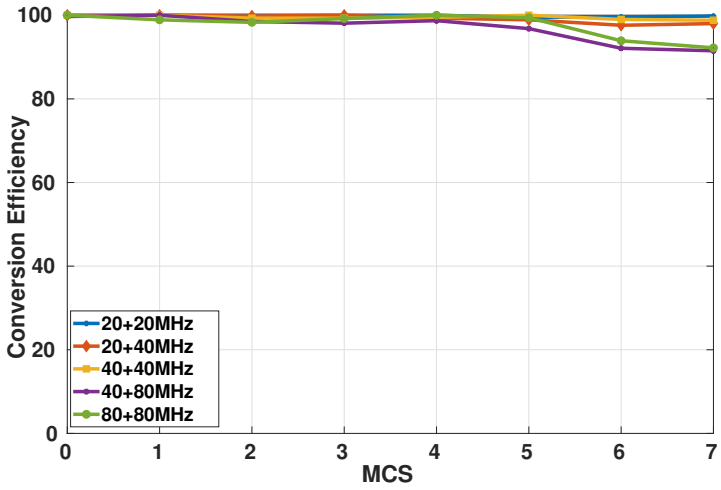

Figure 7.22: WhiteHaul conversion and aggregation efficiency as percentage of best case in all two scenarios

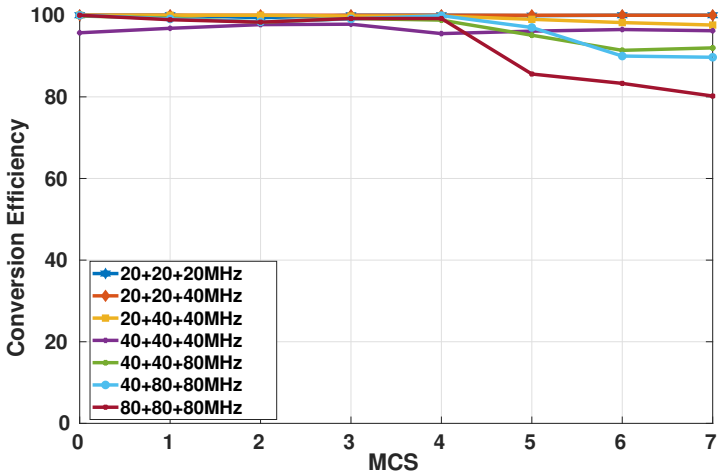

Figure 7.23: WhiteHaul conversion and aggregation efficiency as percentage of best case in all three scenarios

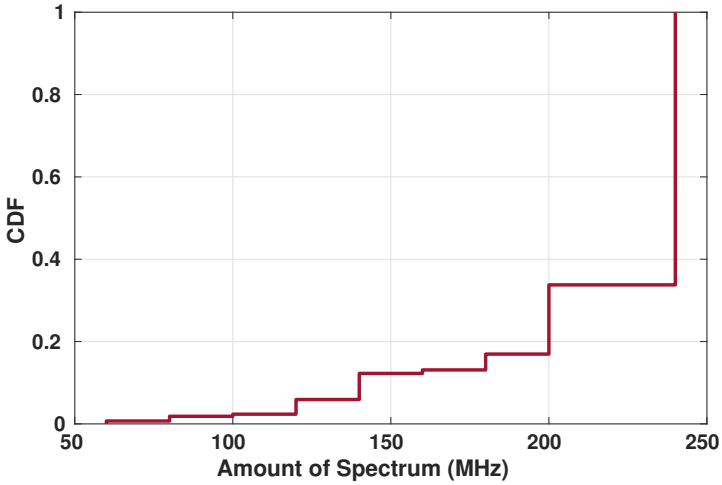

Figure 7.24: The amount and percentage of utilized spectrum for the case with three 802.11ac interfaces.

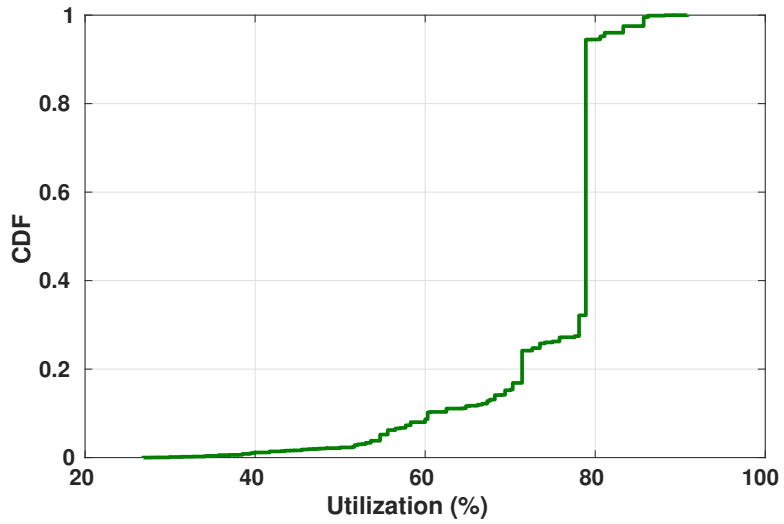

Figure 7.25: The amount and percentage of utilized spectrum for the case with three 802.11ac interfaces.

these few channel widths on available the TVWS spectrum use when aggregating individual narrower (6/8MHz) TVWS channels. We follow the methodology earlier used in §7.1. We first obtain the amount of available TVWS spectrum in rural locations of our case study country by querying a commercial geolocation database. Then, for each of those locations, we find how much of the available spectrum is available with any combination of 20/40/80MHz channel widths and supposing three 802.11ac interfaces at each WhiteHaul node. Results show that with 3 interfaces: more than 200MHz of spectrum can be utilized in more than 70% of the locations (Fig. 7.24); and this is equivalent to nearly 80% (Fig. 7.25). This can be further improved with additional interfaces. Overall, these results indicate that using 802.11ac interfaces and their widths only have a marginal negative impact in being able to fully exploit the available TVWS spectrum.

LoRa based control interface. Here we present our experimental assessment of using LoRa based control interfaces for coordination between WhiteHaul link endpoints. To this end, we experimentally study the data rates and reliability with LoRa under wide range of radio conditions. For reliability, we used packet reception rate (PRR), defined as percentage of successful packet reception, as the measure. We find that LoRa based communication is reliable with PRRs between 99.8% to 100% across a diverse range of link qualities (RSSIs ranging from -115dBm to -70dBm). And it achieves a data rate of $2.8Kbps$ even with the very low RSSI of -115dBm. To put these results into perspective, note that WhiteHaul endpoints need to exchange control

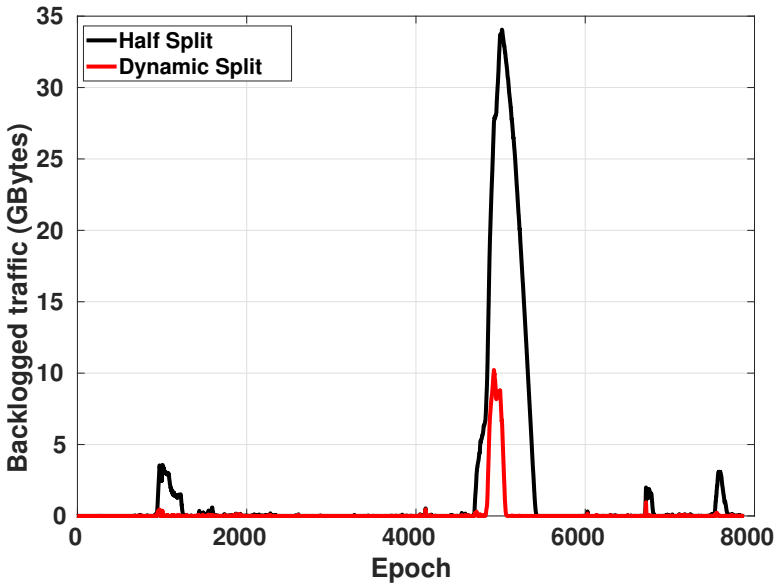

Figure 7.26: Performance benefit with WhiteHaul dynamic time slot allocation compared to commonly used static, half-split approach: the amount of backlogged traffic per epoch for a one week period.

Table 7.1: Simulation Parameters

Parameter	Value
iterations	1000
Number of epoch (T)	7877
Slot Duration (secs)	30
Effective Capacity (Mbps)	[5, 60]
Number of interfaces	2

information every few tens of seconds to aid decision making at the `Master` every epoch (30s). And the size of the control commands from the `Master` to the `Slave` are quite small (few tens of bytes). The largest control message size in WhiteHaul is the spectrum sensing information from `Slave` to the `Master` with a payload size of 797 bytes but this can be exchanged at the timescale of tens of minutes. With a duty cycle of 0.8%, even this message can be delivered 2.3 seconds at the achievable data rate every 5 minutes, and other smaller messages in less than a second.

Slot allocation. Here we evaluate the dynamic time slot allocation between forward and reverse directions in WhiteHaul in comparison with static, equal time split baseline. We use the total backlogged traffic carried forward from epoch to epoch as a performance measure. This evaluation is based on Monte Carlo simulations (1000 iter-

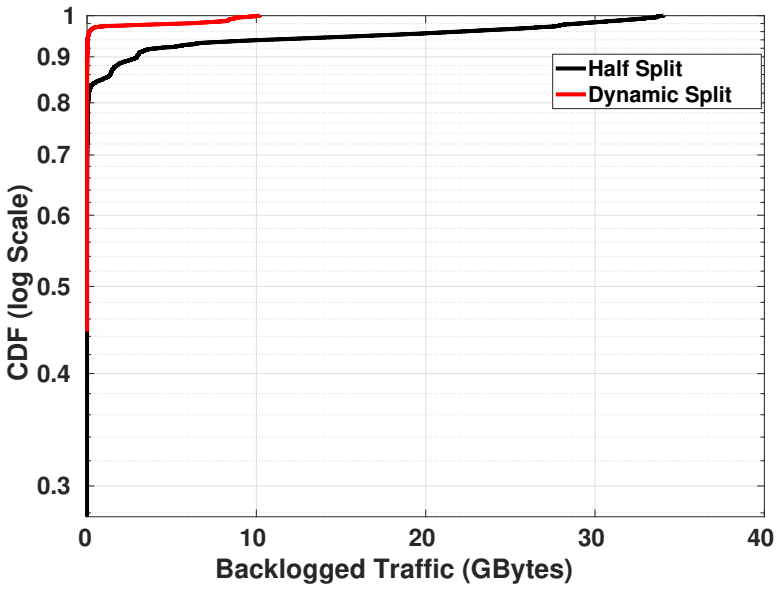

Figure 7.27: Performance benefit with WhiteHaul dynamic time slot allocation compared to commonly used static, half-split approach: CDFs of backlogged traffic.

ations per data point) using MATLAB, each spanning about 8000 epochs (30s long as per analysis in §7.1) and assuming two interfaces per WhiteHaul node. Table.7.1 summarises the simulation parameters. Effective sub-link capacities are randomly generated within the range of 5 to 60$Mbps$ for this case but traffic volumes in forward and reverse directions are from the real-world network trace as described in §7.1. Results shown in Fig. 7.26 indicate that the WhiteHaul the dynamic time split approach significantly reduces the maximum backlogged traffic across the whole one week period of the trace from up to 30GB with half-split approach to less than 7GB. This improvement is also evident from the CDF plot in Fig. 7.27 where there is no backlogged traffic in nearly 90% of the cases with dynamic split as opposed to under 60% with half-split.

Traffic scheduling. Here we experimentally assess the effectiveness of WhiteHaul MPTCP based aggregation in a wide range of capacity and packet loss scenarios, relative to two MPTCP alternatives using coupled congestion control with OLIA [142] and uncoupled congestion control with CUBIC [71]. We approach this in two steps. We first characterize packet loss and effective capacity in different link quality conditions and with different channel widths. This characterization then is used as the basis for emulation based evaluation of WhiteHaul and other MPTCP alternatives.

Packet Loss and Capacity Characterization. Using wider channel bandwidths for high capacity TVWS backhaul links can potentially impact transmission range and cause higher susceptibility to interference due to distribution of the same power over a

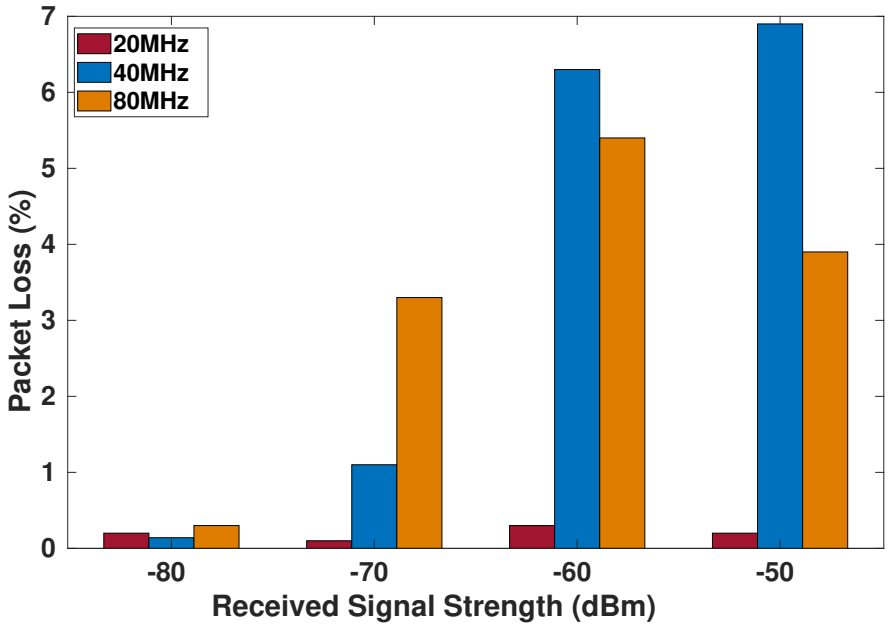

Figure 7.28: Packet loss rate at different link qualities (RSS values) and channel widths.

wider bandwidth [48]. These both manifest as increased packet loss rates, which can have adverse effect on most TCP based alternatives. We therefore conduct a controlled study to understand the nature of packet losses and effective capacities in a TVWS-based long distance setting. For this, we attenuate the transmitted TVWS signal using a combination of step attenuator and transmit power adjustment. The resulting received signal strength (RSS) values range from $-80dBm$ to $-50dBm$, reflecting increasing link distances.

To measure the loss rate and effective capacity, we use *iPerf* with CBR UDP traffic streams and also experiment with three different channel widths (20, 40 and 80MHz). As shown in Fig. 7.28, on narrow channels, e.g., $20MHz$, the link has very low loss rate, almost negligible, and the maximum loss rate observed across different RSS values was 0.3%. At higher channel width, packet losses increase up to 6.9% (with 40MHz channel). Packet loss differences between 40MHz and 80MHz channels are an artifact of the mechanics of underlying rate adaptation mechanism. On the other hand, the effective capacity, measured in terms of UDP throughput, shown in Fig. 7.29 is along expected lines – increasing with increasing RSS and channel width.

WhiteHaul MPTCP in Diverse Conditions. We use the results from the above study to evaluate the performance of WhiteHaul MPTCP in different conditions. We use our Linux kernel implementation for WhiteHaul and compare it with CUBIC [71] and OLIA [142]. The setup for this experiment consists of two Linux desktops, each

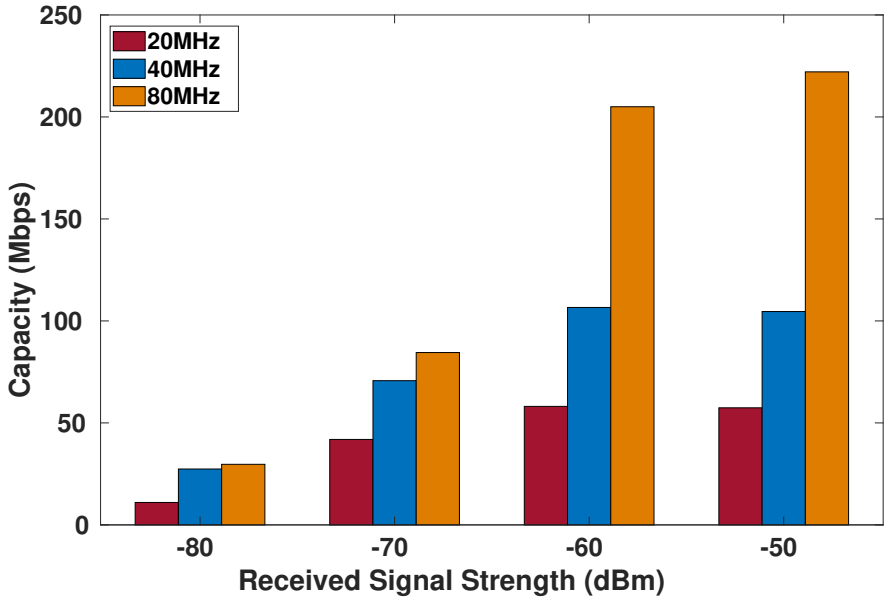

Figure 7.29: Effective capacity at different link qualities (RSS values) and channel widths.

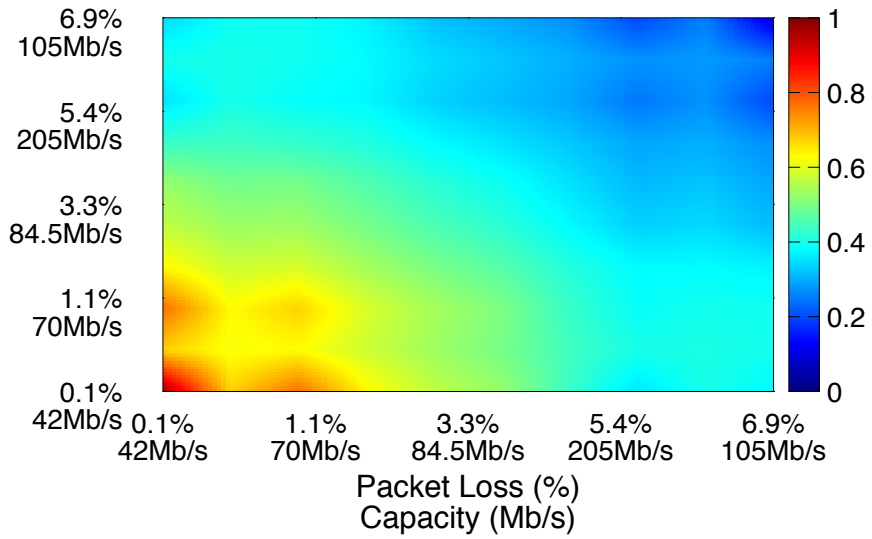

Figure 7.30: Aggregation efficiency of uncoupled MPTCP with CUBIC [71] in different conditions shown as a heatmap – red is best.

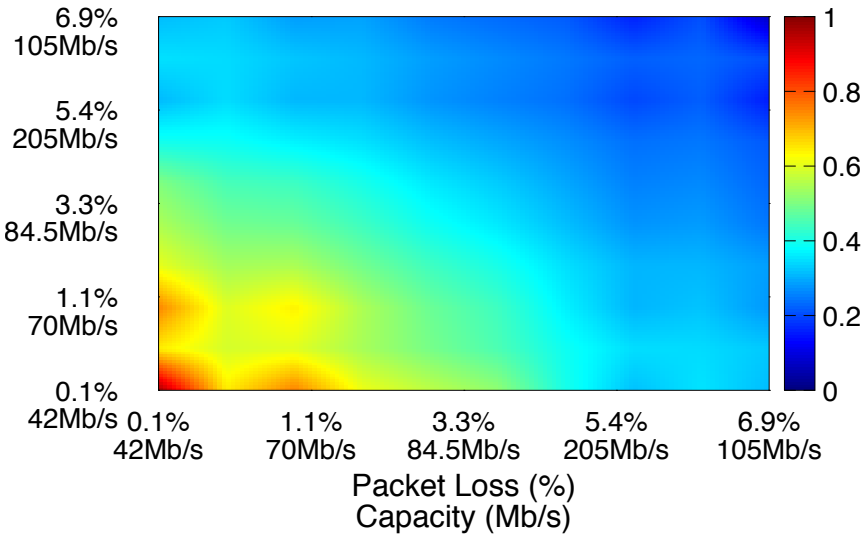

Figure 7.31: Aggregation efficiency of coupled MPTCP with OLIA [142] in different conditions shown as a heatmap – red is best.

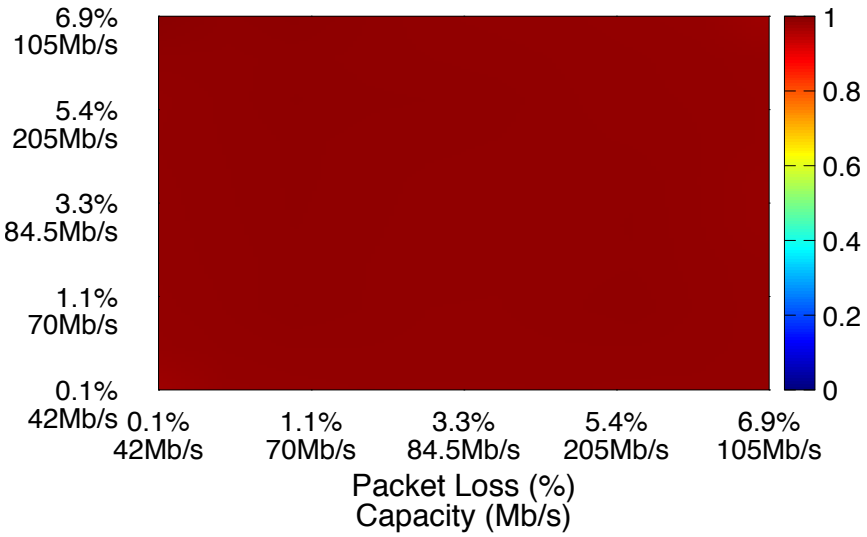

Figure 7.32: Aggregation efficiency of WhiteHaul MPTCP in different conditions shown as a heatmap – red is best.

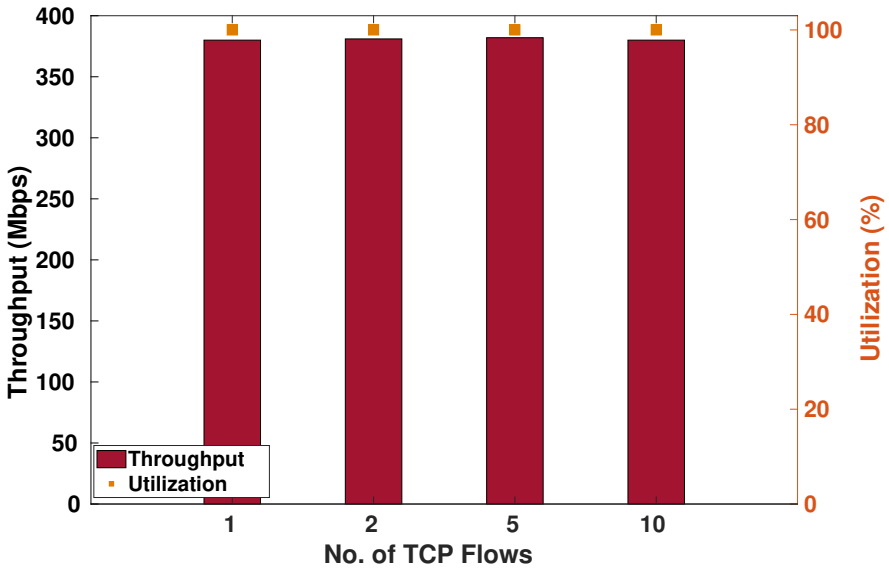

Figure 7.33: Effectiveness of WhiteHaul MPTCP link-level tunnel with varying number of end-to-end TCP flows.

with two Gigabit Ethernet interfaces. We use Linux Network Emulator (NetEm) and Traffic Control (tc) to emulate both losses and sub-link capacities from the above characterization study. For WhiteHaul, we set the queuing delay budget (λ) as $50ms$ and the target size is set as described in §7.3.2.3. We use *iPerf* tool send uni-directional TCP traffic and measure the aggregate throughput across the two interfaces. Figs. 7.30, 7.31 and 7.32 displays the results for the three alternatives as heatmaps of efficiency, defined as the ratio of achieved throughput (in presence of losses) for a given alternative – WhiteHaul, CUBIC or OLIA – to the maximum achieved throughput (without losses) with the same link capacities. We observe that CUBIC in general performs better than OLIA in presence of losses. This can be attributed to the fact that with CUBIC each sub-flow behaves independently with a separate congestion window, so the impact of packet losses of one sub-flow does not affect the congestion window of the other sub-flow. Overall though, WhiteHaul algorithm clearly achieves superior performance, by an order of magnitude, compared to both CUBIC and OLIA. In some scenarios like in the upper right corner, WhiteHaul , CUBIC and OLIA achieve aggregate throughputs of 403.8Mbps, 31.6Mbps and 22.3Mbps, respectively. This significant improvement with WhiteHaul is due to two reasons. First, WhiteHaul relies on a periodic advisory signal from the slot allocation manager to keep track of the optimal target congestion window size and uses it to ramp up the rate instantly to that level and then increases linearly while keep monitoring the queuing delay. If the queuing delay exceeds the

Table 7.2: WhiteHaul link CAPEX costs

Item		Cost (USD)
TVWS Conversion Substrate (per interface per node)	2 IEEE 802.11ac interfaces	200
	2 SDR-based LO	600
	RF Accessories (Amp, Attenuators, filters, etc.)	550
2 Combiner/Splitter		270
2 TVWS Yagi antennas		160
2 Compute Platforms (Raspberry Pis)		75
Link cost with one interface per node		1585
Link cost with two interfaces per node		3205
Link cost with three interfaces per node		4555

delay budget, the congestion window shrinks back again to the target value, preventing self-inflicting losses due to RTOs. Second, the WhiteHaul algorithm is robust in presence of losses to maintain sending rate close to sub-link capacities whereas CUBIC and OLIA have drastic responses to lost packets.

MPTCP use in WhiteHaul is transparent to end-to-end traffic flows (between user devices in the access network and the Internet) as it seeks to create a link-level tunnel abstraction. We evaluated the effectiveness of WhiteHaul to this end through an experiment varying number of end-to-end TCP flows. In this experiment, the WhiteHaul link consists of three sub-links respectively using 20, 40 and 80MHz chunks and aggregate capacity of 385Mbps. Results (Fig. 7.33) confirm that WhiteHaul link throughput and utilization stay unaffected by the number of end-user TCP flows, indicating no undesirable interactions between them and WhiteHaul MPTCP.

Cost analysis. We close this section with a cost analysis of WhiteHaul, which is primarily CAPEX as the OPEX cost includes small nominal fee to access a commercial geolocation database. Table 7.2 provides a breakdown of WhiteHaul link CAPEX costs. We assume a LimeSDR based LO. The basic version consists of one interface per WhiteHaul node making up a link and costs about 1600 USD. This version can aggregate up to 10 contiguous TVWS channels (80MHz spectrum) and provide a throughput up to 240Mbps based on results from earlier in this section. Some items are

per node and unaffected by the number of interfaces per node (combiners/splitters, antennas and compute platforms) while the rest scale with the number of interfaces. With 3 802.11ac interfaces per node, WhiteHaul link costs around 4500 USD and can deliver nearly 600Mbps. For a marginal additional cost, we can use dual polarized Yagi antennas to get the MIMO benefits and double the achievable throughput to over 1Gbps. Cost of our solution is comparable to existing commercial TVWS solutions (e.g., RuralConnect by Carlson Wireless, ACRS2 B1000 Adaptrum, GWS5002 by 6Harmonics, and XR by Redline) that cost around 4500-5000 USD but with an order-of-magnitude or higher throughput. While licensed or unlicensed commercial microwave solutions (e.g., Ubiquiti AirFiber-24-HD) cost a bit cheaper around 3500 USD per link, they can operate only in line-of-sight conditions.

7.5 Summary

In this chapter, we presented WhiteHaul system which, to the best of our knowledge, the first system that enable aggregated N number of non-contiguous channels in TVWS spectrum. WhiteHaul system tackles the fragmented TVWS spectrum by leveraging multiple wireless interfaces to be able to fully utilize the available spectrum and to increase capacity of the backhauling link. In order to allow these radios to share a single antenna, we propose hardware layer architecture for the WhiteHaul system to allow these multiple interfaces to share a single antenna without causing any harmful interference to each others. We also presented the orchestration software layer of WhiteHaul system where we design a new MPTCP congestion control that is robust to the losses of backhauling links. The main limitation of this work is handling the available TVWS chunks that is less than 20MHz or the available chunks these are not in 20, 40 or 80MHz sizes. We will discuss that in more details in the future work chapter.

Chapter 8

Multi-RAT Integration: PDCP Layer or Transport Layer?

In this chapter we focus on the third use case of the multi-connectivity paradigm and investigate the right protocol layer to perform the Multi-RAT integration. In this work, we experimentally study the two integration approaches of Multi-RAT: the transport layer approach and the PDCP layer approach. We also present our PDCP layer rate-based scheduler that leverages a feedback mechanism from the mobile user to estimate the rate on the underlying interfaces.

Next generation 5G networks are expected to provide superior advantages over the existing mobile networks by enabling wider mobile coverage and higher network capacities, thus, creating a better user experience. New challenges are expected to face the future 5G networks due to the rapid advances in computing, Artificial Intelligence (AI) and computer vision. These challenges revolve around the diverse requirements of these services that are expected to evolve in the new future. For instance, the virtual/augmented reality and the autonomous car driving pose stringent requirements on both throughput and per-packet latency and reliability [90, 150]. The autonomous driving requires real-time and reliable communication between the vehicle and the base stations to maintain and handle the vehicle safety. Virtual/augmented reality and tele-presence require continuous real-time feedback to enforce high-precision perception. In order to handle such diverse requirements, the 5G network services have been classified into three categories: Enhanced Mobile Broadband (eMBB), Ultra-reliable and Low-latency Communications (URLLC), and Massive Machine Type Communications (mMTC). eMBB focuses on services that require high bandwidth and capacity

(e.g., high definition (HD) videos and virtual reality/augmented reality). On the other hand, URLLC aims to handle the requirements of latency-sensitive services (e.g., remote driving and tactile Internet [150]). Lastly, mMTC is meant to handle the massive number of machine-to-machine short connections that are expected to be deployed to enable wide applications of smart cities.

To support such diverse services, leveraging multiple radio access technologies (RATs) such as LTE, 5G New Radio (NR) and WiFi simultaneously is vital. The key idea is to exploit the multi-connectivity that exists in modern hand-held devices to efficiently utilize the available resources and provide a better user experience. However, *Multi-RAT Integration* is a challenging task. The key concerns of Multi-RAT integration are the heterogeneity of the different protocol stacks and channel conditions. Multipath-TCP (MPTCP) [167] is one form of the different RAT integration and has attracted much attention in the last few years, not only in the research community but also in industry after Apple integrated MPTCP for the voice assistant application, Siri [162, 42]. MPTCP is a transport layer protocol that splits data streams over multiple paths by creating and maintaining *sub-flows* that are exposed to the application as a standard TCP connection. MPTCP has two main components that maintain the data flow across different paths: (i) congestion control algorithm, and (ii) traffic scheduler. The former acts similarly to the congestion control algorithm in standard TCP to prevent congestion on the path between the sender and receiver. Different new variations of congestion control algorithms have been proposed for MPTCP (e.g., OLIA, BALIA [98, 99, 142, 23]). The traffic scheduler decides on which available path the packet should be dispatched with the default scheduler, *minRTT*, and gives preference to the path with the lowest round-trip time (RTT). LTE-WiFi Aggregation (LWA) is another form of the Multi-RAT Integration. LWA is a Packet Data Convergence Protocol (PDCP) layer integration approach and has been standardized in Release 14 [15]. The PDCP layer integration is expected to be exploited in 5G networks. The PDCP architecture leverages the same outlines of LTE Dual Connectivity (Rel. 12), in which the eNB/base station is connected to wireless termination (WT) (i.e., it could be an access point or central controller that controls multiple access points) through (Xw) interface and the PDCP layer is responsible for the traffic distribution, congestion control and reordering functionality. The PDCP scheduler decides where to route the PDCP packets either on LTE, 5G NR or WiFi interfaces and to perform the reordering process at the reception before passing the packets to the higher layers.

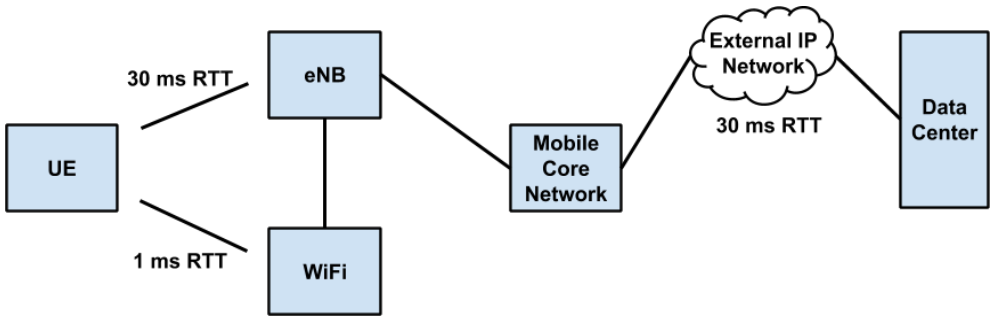

Figure 8.1: The Experimental setup used to evaluate the performance of MPTCP and LWA

8.1 PDCP Layer Integration: LWA Approach

To enable the Multi-RAT integration at the PDCP layer, we implement the LWA approach standardized by 3GPP Rel. 14 [17]. More specifically, we tackle two problems: (i) reordering at the PDCP layer, and (ii) the traffic scheduler. Reordering functionality at the PDCP layer is standardized by the 3GPP in [17] which is a timer-based reordering. Each Protocol Data Unit (PDU) in the PDCP layer has a sequence number that is leveraged by the reordering function either to deliver the received PDU to the higher layer or to insert it in a receiver buffer. Once the out-of-order packet is inserted in the receiver buffer, the reordering timer is started, waiting for the in-order packet to arrive to be able to send the packets to the upper layers. The reordering timer is configured by the Radio Resource Control (RRC) layer. If the timer expires before the in-order packet arrives, the PDCP delivers that PDU and all the in-order consecutive PDUs to the upper layer and stops the timer. Algorithm.3 summarizes the reordering procedure that is implemented in the PDCP layer.

The second problem is the rate estimation on both LTE and WiFi interfaces. We implement a feedback mechanism that leverages control messages sent from the UE to eNB that allows the base station to estimate the rate on each interface. The feedback is realized in the form of bitmap messages, which are sent at a predefined time to notify the base station on the unsuccessfully received packets. The bitmap message consists of 13Bytes as a header and a variable payload length. The header contains: (i) 1Byte of fixed Identifier to differentiate the bitmap packets from the data packets, (ii) 4Bytes of bitmap sequence number, (iii) 4Bytes of the PDCP Start Sequence number which is the PDCP sequence number of the first lost packet, and (iv) 4Bytes of PDCP End Sequence number which is the PDCP sequence number of the last packet received at the PDCP before sending the bitmap message. The actual payload in the bitmap message is N

flags that can be set to 0 or 1 as follows:

$$n^{th}flag = \begin{cases} 1, & \text{if the } n^{th} \text{ packet starting from} \\ & \text{PDCP Start Sequence number is received} \\ & \text{successfully} \\ 0, & \text{otherwise} \end{cases} \tag{8.1}$$

The total size of the bitmap packet is equal to 13 Bytes header and (N/8)Bytes flags.

The base station maintains a transmission table which contains information on each transmitted PDU including its length, transmit timestamp and the interface that is used to send the PDU. Once the bitmap message is received, the rate is estimated on each interface based on the ratio between the successfully received packet on that interface and the inter-arrival time of bitmap messages. The traffic is scheduled based on a simple algorithm that distributes the packets based on a ratio which equals the throughput estimated on that interface to the total throughput of both interfaces. Algorithm 4 summarizes the rate estimation at the eNB.

Algorithm 3: LWA Reordering and Bitmap Creation

```
1  procedure
2      while PDU is received do
3          if Received-PDCP-SN = Last-Submitted-PDCP-RX-SN + 1 then
4              Deliver to the upper layer, in ascending order, this PDU and all PDUs that
                 received in the receive buffer.
5              Last-Submitted-PDCP-RX-SN++;
6              Reset Reordering timer
7          end
8          else
9              Insert the PDU into receive buffer
10         end
11         if Reordering timer is not running then
12             Set Reordering timer with predefined timeout value.
13         end
14         if Reordering timer is expired then
15             Create bitmap for the received PDUs starting from
                 Last-Submitted-PDCP-RX-SN to the last PDU received (end of receive buffer)
16             Send the bitmap to the eNB
17             Deliver all the PDUs in the receive buffer to the upper layer.
18         end
19     end
20 end
```

Algorithm 4: Rate Estimation

```
1  procedure
2      while PDU is received do
3          if Received-PDU is bitmap PDU then
4              ΔT =T_currentbitmap - T_previousbitmap
5              while bitmap != end() do
6                  if bitmap[i] == 1 then
7                      if findSeqInTxtable (sqn) == 0 then
8                          Success-packet-on-LTE+=Length(packet);
9                      end
10                     else
11                         findSeqInTxtable (sqn) == 1
12                     end
13                     Success-packet-on-WiFi+= Length(packet);
14                 end
15             end
16             Rate-LTE = (Success-packet-on-LTE * 8)/ΔT
17             Rate-WiFi = (Success-packet-on-WiFi * 8)/ΔT
18         end
19     end
20 end
```

8.2 Integration Layer: Evaluation

To answer the question of which protocol layer is the right layer to integrate multiple RATs, we aim to experimentally evaluate the performance of two integration approaches: (i) the transport layer approach, represented by MPTCP and (ii) the PDCP layer approach, represented by LWA (realized by the traffic scheduler and reordering function described in the previous section) with a focus on both throughput and latency.

8.2.1 Methodology

The Testbed For the experiments, we consider a realistic architecture in which a download server is hosted in a data center located outside the mobile core network. The latency of the external IP network between the data center and the mobile core network is set to be 30 ms RTT. The download server is running MPTCP version 0.92 for Linux Kernel 4.14 hosted on quad-core Xeon CPUs at 3.4GHz and 16GB of RAM.

Both the eNodeB and UE are realized using srsLTE[1] which is an open-source LTE software that implements the LTE full stack. The eNodeB is connected to another machine acting as the EPC, running the EPC software implementation (OAI openair-cn [2]). Both the UE and eNodeB machines are equipped with dual-core Xeon CPUs at 3.4GHz and 8GB of RAM. Depending on the experiment, the testbed uses either the vanilla version of srsLTE or our modified version, which enable the LWA integration. The LTE air-interface is realized with a real RF front-end (Ettus B210 USRP) at both the UE and eNodeB. All the experiments were conducted with the same eNodeB configuration; namely, FDD with transmission mode 1 and 5MHz bandwidth in band 7. For the WiFi, we use Ubiquiti RouterStation router boards that host Mikrotik R52Hn miniPCI wireless cards that operate in 2.4/5GHz bands. The routers are connected to the eNodeB and UE through Gigabit Ethernet interfaces. We leverage the OpenWRT Linux as an operating system running the WiFi routers to allow us to evaluate the performance in different configurations (i.e., MCS values, bandwidth).

8.2.2 Throughput Evaluation

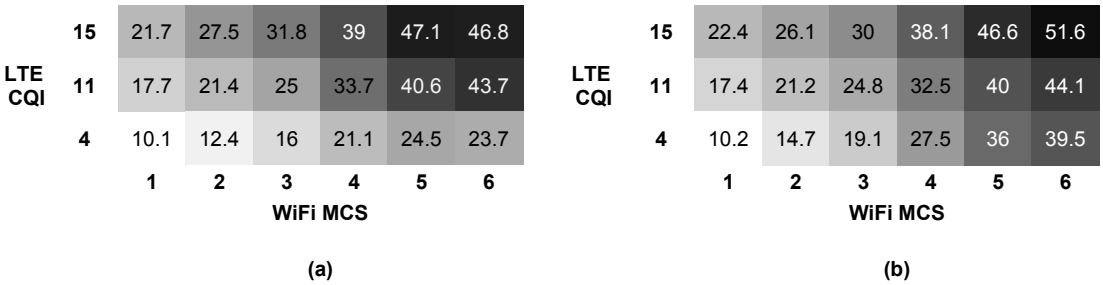

Figure 8.2: (a) MPTCP and (b) LWA performance for 5MHz LTE spectrum and 20MHz WiFi channel

To evaluate the throughput performance of the MPTCP approach, we run MPTCP on both the server and the UE where we consider the *minRTT* default MPTCP scheduler and use CUBIC as an uncoupled congestion control for the two sub-flows (i.e., LTE and WiFi). We focus on the aggregate downlink throughput as a metric to evaluate the performance of MPTCP. The RTT measured is 30 ms on the LTE air-interface and 1 ms on the WiFi air-interface. We consider these RTTs to be realistic and no further delay has been added to the air-interface of both technologies. However, to

[1] https://github.com/srsLTE/srsLTE
[2] https://github.com/OPENAIRINTERFACE/openair-cn/wiki

emulate the latency between the external server and the mobile core network, we use Linux Netem, where we introduce 30 ms RTT on that link. Thus, the end-to-end RTT for the LTE sub-flow is 60 ms, while it is 31 ms for the WiFi sub-flow. The WiFi is configured to operate in 5GHz band (i.e., channel 36) with 20 and 40MHz bandwidth channels. In all the following experiments, we vary the channel conditions on the Wi-Fi by changing the modulation and coding scheme (MCS) on the routers, and we also vary the channel condition on LTE air-interface by adjusting the transmit and receive power of the eNodeB (eNB). Fig. 8.2 shows the comparison between MPTCP and LWA on different channel conditions and when using a 5MHz LTE spectrum and a 20MHz WiFi channel.

As illustrated, both approaches have relatively similar performance in most of the channel conditions. However, in the scenario where the LTE interface experiences low channel quality while the WiFi interface has very superior channel condition (i.e., CQI 4 and MCS 6, the right bottom in Fig.8.2), the LWA approach over-performs the MPTCP with a 40% increase in the aggregate throughput. The severe performance degradation in the MPTCP scenario is due to the Head-of-Line blocking (HoL) at the receiver buffer. MPTCP ensures in-order packet delivery, which means when MPTCP receives an out-of-order packet, it must get buffered in the receiver queue until the packet with the expected sequence number arrives. This phenomenon is known as head-of-line blocking, where out-of-order packets are blocked and not sent to the application layer until the arrival of in-order packets. The *minRTT* scheduler at MPTCP tries to fill the congestion window of the lowest-RTT path first, then the path with the next lowest-RTT. As we have two different RTTs in this setup (i.e., 31ms for WiFi and 60ms for LTE), the LTE sub-flow blocks the faster WiFi sub-flow at the receiver. This phenomenon degrades the performance of MPTCP severely, especially in the cases when the fastest sub-flow is also the interface with the higher bandwidth. In that scenario, the receiver buffer is filled faster (compared to other scenarios) because of the larger send window of high bandwidth sub-flow. The packets are then blocked in the receiver buffer and are not passed to the application layer unless the in-order packets that were sent on the slowest interface arrive to the receiver. That limits the growth of the sender window of the higher bandwidth sub-flow. To confirm that, we run the same experiment but with a 40MHz WiFi channel, focusing on high throughput scenarios that can provide up to 83Mbps for a single TCP flow. As illustrated in Fig.8.3 and at higher throughput values of WiFi interface, we observe severe degradation in the aggregate throughput of MPTCP, where in most cases the aggregate throughput is

Table 8.1: Maximum achieved throughput of different LTE and WiFi channel conditions when using single TCP flow

WiFi MCS Value	Maximum achieved throughput on single TCP flow (20MHz Channel)	Maximum achieved throughput on single TCP flow (40MHz Channel)	LTE CQI Value	Maximum achieved throughput on single TCP flow (5MHz Channel)
MCS 1	9 Mbps	20.4 Mbps	CQI 4	1.6 Mbps
MCS 2	13.3 Mbps	30.2 Mbps	CQI 11	9.5 Mbps
MCS 3	17.6 Mbps	40.2 Mbps	CQI 15	15.5 Mbps
MCS 4	26 Mbps	58.1 Mbps		
MCS 5	34.4 Mbps	77.1 Mbps		
MCS 6	38.5 Mbps	82.3 Mbps		

lower than the throughput that can be achieved on a single TCP flow as summarized in Table. 8.1. For example, in the case of WiFi MCS4 and LTE CQI4, the aggregate theoretical throughput should be approx. 59.7Mbps, while the MPTCP achieves only 26.9Mbps, the LWA approach achieves 58.1Mbps, which is 97% of the theoretical throughput. This phenomenon can be confirmed when looking at the sender congestion window in the scenario of MCS6 and CQI4. Fig.8.1 represents the *bytes-in-flights* captured during that scenario. The congestion window of the WiFi sub-flow should be around 500KBytes according to the bandwidth-delay product formula where the maximum bandwidth of MCS6 is 83Mbps and the average RTT is 48ms. However, Fig.8.4 shows the limited growth of the congestion window which reaches only up to 300KBytes.

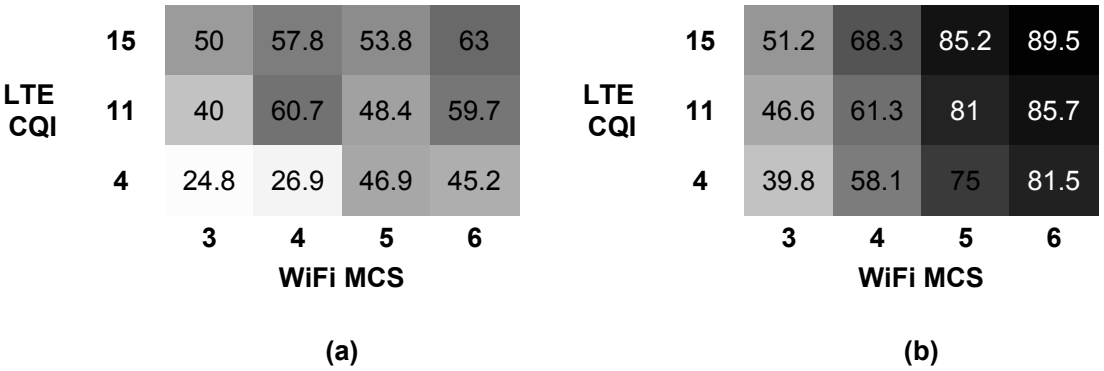

Figure 8.3: (a) MPTCP and (b) LWA performance for 5MHz LTE spectrum and 40MHz WiFi channel

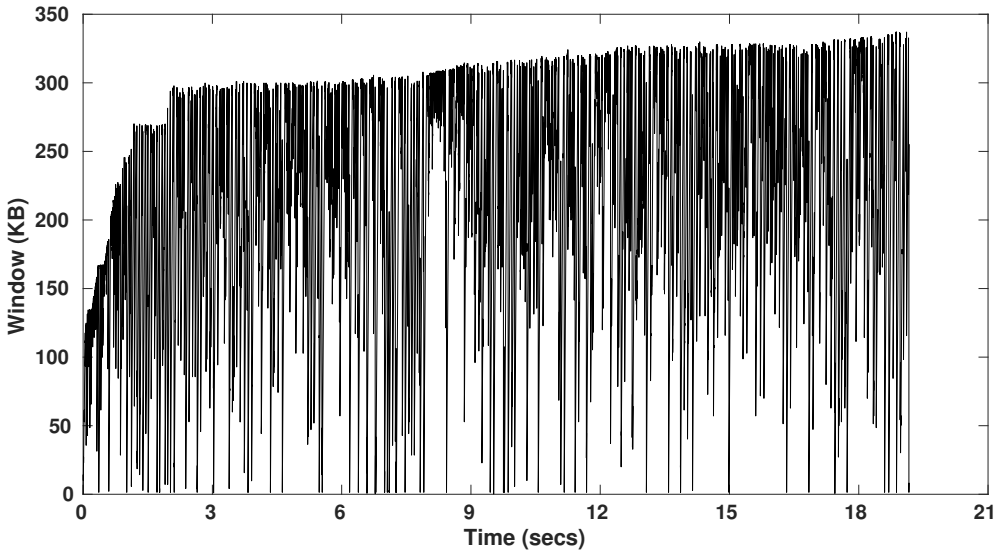

Figure 8.4: Congestion window of the higher capacity WiFi interface

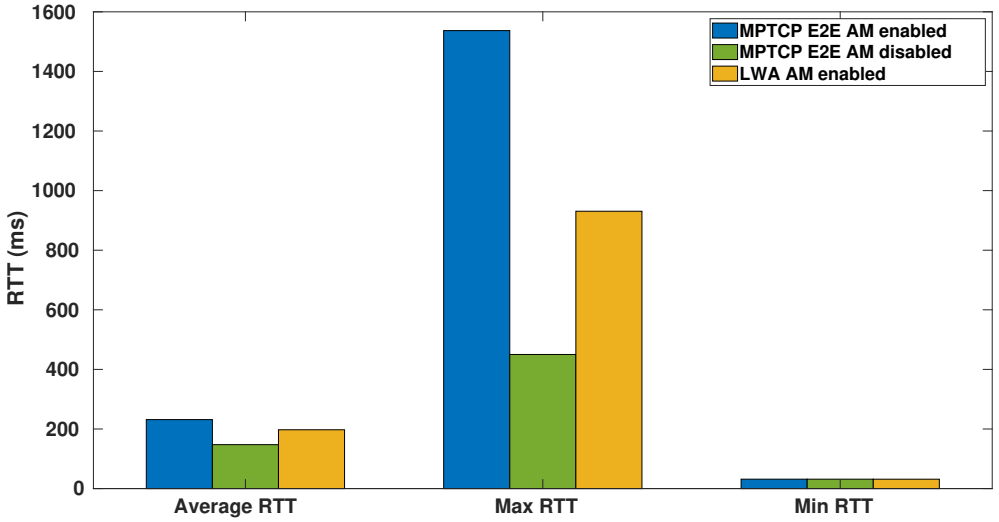

Figure 8.5: RTT comparison between MPTCP and LWA approaches with different RLC layer configurations

8.2.3 Latency Evaluation

In this section, we compare the performance of MPTCP and PDCP layer approaches from the latency perspective. More specifically, we focus on the scenarios where one interface experiences severe interference problem (to create re-transmission conditions) while the other interface is clear. In the following experiments, we introduce an interference to the LTE interface that leads to high number of retransmissions on the LTE air-interface. The key question is: at which layer is the retransmission considered more efficient in terms of latency? We answer the question by examining three sce-

narios: (i) MPTCP is running End-to-End (E2E) (i.e., on the server and the UE) with the RLC Acknowledged Mode (AM) enabled, (ii) MPTCP is running E2E with the RLC Unacknowledged Mode (UM) enabled and (iii) LWA is running with the RLC AM enabled. We use RTT as a metric to measure the latency. Using RF front-end (USRP B210) operating on the same frequency of the LTE base station we introduce an interference to the LTE air-interface that drops the CQI to value of 5 and causes a Block Error Rate (BLER) of around 10%. We ensured that the following results are not due to the head-of-line blocking phenomenon by limiting the WiFi throughput to 9Mbps. Fig.8.5, surprisingly, highlights that the E2E MPTCP with the RLC AM enabled experiences the highest latency, with an average and maximum RTT of 231.5ms and 1537ms, respectively. It also shows that doing the retransmission at the higher transport layer (i.e., going all the way back to the server) is faster than realizing the retransmission at the last hop, in the RLC layer of the eNB. This is due to the fact that in the case of E2E MPTCP with the RLC AM enabled, the failed packets are retransmitted by the RLC layer, where the maximum number of retries is 16 times (according to the 3GPP standards). The failed packets are handled by the transport layer only after reaching the maximum number of retries in the RLC layer. Thus, that is the major drawback of this scenario in which the retransmission occurs on the same interfered interface, where the probability of failed retransmission is high. On the other hand, when the RLC AM is disabled and the RLC layer uses the Unacknowledged Mode (UM), all the retransmission is handled by the transport layer at the server which can retransmit the packets on the other non-interfered interface, in turn reducing the average and maximum RTT to 147.5 and 450ms, respectively. On average, the performance of LWA approach with the RLC AM enabled is similar to the E2E MPTCP with the RLC AM; this is due to the fact that both approaches delegate the retransmission to the RLC layer.

8.3 Discussion

In light of the previous experiments, the PDCP Layer approach shows significant performance gain in terms of throughput and slight improvement from the latency perspective. The gain in terms of throughput is driven by the differences in the reordering mechanism used in the different layers. The LWA reordering mechanism is a timer-based function that avoids the HoL problem by delivering the packets to the upper layer after a predefined time, even if the in-order packet has not arrived. In MPTCP

and as a rule-of-thumb, increasing the receiver buffer might help to alleviate the problem of HoL, however, that will not mitigate the problem. This is due to two reasons. First, the TCP stack does not use a fixed receive buffer; however, it uses an auto-tuning algorithm to dynamically adapt the receive buffer size in order to achieve high performance at the lowest possible memory cost. Therefore, having a fixed large receive buffer is not scalable especially, on mobile devices. Second, in order to react to the event of a stalled receiver buffer, MPTCP penalizes the interface with a higher RTT by reducing its congestion window. Such a penalization mechanism avoids utilizing the higher RTT sub-flow.

From the latency perspective, LWA achieves lower average latency compared to the E2E MPTCP with the RLC AM enabled. However, when the MPTCP is tested with the RLC UM, it outperforms the LWA approach. This proves the need to realize the re-transmission at the PDCP layer rather than relying on the RLC AM. This is due to the fact that the RLC layer is unaware of any other interfaces associated with the LTE base station; therefore, any failed packet on the LTE interface will be retransmitted on the same interface. However, moving the re-transmission one layer up and handling the re-transmission decision at the PDCP layer might result in lower latency, because the PDCP layer has a better view and understanding for all the underlying wireless interfaces associated to the base station, including their channel quality and the radio parameters. This helps the PDCP layer to optimally decide where to re-transmit the failed packet. In addition, realizing the re-transmission at the PDCP layer will result in lower latency compared to the E2E MPTCP with the RLC UM. This is because performing the re-transmission at the last hop allows faster packet failure detection compared to the end-to-end RTT mechanism used by the MPTCP to detect the failure.

Real-time applications (e.g., health care, vehicle-to-vehicle, or factory automation) have stringent requirements in terms of latency and reliability. Thus, the MPTCP, transport-layer approach might fail to achieve these requirements for two reasons. First, in the transport-layer approach, the server (i.e., the sender) is responsible for the packet recovery mechanism. In other words, if any packet is lost or failed due to poor channel conditions, the server should be able to detect and retransmit the lost packets. However, because these servers are usually located several hops away from the users (e.g., those who run the real-time application), the lost packet takes a longer time to be recovered and retransmitted. Such long retransmission time might not be tolerable by real-time applications. Second, the mobile network is dynamic in nature and will be more dynamic in the next generation networks with the adaptation

of mmWave in future 5G networks. The transport-layer approach has a slow reaction to such a dynamic environment and fails to utilize the network resources optimally as such in several studies.

On the other hand, the PDCP layer approach overcomes the limitations of the transport-layer approach. As the PDCP is located on the eNB - in other words, on the last hop from the mobile users - it can detect the lost packets and react faster to the change in the wireless environment. As we discussed above, performing the retransmission at the PDCP layer might significantly benefit real-time applications. Besides, the PDCP scheduler should be intelligent enough to decide on the scheduling policy based on the traffic type. For instance, splitting the traffic of real-time applications between different Radio Access Technologies (RATs) might not be the optimal decision. These RATs have different characteristics (e.g., bandwidth, latency) and different channel conditions; therefore, if the packets are distributed across multiple RATs, they will arrive at the receiver out-of-order. Then they will remain in the receiver buffer to be reordered before being passed to the upper layer. Such a policy of splitting the packets across different RATs is not desirable for real-time applications because it will significantly affect packet latency. On the other hand, for throughput-hungry applications, this splitting scheduling policy will be highly desirable because it will improve the throughput. Thus, the PDCP layer scheduler should have some intelligence to decide on the right scheduling policy based on the traffic type and network conditions.

8.4 Summary

In this chapter, we provided a quantitative comparison between MPTCP and LWA integration approaches in different scenarios and channel conditions. We also proposed the PDCP layer rate-based scheduler that leverages a feedback mechanism to estimate the rate of different interfaces. The study shows the performance gain of LWA approach compared to the E2E MPTCP in terms of throughput and latency. In addition, our experimental study sheds the light on the need to perform the packet retransmission at the last hop, and more specifically at the PDCP layer instead of the RLC, due to the very fact that the PDCP layer has a better view for all the underlying wireless interfaces associated to the base station, including the channel quality and the radio parameters. This helps the PDCP layer to optimally decide where to re-transmit the failed packet. Hence, the lack of the retransmission module in PDCP is the current limitation of this work and we consider to study the effect of that module on overall

system performance in terms of latency in the future work.

Chapter 9

Conclusions & Future Works

9.1 Conclusions

Global mobile data traffic increased by 71% in 2017, reaching 11.5 exabytes per month by the end of 2017 from a previous 6.7 exabytes per month by the end of 2016 [40]. That increasing trend of data traffic demand is expected to continue growing exponentially in the coming years. Both the growing demand and the limited spectrum resources have fueled the need for innovative, efficient techniques that can accommodate the increasing demand and utilize the available spectrum resources. The multi-connectivity paradigm is considered to be the key feature in the next generation of wireless networks. It allows the wireless systems to maintain multiple simultaneous connections to different radio access technologies in order to fully utilize the spectrum resources and boost the wireless system capacity. However, enabling such a paradigm is a non-trivial task due to the challenges that arise from the need to enable the coordination between heterogeneous systems which have dissimilar representation of the spectrum resources and different protocols and standards.

In this thesis, we focused on three different use cases for the multi-connectivity paradigm in emerging wireless networks, investigated the issues and the key problems that arise in these use cases and provided solutions towards enabling an efficient operation. Although each of these solutions focused on different areas, they complement each other in providing a holistic view and better understanding of the several issues that can hinder wireless systems from enabling the multi-connectivity paradigm. The high-level conclusions for each of these issues and their solutions are presented in the

following subsections.

9.1.1 Matching Theory based Decoupled User Association Mechanism

For our first contribution, we focused on dual connectivity as the first use case of the multi-connectivity paradigm; more specifically, the decoupled uplink/downlink user association problem in the HetNets context. We highlighted that the challenges in this environment stem from the conflicting objectives of different entities in such a system, including MBS, SBS and mobile users. We presented a matching theory algorithm that considers these diverse objectives and the decoupling related cost; this algorithm results in a stable allocation and we also empirically demonstrated its convergence. In addition, we used stochastic geometry to model the long-term throughput as the average ergodic rate of a typical mobile user and its associated BS. Mobile users use this model to rank their BS preferences in both the uplink and downlink directions. From the perspective of BSs, the preferences capture the need to offload the traffic from the MBS to SBSs.

9.1.2 Aggregated TVWS Spectrum for Backhaul in Rural and Developing Regions

For our second contribution, we focused on providing a high-capacity and low-cost backhauling solution for rural and low-income regions leveraging the TVWS spectrum. In this work, we shed light on the limitations of the state-of-the-art backhauling solutions in TVWS spectrum, which can only support up to 3 TV channels (i.e., a total of 24 MHz). Through our trial deployment and theoretical analysis, we highlighted the need for a high-capacity backhauling solution that can aggregate the TVWS fragmented spectrum. We presented the WhiteHaul system which is, to the best of our knowledge, the first TVWS spectrum aggregation system that can leverage multiple large non-contiguous chunks of the spectrum. WhiteHaul system composed of three main components: (i) the interface configuration module which is responsible to assess the current available spectrum opportunities and configure the wireless interfaces to maximize the system performance. (ii) The traffic manager orchestrates the traffic distribution and slot allocation between both end of the link. (iii) The conversion circuit which is responsible for the down/up conversion process of the WhiteHaul system.

We demonstrated a prototype of the WhiteHaul system in our lab setup and thoroughly studied its performance.

9.1.3 Quantitative Assessment of the Right Protocol Layer to Integrate Multiple RATs

For our third contribution, we focused on the Multi-RAT integration use case in which different heterogeneous technologies are enabled to be simultaneously utilized. More specifically, we focused on studying the question of what is the right layer in the protocol stack that should be leveraged to enable a seamless integration between different RATs? Towards that objective, we studied the performance of two dominant approaches including the transport layer and PDCP layer approaches. We focused on different service requirements, namely, the URLLC and eMBB, the two main services in the future 5G networks. We quantitatively studied the performance of the MPTCP and LWA using both metrics of throughput and latency. In addition, we proposed a rate-based scheduling algorithm for the PDCP layer approach that aims at distributing the traffic between the different available RATs based on the estimated rates.

9.2 Limitations & Future Work

This section summarizes the limitations of the contributions presented in this thesis, and presents directions for future work.

9.2.1 Aggregated TVWS Spectrum for Backhaul in Rural and Developing Regions

TVWS spectrum is fragmented and crucial requirement of any backhauling system is the capability to aggregate non-contiguous spectrum chunks.

Narrow-band Channel. WhiteHaul system has the capability of aggregating N number of different spectrum chunks with different channel widths. However, as it down/up converts the WiFi signal generated from WiFi devices into TVWS band, these devices operate only with the standard WiFi channel width (i.e., 20, 40, 80 MHz). The WiFi channels are much wider than TV channels; therefore, in scenarios where the availability of TVWS is smaller than 20 MHz channel, the WhiteHaul system might not be able to leverage that available resource. For example, if the TVWS availability in

specific location is four non-contiguous TV channels and the size of each channel is 8 MHz (i.e., 32 MHz total), the WhiteHaul system will not be able to utilize these resources. Due to the fact that these channel widths are smaller than the channels in WiFi systems. To address this limitation, another feature is required to be added to WhiteHaul system which aims at not only down/up-convert the WiFi signal but also to down/up-clock that signal to the standard 8 MHz TV channel.

Losses in the conversion process. As we are using a combiner/splitter components with around 6dB total losses, that might reduce the received signal strength at the receiver side and increase the packet losses probability at high MCS values. One way to mitigate the effect of these losses is to use higher power amplifiers with low noise figure (NF) which will allow the WhiteHaul system to tolerate the losses introduced by the combiner/splitter. A careful configuration of WhiteHaul system parameters (e.g., transmit power, amplifier gain) is essential in order to maintain the signal quality at high MCS values.

Real-world Deployment. Throughout this work, we evaluated the WhiteHaul performance in the lab environment; however, a real-world deployment in a representative rural area would help to better understand the trade-off between the size of the aggregated spectrum and the link distance. In addition, a benchmarking study between the WhiteHaul system and the existing commercial TVWS solutions (e.g., Carlson solution [3]) that can only support up to 3 TV channels would help to highlight the performance gain in terms of the backhauling link capacity.

9.2.2 Quantitative Assessment of the Right Protocol Layer to Integrate Multiple RATs

Re-transmission at PDCP Layer. In this work, we concluded that the PDCP layer approach can be considered to be the better approach for URLLC traffic due to the fact that performing the packet re-transmission at the last hop (i.e., eNodeB) is less time-consuming than re-transmitting the packets at the transport layer. However, the re-transmission at the last hop should be the responsibility of the PDCP layer and not the RLC layer. That is because PDCP layer has a better understanding of the current channel conditions of both Wi-Fi and LTE interfaces, such that the decision of which interface to re-transmit the failed packet on will be optimal. On the other hand, as the RLC layer has limited information about the channel conditions of the other interface, realizing the re-transmission at the RLC layer is inefficient and creates

the high latency, as discussed in the previous chapter. An efficient re-transmission mechanism that leverages the lower layer information of both LTE and WiFi interfaces is essential in order to meet the stringent requirements of URLLC traffic.

Service-Oriented PDCP Layer Scheduler. We proposed a rate-based scheduler that relies on the feedback mechanism from the mobile user to estimate the rate of the underlying interfaces and decides on which interface the next packet should be scheduled. A holistic scheduler that supports different types of services, including URLLC and eMBB is essential for the future 5G network. That scheduler should be able to maintain updated information on the channel conditions of the underlying interfaces and to meet the service requirements of different types of traffic.

Bibliography

[1] Adaptrum. http://www.adaptrum.com/.

[2] *ATT: Project AirGig*. https://about.att.com/story/2018/airgig.html.

[3] Carlson Wireless Technologies. http://www.carlsonwireless.com/.

[4] *Pycom - Next Generation Internet of Things Platform*. https://pycom.io/.

[5] *RF Explorer*. http://j3.rf-explorer.com/.

[6] Splat!: an RF Signal Propagation, Loss, And Terrain analysis tool. http://www.qsl.net/kd2bd/splat.html.

[7] *Tarana Wireless*. https://www.taranawireless.com/intro.html.

[8] *Ubiquiti Networks*. https://www.ui.com/.

[9] UK digital television transmitter details. https://www.ofcom.org.uk/spectrum/information/transmitter-frequency.

[10] Urban Rural Classification 2013-2014, 6 Fold Classification. http://www.gov.scot/Resource/0046/00464780.pdf.

[11] *USRP B210*. http://www.ettus.com/all-products/UB210-KIT/.

[12] 3GPP. 3GPP TS 36.300: Technical Specification Group Radio Access Network. http://www.arib.or.jp/english/html/overview/doc/STD-T104v3_00/5_Appendix/Rel12/36/36300-c50.pdf, 2015. [Online; accessed July-2019].

[13] 3GPP. 3GPP TS 36.323: Packet Data Convergence Protocol (PDCP) specification, Release 14. https://www.etsi.org/deliver/etsi_ts/136300_136399/136323/14.03.00_60/ts_136323v140300p.pdf, 2017. [Online; accessed July-2019].

[14] 3GPP. Evolved Universal Terrestrial Radio Access Network (E-UTRAN) and Wireless LAN (WLAN); Xw signalling transport, Release 14. https://www.etsi.org/deliver/etsi_ts/136400_136499/136462/14.00.00_60/ts_136462v140000p.pdf, 2017. [Online; accessed July-2019].

[15] 3GPP SPECIFICATION. Packet Data Convergence Protocol (PDCP) specification, Release 14" in TS 36.323. Retrieved July, 2019 from https://www.etsi.org/deliver/etsi_ts/136300_136399/136323/14.03.00_60/ts_136323v140300p.pdf.

[16] 3GPP:REL.13. Evolved Universal Terrestrial Radio Access (E-UTRA) Packet Data Converge Protocol (PDCP) specification. Retrieved July, 2018 from https://www.etsi.org/deliver/etsi_ts/136300_136399/136323/13.00.00_60/ts_136323v130000p.pdf.

[17] 3GPP:REL.14. Evolved Universal Terrestrial Radio Access (E-UTRA); Packet Data Convergence Protocol (PDCP) specification. Retrieved July, 2018 from https://www.etsi.org/deliver/etsi_ts/136300_136399/136323/14.03.00_60/ts_136323v140300p.pdf.

[18] 3GPP:REL.16. LTE CA R16 xBDL 2BUL. Retrieved July, 2018 from http://www.3gpp.org/DynaReport/GanttChart-Level-2.htm#bm800063.

[19] AHMAD, T., AND SUBRAMANIAN, L. Virtual Cellular ISPs. In *Proceedings of the 3rd Workshop on Experiences with the Design and Implementation of Smart Objects* (2017), ACM, pp. 35–40.

[20] AIJAZ, A., AGHVAMI, H., AND AMANI, M. A survey on mobile data offloading: technical and business perspectives. *Wireless Communications, IEEE 20*, 2 (2013), 104–112.

[21] AKYILDIZ, I. F., LO, B. F., AND BALAKRISHNAN, R. Cooperative spectrum sensing in cognitive radio networks: A survey. *Physical Communication 4*, 1 (2011), 40–62.

[22] ANAND, A., PEJOVIC, V., BELDING, E. M., AND JOHNSON, D. L. VillageCell: Cost Effective Cellular Connectivity in Rural Areas. In *Proceedings of the Fifth International Conference on Information and Communication Technologies and Development* (2012), ACM, pp. 180–189.

[23] ANWAR WALID, QIUYU PENG, JAEHYUN HWANG, STEVEN H. LOW. Balanced Linked Adaptation Congestion Control Algorithm for MPTCP. Retrieved July, 2019 from `https://tools.ietf.org/html/draft-walid-mptcp-congestion-control-00`.

[24] ARYAFAR, E., KESHAVARZ-HADDAD, A., WANG, M., AND CHIANG, M. RAT Selection Games in HetNets. In *INFOCOM, 2013 Proceedings IEEE* (2013), IEEE, pp. 998–1006.

[25] ASHOK, A., SUBBIAH, I., VARGA, G., SCHREY, M., ACHTZEHN, A., PETROVA, M., AND HEINEN, S. WhiteLAN: Facilitate cost-efficient SDR research with COTS IEEE 802.11 b/g devices. In *ACM SIGCOMM Computer Communication Review* (2014), vol. 44, ACM, pp. 45–52.

[26] BAHL, P., ET AL. White Space Networking with Wi-Fi like Connectivity. In *Proc. ACM SIGCOMM* (2009).

[27] BAIG, G., ALISTARH, D., KARAGIANNIS, T., RADUNOVIC, B., BALKWILL, M., AND QIU, L. Towards unlicensed cellular networks in TV white spaces. In *Proc. ACM CoNEXT* (2017).

[28] BAIG, G., ALISTARH, D., KARAGIANNIS, T., RADUNOVIC, B., BALKWILL, M., AND QIU, L. Towards Unlicensed Cellular Networks in TV White Spaces. In *Proceedings of the 13th International Conference on emerging Networking EXperiments and Technologies (CoNEXT)* (2017).

[29] BAO, W., AND LIANG, B. Structured Spectrum Allocation and User Association in Heterogeneous Cellular Networks. In *INFOCOM, 2014 Proceedings IEEE* (2014), IEEE, pp. 1069–1077.

[30] BOCCARDI, F., ET AL. Why to Decouple the Uplink and Downlink in Cellular Networks and How To Do It. *IEEE Communications Magazine*. in press.

[31] BOCCARDI, F., ET AL. Five Disruptive Technology Directions for 5G. *IEEE Communications Magazine 52*, 2 (2014), 74–80.

[32] BOOSTANIMEHR, H., AND BHARGAVA, V. Joint Downlink and Uplink Aware Cell Association in HetNets with QoS Provisioning. *Wireless Communications, IEEE Transactions on PP* (2015), 1.

[33] BROADBAND COMMISSION FOR SUSTAINSABLE DEVELOPMENT. The State of Broadband: Broadband catalyzing sustainable development, March 2017. Retrieved April, 2018 from https://www.itu.int/dms_pub/itu-s/opb/pol/S-POL-BROADBAND.18-2017-PDF-E.pdf.

[34] BROWN, T. X. An analysis of unlicensed device operation in licensed broadcast service bands. In *New Frontiers in Dynamic Spectrum Access Networks, 2005. DySPAN 2005. 2005 First IEEE International Symposium on* (2005), IEEE, pp. 11–29.

[35] CEPT. Draft CEPT Report 57 (A), 5 GHz. http://tinyurl.com/q5dg33f, 2014. [Online; accessed 10-August-2015].

[36] CHAKRABORTY, A., AND DAS, S. R. Measurement-augmented spectrum databases for white space spectrum. In *Proc. ACM CoNEXT* (2014).

[37] CHANDRA, R., ET AL. A Campus-Wide Testbed over the TV White Spaces. *ACM SIGMOBILE MC2R 15*, 3 (Jul 2011).

[38] CHEN, Q., YU, G., SHAN, H., MAAREF, A., LI, G. Y., AND HUANG, A. Cellular meets WiFi: Traffic offloading or resource sharing? *IEEE Transactions on Wireless Communications 15*, 5 (2016), 3354–3367.

[39] CHIARAVIGLIO, L., BLEFARI-MELAZZI, N., LIU, W., GUTIÉRREZ, J. A., VAN DE BEEK, J., BIRKE, R., CHEN, L., IDZIKOWSKI, F., KILPER, D., MONTI, P., ET AL. Bringing 5G into Rural and Low-Income Areas: Is It Feasible? *IEEE Communications Standards Magazine 1*, 3 (2017), 50–57.

[40] CISCO. Cisco VNI Forecasting. http://www.cisco.com/c/en/us/solutions/collateral/service-provider/visual-networking-index-vni/white_paper_c11-520862.html, 2014. [Online; accessed 10-August-2015].

[41] CISCO. IEEE 802.11ax: The Sixth Generation of Wi-Fi. https://www.cisco.com/c/dam/en/us/products/collateral/wireless/white-paper-c11-740788.pdf, 2018. [Online; accessed July-2019].

[42] CONINCK, Q. D., BAERTS, M., HESMANS, B., AND BONAVENTURE, O. Observing real smartphone applications over multipath TCP. *IEEE Communications Magazine 54*, 3 (Mar 2016), 88–93.

[43] CORDEIRO, C., CHALLAPALI, K., BIRRU, D., AND SHANKAR, N. S. IEEE 802.22: The First Worldwide Wireless Standard based on Cognitive Radios. In *Proc. IEEE DySPAN* (2005).

[44] DAHLMAN, E., PARKVALL, S., AND SKOLD, J. *4G: LTE/LTE-advanced for Mobile Broadband*. Academic press, 2013.

[45] DCMS. Enabling UK growth - Releasing public spectrum. `https://www.gov.uk/government/uploads/system/uploads/attachment_data/file/287992/PSSRP_update_5_March_2014_Final.pdf`, 2014. [Online; accessed 10-August-2015].

[46] DE CONINCK, Q., AND BONAVENTURE, O. Multipath QUIC: Design and evaluation. In *Proceedings of the 13th International Conference on Emerging Networking EXperiments and Technologies* (2017), ACM, pp. 160–166.

[47] DE CONINCK, Q., AND BONAVENTURE, O. MultipathTester: Comparing MPTCP and MPQUIC in Mobile Environments. In *2019 Network Traffic Measurement and Analysis Conference (TMA)* (2019), IEEE, pp. 221–226.

[48] DEEK, L., GARCIA-VILLEGAS, E., BELDING, E., LEE, S.-J., AND ALMEROTH, K. The impact of channel bonding on 802.11 n network management. In *Proceedings of the Seventh COnference on emerging Networking EXperiments and Technologies* (2011), ACM, p. 11.

[49] DEHOS, C., GONZÁLEZ, J. L., DE DOMENICO, A., KTENAS, D., AND DUSSOPT, L. Millimeter-wave access and backhauling: The solution to the exponential data traffic increase in 5G mobile communications systems? *IEEE Communications Magazine 52*, 9 (2014), 88–95.

[50] DEMANGE, G., AND GALE, D. The Strategy Structure of Two-sided Matching Markets. *Econometrica: Journal of the Econometric Society* (1985), 873–888.

[51] DIMATTEO, S., HUI, P., HAN, B., AND LI, V. O. Cellular traffic offloading through WiFi networks. In *Mobile Adhoc and Sensor Systems (MASS), 2011 IEEE 8th International Conference on* (2011), IEEE, pp. 192–201.

[52] DJUKIC, P., AND MOHAPATRA, P. Soft-TDMAC: A software TDMA-based MAC over commodity 802.11 hardware. In *INFOCOM 2009, IEEE* (2009), IEEE, pp. 1836–1844.

[53] ELAYOUBI, S. E., ALTMAN, E., HADDAD, M., AND ALTMAN, Z. A Hybrid Decision Approach for the Association Problem in Heterogeneous Networks. In *INFOCOM, 2010 Proceedings IEEE* (2010), IEEE, pp. 1–5.

[54] ELSHAER, H., BOCCARDI, F., DOHLER, M., AND IRMER, R. Downlink and Uplink Decoupling: A Disruptive Architectural Design for 5G Networks. In *Global Communications Conference (GLOBECOM), 2014 IEEE* (2014), IEEE, pp. 1798–1803.

[55] ELSHAER, H., BOCCARDI, F., DOHLER, M., AND IRMER, R. Load & Backhaul Aware Decoupled Downlink/Uplink Access in 5G Systems. In *Communications Workshops (ICC), 2015 IEEE International Conference on* (2015), IEEE, pp. 5380–5385.

[56] ERICSSON. Ericsson Mobility Report 2019. https://www.ericsson.com/assets/local/mobility-report/documents/2019/ericsson-mobility-report-june-2019.pdf, 2019. [Online; accessed July-2019].

[57] ETSI. ETSI TR 103 588: Reconfigurable Radio Systems (RRS);Feasibility study on temporary spectrum access for local high-quality wireless networks. https://www.etsi.org/deliver/etsi_tr/103500_103599/103588/01.01.01_60/tr_103588v010101p.pdf, Feb 2018.

[58] ETSI. White Space Devices (WSD) Wireless Access Systems operating in the 470 MHz to 790 MHz TV broadcast band, 2018. ETSI EN 301 598 V2.1.1.

[59] ETSI. ETSI TS 103 652-1: Reconfigurable Radio Systems (RRS); evolved Licensed Shared Access (eLSA); Part 1: System requirements. https://www.etsi.org/deliver/etsi_ts/103600_103699/10365201/01.01.01_60/ts_10365201v010101p.pdf, Feb 2019.

[60] FACEBOOK. Introducing Facebook's new terrestrial connectivity systems - Terragraph and Project ARIES, April 2016. Retrieved May, 2018 from https://bit.ly/2SgSVNM.

[61] FACEBOOK. Introducing OpenCellular: An Open Source Wireless Access Platform, July 2016. Retrieved May, 2018

from https://code.facebook.com/posts/1754757044806180/introducing-opencellular-an-open-source-wireless-access-platform/.

[62] FERLIN, S., ALAY, Ö., MEHANI, O., AND BORELI, R. BLEST: Blocking estimation-based mptcp scheduler for heterogeneous networks. In *IFIP Networking Conference (IFIP Networking) and Workshops, 2016* (2016), IEEE, pp. 431–439.

[63] FITCH, M., NEKOVEE, M., KAWADE, S., BRIGGS, K., AND MACKENZIE, R. Wireless service provision in tv white space with cognitive radio technology: A telecom operator's perspective and experience. *Communications Magazine, IEEE 49*, 3 (2011), 64–73.

[64] FLICKENGER, R., OKAY, S., PIETROSEMOLI, E., ZENNARO, M., AND FONDA, C. Very long distance Wi-Fi Networks. In *Proceedings of the second ACM SIGCOMM workshop on Networked systems for developing regions* (2008), pp. 1–6.

[65] FLORES, A. B., ET AL. IEEE 802.11af: A Standard for TV White Space Spectrum Sharing. *IEEE Communications 51*, 10 (Oct 2013).

[66] FORD, A., RAICIU, C., HANDLEY, M., BARRE, S., IYENGAR, J., ET AL. Architectural guidelines for multipath tcp development. *IETF, Informational RFC 6182* (2011), 2070–1721.

[67] FORD, A., RAICIU, C., HANDLEY, M., BONAVENTURE, O., ET AL. Tcp extensions for multipath operation with multiple addresses.

[68] FRIAS, Z., AND PÉREZ, J. Techno-economic analysis of femtocell deployment in long-term evolution networks. *EURASIP Journal on Wireless Communications and Networking 2012*, 1 (2012), 1–15.

[69] GSMA. The Mobile Economy 2019. https://www.gsmaintelligence.com/research/?file=b9a6e6202ee1d5f787cfebb95d3639c5&download, 2019. [Online; accessed July-2019].

[70] GUO, Y. E., NIKRAVESH, A., MAO, Z. M., QIAN, F., AND SEN, S. Accelerating multipath transport through balanced subflow completion. In *Proceedings of the 23rd Annual International Conference on Mobile Computing and Networking* (2017), ACM, pp. 141–153.

[71] HA, S., RHEE, I., AND XU, L. CUBIC: a new TCP-friendly high-speed TCP variant. *ACM SIGOPS operating systems review 42*, 5 (2008), 64–74.

[72] HAGOS, D. H., AND KAPITZA, R. Study on performance-centric offload strategies for lte networks. In *6th Joint IFIP Wireless and Mobile Networking Conference (WMNC)* (2013), IEEE, pp. 1–10.

[73] HANDLEY, M., RAICIU, C., AND WISCHIK, D. Coupled congestion control for multipath transport protocols.

[74] HARRISON, K., MISHRA, S. M., AND SAHAI, A. How much white-space capacity is there? In *New Frontiers in Dynamic Spectrum, 2010 IEEE Symposium on* (2010), IEEE, pp. 1–10.

[75] HARTUNG, L., AND MILIND, M. Policy driven multi-band spectrum aggregation for ultra-broadband wireless networks. In *Dynamic Spectrum Access Networks (DySPAN), 2015 IEEE International Symposium on* (2015), IEEE, pp. 82–93.

[76] HATFIELD, J. W., AND MILGROM, P. R. Matching with Contracts. *American Economic Review* (2005), 913–935.

[77] HE, Y., CHEN, M., GE, B., AND GUIZANI, M. On wifi offloading in heterogeneous networks: Various incentives and trade-off strategies. *IEEE Communications Surveys & Tutorials 18*, 4 (2016), 2345–2385.

[78] HEIMERL, K., ALI, K., BLUMENSTOCK, J. E., GAWALT, B., AND BREWER, E. A. Expanding Rural Cellular Networks with Virtual Coverage. In *NSDI* (2013), pp. 283–296.

[79] HEIMERL, K., HASAN, S., ALI, K., BREWER, E., AND PARIKH, T. Local, Sustainable, Small-Scale Cellular Networks. In *Proceedings of the Sixth International Conference on Information and Communication Technologies and Development: Full Papers-Volume 1* (2013), ACM, pp. 2–12.

[80] HEO, J., NOH, G., PARK, S., LIM, S., KIM, E., AND HONG, D. Mobile TV white space with multi-region based mobility procedure. *IEEE Wireless Communications Letters 1*, 6 (2012), 569–572.

[81] HOLLAND, O. Some Are Born With White Space, Some Achieve White Space, And Some Have White Space Thrust Upon Them. *IEEE Transactions on Cognitive Communications and Networking 2*, 2 (2016), 178–193.

[82] HOLLAND, O., AIJAZ, A., PING, S., WONG, S., MACK, J., LAM, L., AND DE LA FUENTE, A. Aggregation in TV white space and assessment of an aggregation-capable IEEE 802.11 white space device. In *Communications (ICC), 2016 IEEE International Conference on* (2016), IEEE, pp. 1–5.

[83] IBARRA, D., DESAI, N., AND DEMIRKOL, I. Software-based implementation of LTE/Wi-Fi aggregation and its impact on higher layer protocols. In *2018 IEEE International Conference on Communications (ICC)* (2018), IEEE, pp. 1–6.

[84] IHS ECONOMICS AND IHS TECHNOLOGY. The 5G economy: How 5G Technology will Contribute to the Global Economy, January 2017. Retrieved May, 2018 from `https://cdn.ihs.com/www/pdf/IHS-Technology-5G-Economic-Impact-Study.pdf`.

[85] ILAND, D., AND BELDING, E. M. Emergenet: Robust, rapidly deployable cellular networks. *IEEE Communications Magazine 52*, 12 (2014), 74–80.

[86] IP.ACCESS. Enterprise and Public Access, 2018. Retrieved May, 2018 from `http://www.ipaccess.com/`.

[87] JABBARI, B., PICKHOLTZ, R., AND NORTON, M. Dynamic spectrum access and management [dynamic spectrum management]. *Wireless Communications, IEEE 17*, 4 (2010), 6–15.

[88] JAUME, D., MASSÓ, J., AND NEME, A. The Multiple-partners Assignment Game with Heterogeneous Sales and Multi-unit Demands: Competitive Equilibria. *Mathematical Methods of Operations Research 76*, 2 (2012), 161–187.

[89] JOHNSON, D. L., AND MIKEKA, C. Bridging Africa's Broadband Divide. *IEEE Spectrum 53*, 9 (Sept 2016).

[90] KANG, L., ZHAO, W., QI, B., AND BANERJEE, S. Augmenting self-driving with remote control: Challenges and directions. In *Proc. ACM HotMobile* (2018), pp. 19–24.

[91] KASSEM, M., HASAN, C., AND MARINA, M. Decoupled uplink/downlink user association in hetnets: A matching with contracts approach. In *Proceedings of the 12th ACM Symposium on QoS and Security for Wireless and Mobile Networks* (2016), ACM, pp. 19–28.

[92] KASSEM, M. M., AND MARINA, M. K. Future wireless spectrum below 6 GHz: A UK perspective. In *2015 IEEE International Symposium on Dynamic Spectrum Access Networks (DySPAN)* (2015), IEEE, pp. 59–70.

[93] KASSEM, M. M., MARINA, M. K., AND HOLLAND, O. On the potential of TVWS spectrum to enable a low cost middle mile network infrastructure. In *Communication Systems & Networks (COMSNETS), 2018 10th International Conference on* (2018), IEEE, pp. 159–166.

[94] KASSEM, M. M., MARINA, M. K., AND RADUNOVIC, B. DIY Model for Mobile Network Deployment: A Step Towards 5G for All. In *Proceedings of the 1st ACM SIGCAS Conference on Computing and Sustainable Societies* (2018), ACM, p. 47.

[95] KENNEDY, R., GEORGE, K., VITALICE, O., AND OKELLO-ODONGO, W. TV white spaces in Africa: Trials and role in improving broadband access in Africa. In *AFRICON 2015* (2015), IEEE, pp. 1–5.

[96] KHADRAOUI, Y., LAGRANGE, X., AND GRAVEY, A. TCP performance for practical implementation of very tight coupling between LTE and WiFi. In *2016 IEEE 84th Vehicular Technology Conference (VTC-Fall)* (2016), IEEE, pp. 1–6.

[97] KHALIL, M., QADIR, J., ONIRETI, O., IMRAN, M. A., AND YOUNIS, S. Feasibility, Architecture and Cost Considerations of Using TVWS for Rural Internet Access in 5G. In *Innovations in Clouds, Internet and Networks (ICIN), 2017 20th Conference on* (2017), IEEE, pp. 23–30.

[98] KHALILI, R., GAST, N., POPOVIC, M., ET AL. Opportunistic linked-increases congestion control algorithm for MPTCP.

[99] KHALILI, R., GAST, N., POPOVIC, M., AND LE BOUDEC, J.-Y. MPTCP is not pareto-optimal: performance issues and a possible solution. *IEEE/ACM Transactions on Networking (ToN) 21*, 5 (2013), 1651–1665.

[100] KHAN, Z., AHMADI, H., HOSSAIN, E., COUPECHOUX, M., DASILVA, L. A., ET AL. Carrier aggregation/channel bonding in next generation cellular networks: methods and challenges. *Network, IEEE 28*, 6 (2014), 34–40.

[101] KUHN, N., LOCHIN, E., MIFDAOUI, A., SARWAR, G., MEHANI, O., AND BORELI, R. DAPS: Intelligent delay-aware packet scheduling for multipath transport. In *Communications (ICC), 2014 IEEE International Conference on* (2014), IEEE, pp. 1222–1227.

[102] KUMAR, A., ET AL. Toward Enabling Broadband for a Billion Plus Population with TV White Spaces. *IEEE Communications 54*, 7 (July 2016), 28–34.

[103] KUMAR, A., KUMAR, R., RATHOD, P., AND KARANDIKAR, A. How much TV UHF band spectrum is sufficient for rural broadband coverage? In *2015 13th International Symposium on Modeling and Optimization in Mobile, Ad Hoc, and Wireless Networks (WiOpt)* (2015), IEEE, pp. 419–426.

[104] LEE, H., FLINN, J., AND TONSHAL, B. RAVEN: Improving Interactive Latency for the Connected Car. In *Proceedings of the 24th Annual International Conference on Mobile Computing and Networking* (2018), ACM, pp. 557–572.

[105] LEE, K., LEE, J., YI, Y., RHEE, I., AND CHONG, S. Mobile data offloading: how much can WiFi deliver? In *Proceedings of the 6th International COnference, Co-NEXT'10* (2010), ACM, p. 26.

[106] LIM, Y.-S., NAHUM, E. M., TOWSLEY, D., AND GIBBENS, R. J. ECF: An MPTCP path scheduler to manage heterogeneous paths. In *Proceedings of the 13th International Conference on emerging Networking EXperiments and Technologies* (2017), ACM, pp. 147–159.

[107] LIU, D., WU, Z., WU, F., ZHANG, Y., AND CHEN, G. FIWEX: Compressive sensing based cost-efficient indoor white space exploration. In *Proceedings of the 16th ACM International Symposium on Mobile Ad Hoc Networking and Computing* (2015), ACM, pp. 17–26.

[108] LYSKO, A. A., MASONTA, M. T., AND JOHNSON, D. L. The television white space opportunity in southern africa: from field measurements to quantifying white spaces. In *White Space Communication*. Springer, 2015, pp. 75–116.

[109] MACCARTNEY, G. R., AND RAPPAPORT, T. S. Rural macrocell path loss models for millimeter wave wireless communications. *IEEE Journal on selected areas in communications 35*, 7 (2017), 1663–1677.

[110] MACCARTNEY JR, G. R., SUN, S., RAPPAPORT, T. S., XING, Y., YAN, H., KOKA, J., WANG, R., AND YU, D. Millimeter wave wireless communications: New results for rural connectivity. In *Proceedings of the 5th workshop on all things cellular: operations, applications and challenges* (2016), ACM, pp. 31–36.

[111] MALIWATU, R., ZLOBINSKY, N., LAMOLA, M., TAKYI, A., JOHNSON, D. L., AND DENSMORE, M. Experimental Analysis of 5 GHz WiFi and UHF-TVWS Hybrid Wireless Mesh Network Back-Haul Links. In *International Conference on Cognitive Radio Oriented Wireless Networks* (2018), Springer, pp. 3–14.

[112] MASONTA, M. T., JOHNSON, D., AND MZYECE, M. The white space opportunity in southern africa: Measurements with meraka cognitive radio platform. In *International Conference on e-Infrastructure and e-Services for Developing Countries* (2011), Springer, pp. 64–73.

[113] MATINMIKKO, M., OKKONEN, H., PALOLA, M., YRJOLA, S., AHOKANGAS, P., AND MUSTONEN, M. Spectrum sharing using licensed shared access: the concept and its workflow for LTE-advanced networks. *Wireless Communications, IEEE 21*, 2 (2014), 72–79.

[114] MOGENSEN, R. S., MARKMOLLER, C., MADSEN, T. K., KOLDING, T., POCOVI, G., AND LAURIDSEN, M. Selective Redundant MP-QUIC for 5G Mission Critical Wireless Applications. In *2019 IEEE 89th Vehicular Technology Conference (VTC2019-Spring)* (2019), IEEE, pp. 1–5.

[115] NAIK, G., SINGHAL, S., KUMAR, A., AND KARANDIKAR, A. Quantitative assessment of tv white space in india. In *2014 Twentieth National Conference on Communications (NCC)* (2014), IEEE, pp. 1–6.

[116] NARLANKA, S., CHANDRA, R., BAHL, P., AND FERRELL, J. I. A hardware platform for utilizing tv bands with a wi-fi radio. In *Local & Metropolitan Area Networks, 2007. LANMAN 2007. 15th IEEE Workshop on* (2007), IEEE, pp. 49–53.

[117] NEKOVEE, M. Quantifying the availability of TV white spaces for cognitive radio operation in the UK. In *Communications Workshops, 2009. ICC Workshops 2009. IEEE International Conference on* (2009), IEEE, pp. 1–5.

[118] NGUYEN, B., ZHANG, T., RADUNOVIC, B., STUTSMAN, R., KARAGIANNIS, T., KOCUR, J., AND VAN DER MERWE, J. A reliable distributed cellular core network for hyper-scale public clouds. Tech. rep., 2018. https://www.microsoft.com/en-us/research/uploads/prod/2018/02/ECHO-TR.pdf.

[119] NIKAEIN, N., MARINA, M. K., MANICKAM, S., DAWSON, A., KNOPP, R., AND BONNET, C. Openairinterface: A flexible platform for 5g research. *ACM SIGCOMM Computer Communication Review 44*, 5 (2014), 33–38.

[120] NIYATO, D., AND HOSSAIN, E. Dynamics of Network Selection in Heterogeneous Wireless Networks: An Evolutionary Game Approach. *Vehicular Technology, IEEE Transactions on 58*, 4 (2009), 2008–2017.

[121] OFCOM. Digital Dividend Statement: Cognitive Access — Statement on License-Exempt Cognitive Devices Using Interleaved Spectrum. http://stakeholders.ofcom.org.uk/binaries/consultations/cognitive/statement/statement.pdf, 2009. [Online; accessed 10-August-2015].

[122] OFCOM. Consultation — Implementing Geolocation. http://stakeholders.ofcom.org.uk/binaries/consultations/geolocation/summary/geolocation.pdf, 2010. [Online; accessed 10-August-2015].

[123] OFCOM. Regulatory Requirements for White Space Device in the UHF TV Band. www.cept.org/Documents/se-43/6161/, 2012. [Online; accessed 10-August-2015].

[124] OFCOM. TV white spaces: A consultation on white space device requirements. https://www.ofcom.org.uk/consultations-and-statements/category-2/whitespaces, Nov 2012.

[125] OFCOM. Public Sector Spectrum Release Amateur use of 2310 to 2450 and 3400 to 3475 MHz. http://stakeholders.ofcom.org.uk/binaries/consultations/public-sector-spectrum-release/summary/condoc.pdf, 2013. [Online; accessed 10-August-2015].

[126] OFCOM. TV white spaces: approach to coexistence. https://www.ofcom.org.uk/__data/assets/pdf_file/0023/69305/white-spaces.pdf, September 2013.

[127] OFCOM. Utilisation of key licence exempt bands and the effects on WLAN performance. http://stakeholders.ofcom.org.uk/binaries/research/technology-research/2013/report.pdf, 2013. [Online; accessed 10-August-2015].

[128] OFCOM. Public Sector Spectrum Release (PSSR) Technical coexistence issues for the 2.3 and 3.4 GHz award. http://stakeholders.ofcom.org.uk/binaries/consultations/pssr-2014/summary/pssr.pdf, 2014. [Online; accessed 10-August-2015].

[129] OFCOM. Spectrum management strategy: Ofcom's approach to and priorities for spectrum management over the next ten years. http://stakeholders.ofcom.org.uk/binaries/consultations/spectrum-management-strategy/summary/spectrum_management_strategy.pdf, 2014. [Online; accessed 10-August-2015].

[130] OFCOM. Study on the future UK spectrum demand for terrestrial mobile broadband applications. http://stakeholders.ofcom.org.uk/binaries/consultations/cfi-mobile-bb/annexes/RW_report.pdf, 2014. [Online; accessed 10-August-2015].

[131] OFCOM. Communications Market Report 2015. http://stakeholders.ofcom.org.uk/binaries/research/cmr/cmr15/CMR_UK_2015.pdf, 2015. [Online; accessed 10-August-2015].

[132] OFCOM. Implementing TV White Spaces. https://www.ofcom.org.uk/__data/assets/pdf_file/0034/68668/tvws-statement.pdf, Feb 2015.

[133] OFCOM. Implementing TV White Spaces . http://stakeholders.ofcom.org.uk/consultations/white-space-coexistence/statement, 2015. [Online; accessed 10-August-2015].

[134] OFCOM. Award of the 700 MHz and 3.6-3.8 GHz spectrum bands. https://www.ofcom.org.uk/__data/assets/pdf_file/0019/130726/

Award-of-the-700-MHz-and-3.6-3.8-GHz-spectrum-bands.pdf, December 2018.

[135] OFCOM. Improving spectrum access for Wi-Fi: Spectrum use in the 5 and 6 GHz band. https://www.ofcom.org.uk/__data/assets/pdf_file/0038/189848/consultation-spectrum-access-wifi.pdf, January 2020.

[136] ONIRETI, O., QADIR, J., IMRAN, M. A., AND SATHIASEELAN, A. Will 5G see its blind side? evolving 5G for universal internet access. In *Proceedings of the 2016 workshop on Global Access to the Internet for All* (2016), ACM, pp. 1–6.

[137] PANIGRAHI, D., AND RAMAN, B. Tdma scheduling in long-distance wifi networks. In *IEEE INFOCOM 2009* (2009), IEEE, pp. 2931–2935.

[138] PASCA, S. T. V., PATRO, S., TAMMA, B. R., AND FRANKLIN, A. A. A real-time performance evaluation of tightly coupled LTE Wi-Fi radio access networks. In *2017 IEEE International Conference on Advanced Networks and Telecommunications Systems (ANTS)* (2017), IEEE, pp. 1–6.

[139] PASCA, S. T. V., PATRO, S., TAMMA, B. R., AND FRANKLIN, A. A. Tightly coupled lte wi-fi radio access networks: A demo of lwip. In *2017 9th International Conference on Communication Systems and Networks (COMSNETS)* (2017), IEEE, pp. 419–420.

[140] PATRA, R. K., NEDEVSCHI, S., SURANA, S., SHETH, A., SUBRAMANIAN, L., AND BREWER, E. A. WiLDNet: Design and Implementation of High Performance WiFi Based Long Distance Networks. In *NSDI* (2007), vol. 1, p. 1.

[141] PYATTAEV, A., JOHNSSON, K., ANDREEV, S., AND KOUCHERYAVY, Y. 3GPP LTE traffic offloading onto WiFi direct. In *2013 IEEE Wireless Communications and Networking Conference Workshops (WCNCW)* (2013), IEEE, pp. 135–140.

[142] RAMIN KHALILI, NICOLAS GAST, MIROSLAV POPOVIC, JEAN-YVES LE BOUDEC. Opportunistic Linked-Increases Congestion Control Algorithm for MPTCP. Retrieved July, 2019 from https://tools.ietf.org/html/draft-khalili-mptcp-congestion-control-00.

[143] RAMJEE, R., ROY, S., AND CHINTALAPUDI, K. A Critique of FCC'S TV White Space regulations. *GetMobile: Mobile Computing and Communications 20*, 1 (2016), 20–25.

[144] RAZA, U., KULKARNI, P., AND SOORIYABANDARA, M. Low power wide area networks: An overview. *IEEE Communications Surveys & Tutorials 19*, 2 (2017), 855–873.

[145] REIGADAS, J. S., MARTINEZ-FERNANDEZ, A., RAMOS-LOPEZ, J., AND SEOANE-PASCUAL, J. Modeling and optimizing IEEE 802.11 DCF for long-distance links. *IEEE Transactions on Mobile Computing 9*, 6 (2010), 881–896.

[146] RHIZOMATICA. Community Telecommunications Infrastructure. Retrieved May, 2018 from `https://www.rhizomatica.org/`.

[147] ROBERTS, S., GARNETT, P., AND CHANDRA, R. Connecting Africa Using the TV White Spaces: From Research to Real World Deployments. In *Local and Metropolitan Area Networks (LANMAN), 2015 IEEE International Workshop on* (2015), IEEE, pp. 1–6.

[148] ROTH, A. E., AND SOTOMAYOR, M. A. O. *Two-sided Matching: A Study in Game-theoretic Modeling and Analysis*. No. 18. Cambridge University Press, 1992.

[149] SAAD, W., HAN, Z., ZHENG, R., DEBBAH, M., AND POOR, H. V. A College Admissions Game for Uplink User Association in Wireless Small Cell Networks. In *INFOCOM, 2014 Proceedings IEEE* (2014), IEEE, pp. 1096–1104.

[150] SACHS, J., ANDERSSON, L. A. A., ARAÚJO, J., CURESCU, C., LUNDSJÖ, J., RUNE, G., STEINBACH, E., AND WIKSTRÖM, G. Adaptive 5G low-latency communication for tactile internet services. *Proceedings of the IEEE 107*, 2 (Feb 2019), 325–349.

[151] SAHA, S. K., AGGARWAL, S., PATHAK, R., KOUTSONIKOLAS, D., AND WIDMER, J. MuSher: An Agile Multipath-TCP Scheduler for Dual-Band 802.11 ad/ac Wireless LANs. In *The 25th Annual International Conference on Mobile Computing and Networking* (2019), pp. 1–16.

[152] SAPOUNTZIS, N., SPYROPOULOS, T., NIKAEIN, N., AND SALIM, U. Optimal Downlink and Uplink User Association in Backhaul-limited HetNets. In *INFOCOM, 2016 Proceedings IEEE* (2016), IEEE.

[153] SCHMITT, P., ILAND, D., BELDING, E., AND ZHELEVA, M. Phonehome: Robust Extension of Cellular Coverage. In *Computer Communication and Networks (ICCCN), 2016 25th International Conference on* (2016), IEEE, pp. 1–8.

[154] SCHMITT, P., ILAND, D., ZHELEVA, M., AND BELDING, E. Hybridcell: Cellular connectivity on the fringes with demand-driven local cells. In *INFOCOM 2016-The 35th Annual IEEE International Conference on Computer Communications, IEEE* (2016), IEEE, pp. 1–9.

[155] SEKANDER, S., TABASSUM, H., AND HOSSAIN, E. A Matching Game for Decoupled Uplink-downlink User Association in Full-duplex Small Cell Networks. In *2015 IEEE Globecom Workshops (GC Wkshps)* (2015), IEEE, pp. 1–6.

[156] SEKANDER, S., TABASSUM, H., AND HOSSAIN, E. Decoupled uplink-downlink user association in multi-tier full-duplex cellular networks: A two-sided matching game. *IEEE Transactions on Mobile Computing 16*, 10 (2016), 2778–2791.

[157] SEKANDER, S., TABASSUM, H., AND HOSSAIN, E. Multi-Tier Drone Architecture for 5G/B5G Cellular Networks: Challenges, Trends, and Prospects. *IEEE Communications Magazine 56*, 3 (2018), 96–103.

[158] SEVILLA, S., JOHNSON, M., KOSAKANCHIT, P., LIANG, J., AND HEIMERL, K. Experiences: Design, Implementation, and Deployment of CoLTE, a Community LTE Solution. In *The 25th Annual International Conference on Mobile Computing and Networking* (2019), ACM, p. 45.

[159] SHETH, A., NEDEVSCHI, S., PATRA, R., SURANA, S., BREWER, E., AND SUBRAMANIAN, L. Packet loss characterization in WiFi-based long distance networks. In *IEEE INFOCOM 2007-26th IEEE International Conference on Computer Communications* (2007), IEEE, pp. 312–320.

[160] SHIMOMURA, T., OYAMA, T., AND SEKI, H. Analysis of TV white space availability in Japan. *IEICE Transactions on Communications 97*, 2 (2014), 350–358.

[161] SINGH, S., ZHANG, X., AND ANDREWS, J. G. Joint Rate and SINR Coverage Analysis for Decoupled Uplink-Downlink Biased Cell Associations in HetNets. *Wireless Communications, IEEE Transactions on PP* (2015), 1.

[162] TRAN, V., TAZAKI, H., DE CONINCK, Q., AND BONAVENTURE, O. Voice-activated applications and multipath TCP: A good match? In *Proc. TMA* (Jun 2018), pp. 1–6.

[163] VAN DE BEEK, J., RIIHIJARVI, J., ACHTZEHN, A., AND MAHONEN, P. TV White Space in Europe. *IEEE Transactions on Mobile Computing 11*, 2 (2012), 178–188.

[164] VASISHT, D., KAPETANOVIC, Z., WON, J., JIN, X., CHANDRA, R., SINHA, S. N., KAPOOR, A., SUDARSHAN, M., AND STRATMAN, S. FarmBeats: An IoT Platform for Data-Driven Agriculture. In *NSDI* (2017), pp. 515–529.

[165] VIERNICKEL, T., FROEMMGEN, A., RIZK, A., KOLDEHOFE, B., AND STEINMETZ, R. Multipath QUIC: A deployable multipath transport protocol. In *2018 IEEE International Conference on Communications (ICC)* (2018), IEEE, pp. 1–7.

[166] WANG, J., GAO, Y., AND XU, C. A Multipath QUIC Scheduler for Mobile HTTP/2. In *Proceedings of the 3rd Asia-Pacific Workshop on Networking 2019* (2019), pp. 43–49.

[167] WISCHIK, D., RAICIU, C., GREENHALGH, A., AND HANDLEY, M. Design, implementation and evaluation of congestion control for multipath TCP. In *Proc. USENIX NSDI* (2011), pp. 99–112.

[168] YING, X., ZHANG, J., YAN, L., ZHANG, G., CHEN, M., AND CHANDRA, R. Exploring indoor white spaces in metropolises. In *Proceedings of the 19th annual international conference on Mobile computing & networking* (2013), ACM, pp. 255–266.

[169] YUCEK, T., AND ARSLAN, H. A survey of spectrum sensing algorithms for cognitive radio applications. *Communications Surveys & Tutorials, IEEE 11*, 1 (2009), 116–130.

[170] ZHANG, H., DONG, Y., CHENG, J., HOSSAIN, M. J., AND LEUNG, V. C. Fronthauling for 5G LTE-U ultra dense cloud small cell networks. *IEEE Wireless Communications 23*, 6 (2016), 48–53.

[171] ZHANG, J., ZHANG, W., CHEN, M., AND WANG, Z. WINET: Indoor white space network design. In *Computer Communications (INFOCOM), 2015 IEEE Conference on* (2015), IEEE, pp. 630–638.

[172] ZHANG, T., LENG, N., AND BANERJEE, S. A vehicle-based measurement framework for enhancing whitespace spectrum databases. In *Proc. ACM MobiCom* (2014).

[173] ZHELEVA, M., PAUL, A., JOHNSON, D. L., AND BELDING, E. Kwiizya: Local cellular network services in remote areas. In *Proceeding of the 11th annual international conference on Mobile systems, applications, and services* (2013), ACM, pp. 417–430.